

Development of Digital Readout Electronics for the CMS Tracker

Emlyn Peter Corrin

High Energy Physics
Imperial College London
Prince Consort Road
London SW7 2BW

Thesis submitted to the University of London
for the degree of Doctor of Philosophy

November 2002



Abstract

The Compact Muon Solenoid (CMS) is a general-purpose detector, based at CERN in Switzerland, designed to look for new physics in high-energy proton-proton collisions provided by the Large Hadron Collider. The CMS tracker has 10 million readout channels being sampled at a rate of 40 MHz, then read out at up to 100 kHz, generating huge volumes of data; it is essential that the system can handle these rates without any of the data being lost or corrupted. The CMS tracker FED processes the data, removing pedestal and common mode-noise, and then performing hit and cluster finding. Strips below threshold are discarded, resulting in a significant reduction in data size. These zero suppressed data are stored in a buffer before being sent to the DAQ. The processing on the FEDs is done using FPGAs. Programmable logic was chosen over custom ASICs because of the lower cost, faster design and verification process, and the ability to easily upgrade the firmware at a later date.

This thesis is concerned with the digital readout electronics for the CMS tracker, working on the development of the FED, and verifying that it will meet the requirements of the detector. Firmware was developed for the back-end FPGA of the FED, implementing the CMS-wide common data format. Each event is wrapped in a header/trailer containing information such as the trigger number, bunch-crossing number and error-detection information. The firmware was developed in VHDL, and will be incorporated into the back-end FPGA of the FED, both in the tracker, and in the other subdetectors.

A study was performed, looking into the flow of data and buffer levels in the FED. A program was written in C++ that models the behaviour of the FED buffers. It was shown that during normal operation the FED can handle occupancies of up to 4 % with 100 kHz random triggers, assuming a sustainable output rate of 200 Mbyte/s. Even when the trigger rate was increased to its maximum of 140 kHz, the FED buffers did not overflow as long as the occupancy remained below 2.5 %. These results confirmed that the FED buffers should never overflow in normal operating conditions.

Acknowledgements

I would like to thank everyone in the High Energy Physics group for their help and support during my three years there. In particular Geoff Hall for his supervision and guidance, Costas Foudas for his help and for spending so much time proofreading my thesis, and Peter Dornan for letting me work with the group. Thanks also to John Coughlan, Rob Halsall, Bill Haynes, Peter Sharp, and Mike Johnson at RAL. I would also like to thank the Particle Physics and Astronomy Research Council (PPARC) and the Rutherford Appleton Laboratory (RAL) for funding my project.

I would especially like to thank Greg, Mark, Barry, Jonni, Etam, Rob, and Matt for the great atmosphere both in the lab and also over a coffee or a pint. Above all I would like to thank my girlfriend Sandra for her help and moral support while writing my thesis. Thanks also to my grandmother Win, my sister Naomi, my mum Marie-Pierre, Laurent, and all the rest of my family.

I dedicate this thesis to my dad, Ian, and my grandfather, George, for inspiring me towards an inquisitive mind.

Contents

Abstract.....	2
Acknowledgements.....	3
Contents	4
List of Figures.....	8
List of Tables	11
Glossary	12
Chapter 1: Introduction.....	15
1.1 The Large Hadron Collider (LHC).....	15
1.2 Physics at the LHC	16
1.2.1 The Higgs.....	16
1.2.2 CP Violation	18
1.2.3 Supersymmetry	18
1.3 The Compact Muon Solenoid (CMS).....	19
1.3.1 The Magnet.....	20
1.3.2 The Tracker.....	22
1.3.3 The Electronic Calorimeter (ECAL)	24
1.3.4 The Hadronic Calorimeter (HCAL).....	25
1.3.5 The Muon Detectors	26
1.3.6 The Trigger	28
1.4 Summary.....	29
Chapter 2: Field Programmable Devices.....	30
2.1 Digital Logic	30
2.1.1 Combinatorial Logic	32
2.1.2 Sequential Logic	34
2.2 Programmable Logic	34
2.3 History of Programmable Logic	36
2.3.1 The PROM.....	36
2.3.2 The PLA and PAL	37
2.3.3 The CPLD.....	38
2.3.4 The FPGA	39

2.4	Memory Technology	40
2.4.1	Fuses and Antifuses	40
2.4.2	The EPROM and EEPROM	41
2.4.3	SRAM	42
2.5	The Xilinx Virtex-II Range of FPGAs	43
2.5.1	Logic Blocks	45
2.5.2	I/O Blocks	47
2.5.3	Routing Resources	49
2.6	The Design Process.....	50
2.6.1	Design Entry	50
2.6.2	Verilog	52
2.6.3	VHDL	52
2.6.4	Simulation and Synthesis.....	54
2.6.5	Device Programming.....	54
2.7	Summary.....	56
Chapter 3:	The CMS Tracker Readout System	57
3.1	Overview.....	57
3.2	The Silicon Detectors	58
3.3	The APV Readout Chip.....	59
3.3.1	Preamplifier	61
3.3.2	Shaping Filter.....	61
3.3.3	Pipeline and FIFO	61
3.3.4	APSP.....	61
3.3.5	Analogue Multiplexer.....	63
3.3.6	Slow Control.....	64
3.4	The APVMUX.....	65
3.5	The Optical Link.....	65
3.6	The Front-End Driver	66
3.7	The S-LINK64	67
3.8	The DAQ	67
3.9	Control and Monitoring.....	68
3.9.1	Timing, Trigger and Control (TTC)	68

3.9.2	The Tracker Control System (TCS).....	69
3.10	Summary.....	69
Chapter 4:	The Front-End Driver	70
4.1	The FED Front-End Modules	71
4.2	The Front-End FPGA	75
4.2.1	Housekeeping	76
4.2.2	Monitoring.....	77
4.2.3	Configuration.....	77
4.2.4	Data Path.....	78
4.3	The Back-End FPGA.....	82
4.3.1	Common Data Format	83
4.3.2	CRC	84
4.4	Implementation of Common Data Format.....	86
4.5	Summary.....	92
Chapter 5:	Analysis of Data Flow and Buffering in the FED	93
5.1	The APV Buffers	94
5.1.1	The APV Emulator	94
5.2	Modelling the FED	95
5.2.1	Source Data.....	97
5.3	Simulation Results.....	99
5.3.1	Zero-Suppression Mode.....	99
5.3.2	Raw-Data Mode.....	108
5.4	Summary.....	110
Chapter 6:	Perspectives	111
6.1	FED Schedule	111
6.2	FED Testing.....	111
6.2.1	JTAG and Boundary Scan Testing	112
6.2.2	Basic Analogue Tests	112
6.2.3	Basic Digital Tests.....	112
6.2.4	More Advanced Tests	113
6.3	Conclusions.....	113

Appendix A: Common Data Format Implementation	115
A.1 fed_data_format.vhd	115
A.2 builder.vhd	118
A.3 fifo.vhd	122
A.4 mem64_general.vhd	124
A.5 mux.vhd	125
A.6 pck_crc16_d64_ccitt.vhd	126
A.7 pck_crc16_d64_x25.vhd	128
Appendix B: Common Data Format Verification Code	132
B.1 testbench.vhd	132
B.2 tester.vhd	135
B.3 main.c	139
B.4 crcmodel.h	141
B.5 crcmodel.c	144
References	147

List of Figures

Figure 1.1: The LHC site, (a) map, (b) aerial view.	15
Figure 1.2: Higgs production at the LHC.	16
Figure 1.3: Principle decay modes of the Higgs at CMS.	17
Figure 1.4: The CMS detector.	19
Figure 1.5: Transverse view of the CMS detector.	20
Figure 1.6: Diagram of the CMS superconducting magnet system.	21
Figure 1.7: The CMS tracker.	22
Figure 1.8: A prototype microstrip detector module from the tracker.	23
Figure 1.9: An ECAL crystal.	24
Figure 1.10: An assembled half-barrel of the HCAL.	25
Figure 1.11: A Muon drift tube.	26
Figure 1.12: A Muon cathode strip chamber.	27
Figure 1.13: A Muon resistive plate chamber.	28
Figure 1.14: The CMS level-1 global trigger.	29
Figure 2.1: Bipolar transistors (nnp and pnp) and their symbols.	30
Figure 2.2: JFET transistors (n-channel and p-channel) and their symbols.	31
Figure 2.3: MOSFET transistors (n-channel and p-channel) and their symbols. ...	32
Figure 2.4: A CMOS inverter and transmission gate, and their symbols.	32
Figure 2.5: CMOS NAND and NOR gates and their symbols.	33
Figure 2.6: CMOS transparent latch and flip-flop and their symbols.	34
Figure 2.7: Memory used as programmable logic.	36
Figure 2.8: A very small PLA.	37
Figure 2.9: Architecture of a CPLD.	38
Figure 2.10: Architecture of an FPGA.	39
Figure 2.11: Example of a fine-grained logic cell.	40
Figure 2.12: Antifuses: (a) ONO, (b) amorphous silicon.	40
Figure 2.13: An EPROM memory cell: a) schematic, b) use in wired-AND.	41
Figure 2.14: An SRAM memory cell.	42
Figure 2.15: Xilinx Virtex-II Architecture.	44
Figure 2.16: Virtex-II logic blocks: (a) CLB, (b) slice.	45

Figure 2.17: (a) I/O banks in Virtex-II flip-chip packages, (b) an I/O block.	48
Figure 2.18: Virtex-II routing resources.	49
Figure 2.19: The FPGA Design Process.	50
Figure 3.1: An overview of the tracker readout system.	57
Figure 3.2: A silicon microstrip detector.	58
Figure 3.3: The APV25-S1.	60
Figure 3.4: The APV25 APSP circuit.	63
Figure 3.5: A typical APV output frame.	64
Figure 3.6: The FED and DAQ racks (top) and a FED crate (bottom).	66
Figure 3.7: Overview of the CMS DAQ system.	67
Figure 3.8: Schematic of the tracker control system.	69
Figure 4.1: Schematic of the Front-end driver.	70
Figure 4.2: Schematic of a FED front-end module.	71
Figure 4.3: Schematic of a FED front-end module analogue section.	72
Figure 4.4: Schematic of a FED front-end module two channel ADC.	73
Figure 4.5: Schematic of the FED front-end FPGA.	75
Figure 4.6: Basic schematic of the housekeeping block.	76
Figure 4.7: A pair of channels from the datapath block.	78
Figure 4.8: Graphical representation of the clustering algorithm.	80
Figure 4.9: Diagram of the back-end FPGA.	82
Figure 4.10: Common data format header and trailer.	83
Figure 4.11: Graphical representation of the CRC algorithm (for CRC-8).	85
Figure 4.12: Block diagram of the header formatting block.	88
Figure 4.13: A short period of the simulation.	90
Figure 5.1: Data flow and buffers in the tracker readout system.	93
Figure 5.2: The APV Emulator System.	94
Figure 5.3: Graphical representation of the FED buffer model.	96
Figure 5.4: Distribution of event sizes in strips per detector, from Monte-Carlo.	97
Figure 5.5: Estimated distribution of event sizes in strips per APV.	98
Figure 5.6: Zero-suppression, front-end: events lost vs. output rate.	100
Figure 5.7: Zero-suppression, front-end: events lost vs. occupancy.	101
Figure 5.8: Zero-suppression, back-end: events lost vs. output rate.	102

Figure 5.9: Zero-suppression, back-end: events lost vs. occupancy..... 103

Figure 5.10: Zero-suppression, back-end: maximum occupancy vs. output rate.104

Figure 5.11: Zero-suppression: peak level of data buffer vs. occupancy. 105

Figure 5.12: Zero suppression: peak level of header buffer vs. occupancy. 106

Figure 5.13: Raw data, front-end: events lost vs. trigger rate..... 108

Figure 5.14: Raw data, back-end: events lost vs. trigger rate..... 109

Figure 5.15: Raw data: maximum trigger rate vs. output rate..... 110

List of Tables

Table 2.1: Truth tables for NAND and NOR gates.	33
Table 2.2: Summary of Programming Technologies.....	43
Table 2.3: Virtex-II family members.....	45
Table 2.4: Virtex-II block-RAM configurations.	47
Table 4.1: Rules for data size reduction in the FED.....	81
Table 4.2: Common data format header and trailer fields.	84
Table 4.3: Parameters for the reference CRC.....	91
Table 4.4: Synthesis results for the header building code.	91
Table 5.1: Peak header buffer levels.....	107

Glossary

ADC	Analogue-to-Digital Converter.
APSP	Analogue Pulse Shape Processor: Processing stage in the APV readout chip.
APV	Analogue Pipeline (Voltage Mode): Front-end readout chip.
APV25	APV built on 0.25 μm process.
APV6	Early version of the APV built on 1.2 μm process.
APVE	APV Emulator.
APVM	Early version of the APV built on 1.2 μm process, for MSGCs.
APVMUX	APV Multiplexer: Combines the outputs from pairs of APVs to send to laser driver.
ASIC	Application Specific Integrated Circuit.
BPM	BiPhase Mark: Encoding scheme used by the TTC system.
BRAM	Block-RAM: One of several logic blocks in an FPGA.
CCITT	Comité Consultatif International de Télégraphique et Téléphonique: International consultative committee on telecommunications and telegraphy.
CCU	Communications and Control Unit: Distributes clock, trigger, control and monitoring data within the tracker.
CERN	The European Laboratory for Particle Physics Research, in Geneva, Switzerland.
CLB	Configurable Logic Block: Basic unit of logic functionality in FPGAs.
CMOS	Complementary Metal Oxide Semiconductor: A semiconductor technology consisting of both p-type and n-type devices, and having low power dissipation.
CMS	Compact Muon Solenoid.
CPLD	Complex Programmable Logic device.
CRC	Cyclic Redundancy Check: An error detection code.
CSC	Cathode Strip Chamber: A type of muon detector used at CMS.
DAC	Digital-to-Analogue Converter.
DAQ	Data Acquisition system.
DCM	Digital Clock Manager: One of several logic blocks in an FPGA.
DCU	Detector Control Unit: Interface to monitor slowly varying parameters in the tracker.
DDR	Double Data Rate: Port in which data is latched on both clock edges, resulting in a doubling of the data rate.
DPM	Dual Port Memory.
DT	Drift Tube: A type of muon detector used at CMS.
DUT	Device Under Test.
ECAL	Electromagnetic Calorimeter.
EEPROM	Electrically Erasable Programmable Read Only Memory.
EPROM	Erasable Programmable Read Only Memory.
FEC	Front End Controller: Distributes clock, trigger and control data to, and receives monitoring data from, the tracker readout system via digital optical links.

FED	Front End Driver.
FET	Field Effect Transistor.
FIFO	First In First Out: Type of buffer in which the data are read out in the same order in which they were written.
FIR	Finite Impulse Response: Type of signal-processing filter.
FLASH	Type of EEPROM in which large areas of memory can be erased at once.
FPD	Field Programmable device: A general term for all types of user-programmable integrated circuits.
FPGA	Field Programmable Gate Array: an FPD with a structure allowing very high logic capacity.
HCAL	Hadronic Calorimeter.
HDL	Hardware Description Language.
I ² C	Inter-IC: Two-wire serial communications protocol developed by Philips.
IC	Integrated Circuit.
IEEE	Institute of Electrical and Electronic Engineers: Standards committee.
IIR	Infinite Impulse Response: Type of signal-processing filter.
ILA	Integrated Logic Analyzer: Part of the Chipscope debugging tool for FPGAs from Xilinx.
IOB	Input/Output Block.
ISP	In System Programmable.
JFET	Junction Field Effect Transistor.
JTAG	Joint Test Action Group: Standard for controlling and monitoring pins and internal registers of electronic devices such as FPGAs.
L1A	Level-1 Accept: First-level trigger decision signal (up to 100 kHz).
LEP	Large Electron Positron Collider.
LHC	Large Hadron Collider.
LSP	Lightest Supersymmetric Particle.
LVDS	Low Voltage Differential Signalling: High performance, low power, and low noise signalling standard.
MIP	Minimum Ionising Particle: Corresponds to roughly 25 000 electrons in a 300 μm thick silicon detector.
MOSFET	Metal-Oxide-Semiconductor Field Effect Transistor.
MPGA	Mask Programmable Gate Array: ASIC technology consisting of standard logic cells (as in an FPGA) but programmed by a custom metal layer during the manufacturing process.
MSGC	Microstrip Gas Chamber.
MSSM	Minimal Supersymmetric Standard Model.
NMOS	Negative-channel Metal Oxide Semiconductor.
OVI	Open Verilog International: Non-profit organisation that maintains Verilog HDL.
PAL	Programmable Array Logic: Simple FPD with programmable AND-plane and fixed OR-plane (registered trademark of Advanced Micro Devices Inc.).
PAR	Place-and-Route.
PCB	Printed Circuit Board.

PCI	Peripheral Component Interconnect: Widely used bus designed by Intel.
PLA	Programmable Logic Array: Simple FPD with a programmable AND-plane and OR-plane.
PLD	Programmable Logic Device: See FPD, often used to refer to relatively simple types of devices.
PMC	PCI Mezzanine Card.
PMOS	Positive-channel Metal Oxide Semiconductor.
PPARC	Particle Physics and Astronomy Research Council.
PROM	Programmable Read Only Memory.
QDR	Quad Data Rate.
RAL	Rutherford Appleton Laboratory, in Didcot, Oxfordshire.
RAM	Random Access Memory.
ROM	Read Only Memory.
RPC	Resistive Plate Chamber: A type of muon detector used at CMS.
SDF	Standard Delay Format.
S-LINK	Protocol for transmission of data in 8-32-bit words at up to 40 MHz
S-LINK64	Extension of S-LINK allowing 64-bit data at a rate of 100 MHz.
SM	Standard Model.
SOP	Sum of Products.
SPLD	Simple Programmable Logic Device.
SRAM	Static RAM.
SUSY	Supersymmetry.
TCS	Tracker Control System.
TTC	Timing, Trigger and Control System.
TTCrx	TTC Receiver: Custom IC
TTL	Transistor-Transistor Logic: A semiconductor technology using bipolar transistors.
VHDL	VHSIC (Very High Speed Integrated Circuit) Hardware Description Language.
VME	Versa Module Europa: A flexible backplane interconnection bus system, using the Eurocard standard circuit board sizes and defined by IEEE standard 1014-1987.

Chapter 1: Introduction

1.1 The Large Hadron Collider (LHC)

The LHC is a particle accelerator being built at CERN, the European Laboratory for Particle Physics Research near Geneva in Switzerland. It is located in the 27 km circumference circular tunnel previously used for the Large Electron-Positron (LEP) collider (see figure 1.1).

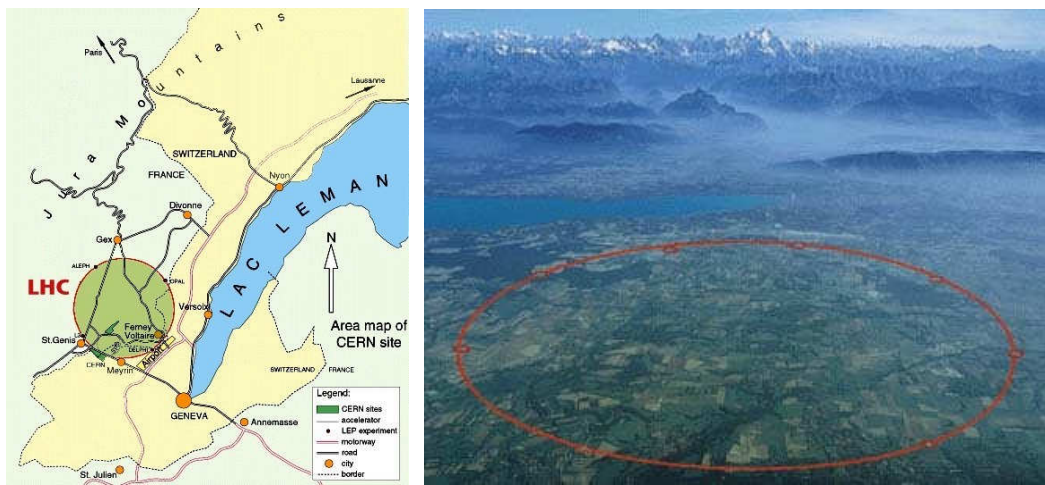


Figure 1.1: The LHC site, (a) map, (b) aerial view.

When operational, it will provide proton-proton collisions with a centre-of-mass energy of 14 TeV and a luminosity of $10^{34} \text{ cm}^{-2}\text{s}^{-1}$. This is orders-of-magnitude higher than any previous accelerator, leading to an extremely demanding radiation environment. In order to sustain such a high luminosity, bunches of particles are separated by only 25 ns, and the readout electronics must be capable of determining from exactly which bunch crossing each signal originated, leading to very strict timing requirements.

In addition to proton-proton collisions, heavy ions, such as lead, will be collided at energies in excess of 1000 TeV/ion and luminosity over $10^{27} \text{ cm}^{-2}\text{s}^{-1}$.

1.2 Physics at the LHC

The LHC will open up new, previously unexplored, areas of physics. The energies available will allow many predictions to be either confirmed by experiment, or rejected. In addition it will allow much more accurate measurement of many fundamental parameters of physics.

1.2.1 The Higgs

The Standard Model (SM) of particle physics requires the existence of a new particle, the Higgs. Particles acquire mass through their interaction with the Higgs field. There is a theoretical upper limit on the mass of the Higgs, of about 1 TeV, and masses up to 114 GeV have been ruled out by direct searches at LEP [1] and other experiments, although there were hints of a possible Higgs at a mass of 115.6 GeV [2]. Depending on its mass, there are a number of ways in

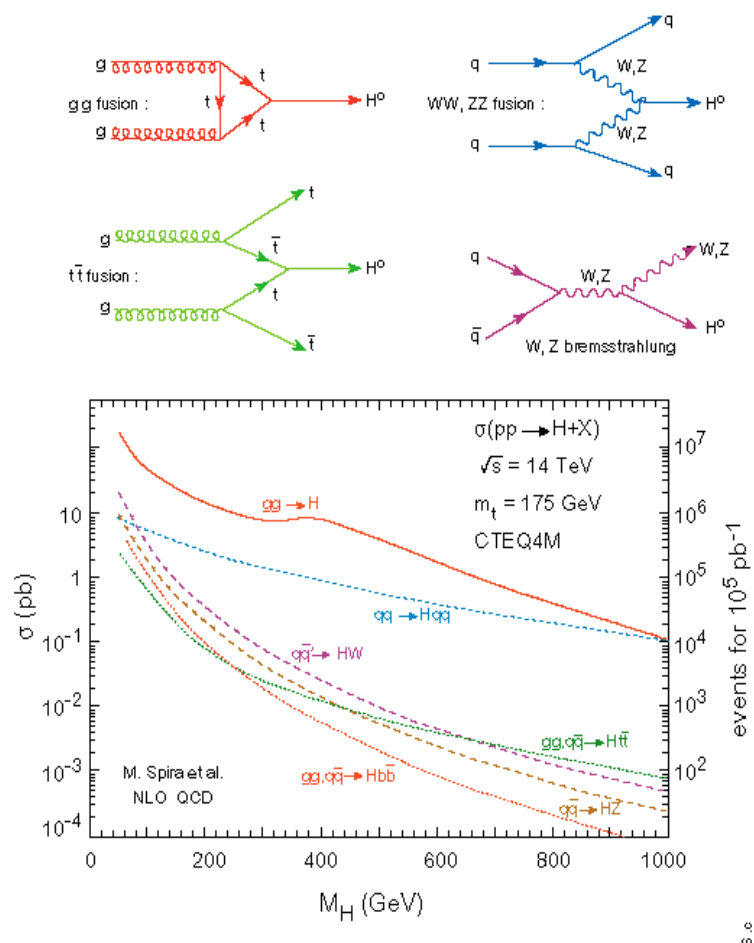


Figure 1.2: Higgs production at the LHC.

which Higgs particles may be produced at the LHC (see figure 1.2), but the dominant production channel is by gluon fusion. Once produced, there are a number of different ways the Higgs may decay, also depending on its mass. The branching ratios for the various modes are depicted in figure 1.3, along with a table of the decay modes best suited for a search at CMS.

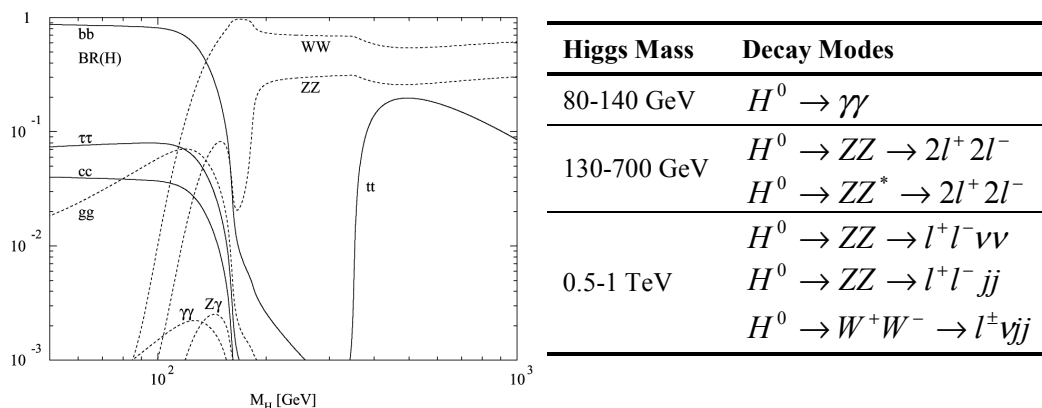


Figure 1.3: Principle decay modes of the Higgs at CMS.

For a light Higgs, up to around 140 GeV, the dominant decay channel is $H^0 \rightarrow b\bar{b}$, but this channel will be difficult to observe due to a large background of QCD jets. A better channel will be the much rarer $H^0 \rightarrow \gamma\gamma$ channel, with a branching ratio of around 10^{-3} . There will also be a large irreducible photon-photon background, but over the relevant mass range this will be smoothly varying, and the Higgs particle would therefore produce a slight hump superimposed on top of a well-calibrated background. For this to be possible, very accurate energy resolution is needed for the photons, and the ECAL has been optimised with this in mind.

For a slightly heavier Higgs, up to about 700 GeV, the most promising decay channels are $H^0 \rightarrow ZZ, ZZ^* \rightarrow 2l^+ 2l^-$. In this case, detection relies on the excellent performance of the muon chambers along with the crystal ECAL and the tracker.

For the highest Higgs mass, there are a number of promising decay modes, with detection relying on leptons, jets, and missing transverse energy in the case of neutrinos. For this the performance of the HCAL is very important.

If the Higgs boson exists, it is expected that it will be produced and detected once in about every 10^{13} collisions, which, with 800 million collisions per second, corresponds to about once a day.

1.2.2 CP Violation

The known universe is dominated by matter, as opposed to antimatter, and yet the four known forces seem to act equally on matter and antimatter. This introduces the question of how the universe evolved into its current asymmetric state. A clue may be provided by the phenomenon of charge-parity (CP) violation, discovered in 1964 in the decays of the neutral kaon (K^0), an s-quark containing meson. There is a small difference in the decay rates of K^0 and \bar{K}^0 mesons. This implies that either there exists another, as yet unknown, force of nature, which is matter-antimatter asymmetric, or that the weak interaction, through which kaons decay, can actually distinguish between matter and antimatter. If this is the case, then mesons made of quarks heavier than the s quark should display an even larger asymmetry in their decay rates. The best candidate is the b quark, which forms B mesons. Although the LHCb experiment at the LHC is dedicated to B physics, CMS will also play a role in the study of CP violation especially during the initial low luminosity phase of the LHC [3].

1.2.3 Supersymmetry

Supersymmetry (SUSY) introduces a new symmetry, not present in the standard model, between fermions and bosons. It proposes that each fermion (spin- $1/2$) has a superpartner of spin-0, while each boson (integer-spin) has a spin- $1/2$ superpartner. In the minimal supersymmetric standard model (MSSM) there are at least five Higgs bosons, as well as a host of new superpartners for currently known particles, called sparticles (supersymmetric particles). The heavier sparticles will rapidly decay, while the lightest supersymmetric particle (LSP) will be stable, and can be detected from missing transverse energy.

1.3 The Compact Muon Solenoid (CMS)

The Compact Muon Solenoid is one of the several experiments based at the LHC. It is a general-purpose detector designed to detect cleanly a diverse range of signatures of possible new physics, and is optimised to search for the standard model Higgs boson in the mass range from 90 GeV to 1 TeV.

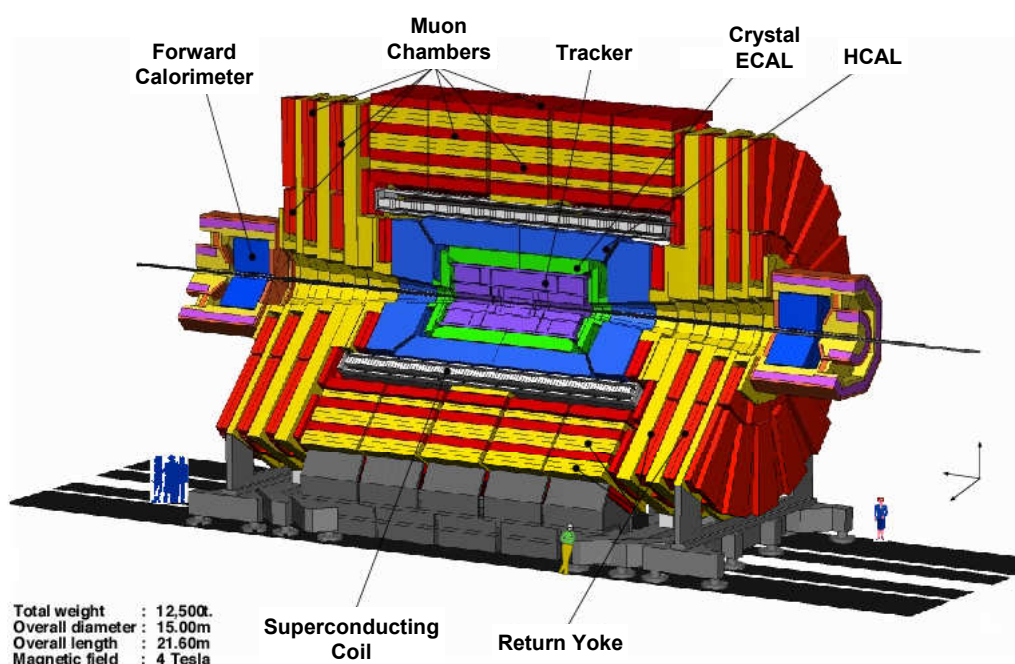


Figure 1.4: The CMS detector.

CMS is built around a large toroidal superconducting electromagnet of length 13 m and inner diameter 5.9 m, which generates a magnetic field of 4 Tesla [4] (see figure 1.4 and figure 1.5). It consists of several sub-detectors each optimised to detect certain types of particles. The tracker is made of layers of silicon pixel and microstrip detectors, and is designed to track all ionising particles without significantly affecting their energy or momentum. Surrounding the tracker is the electronic calorimeter, made of lead tungstate (PbWO_4) crystals. This is designed to absorb all electrons and photons and measure their energy from the scintillation produced by the deposited energy, while other particles such as hadrons, muons and neutrinos, pass through. Outside this is the hadronic calorimeter, which measures the energy and position of the hadrons.

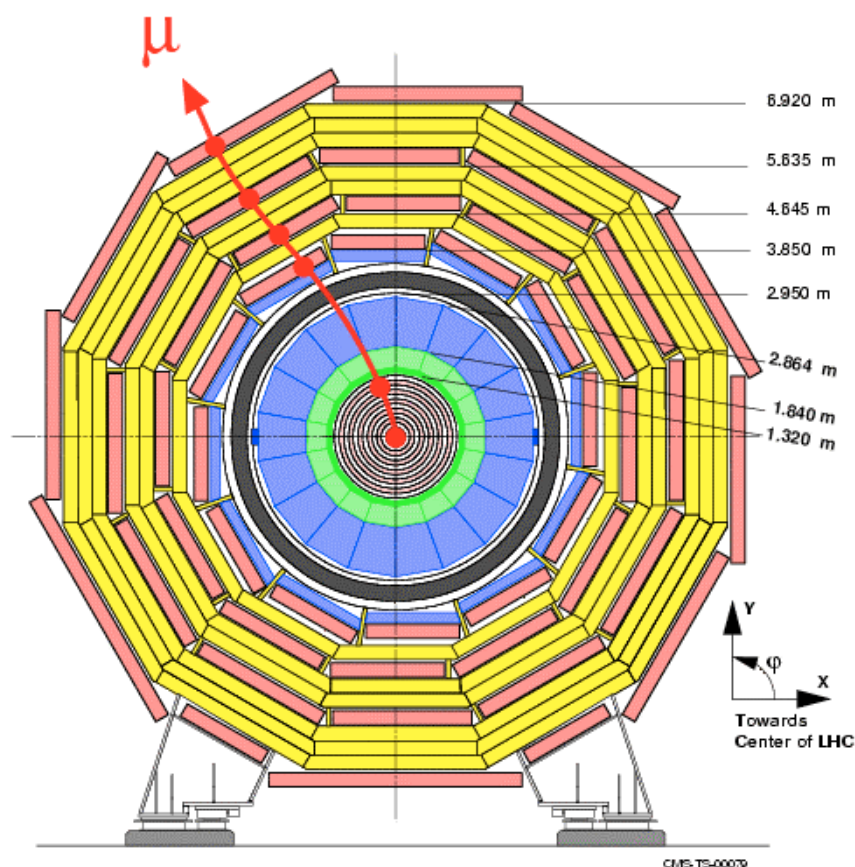


Figure 1.5: Transverse view of the CMS detector.

The only particles that escape through all these layers of detectors and the magnet are muons and neutrinos. Muons lose energy almost solely through ionisation along their path, and even in dense materials like steel or copper, this amounts to a loss of only 1 MeV per millimetre. The muons are detected by the muon chambers surrounding the detector, and the neutrinos have to be inferred from missing energy.

1.3.1 The Magnet

The CMS magnet system consists of a large superconducting coil capable of generating a magnetic field of 4 Tesla, and a return yoke to contain the generated magnetic field. With a length of 13 m and an inner diameter of 5.9 m, it will be the largest superconducting magnet in the world; the stored energy (2.5 GJ) is

enough to melt 18 tonnes of gold. The use of such a high magnetic field allows a much more efficient first-level trigger [5] by improving the momentum resolution of the muon detectors. It also improves the momentum resolution of the tracker, and allows the electromagnetic calorimeter to be accurately calibrated by comparing the energies of electrons with their momentum in the tracker. A reduction of the magnetic field strength to 3 Tesla, would require the running time to increase by one third to achieve the same level of significance for a mass measurement from multi-charged particle states [5].

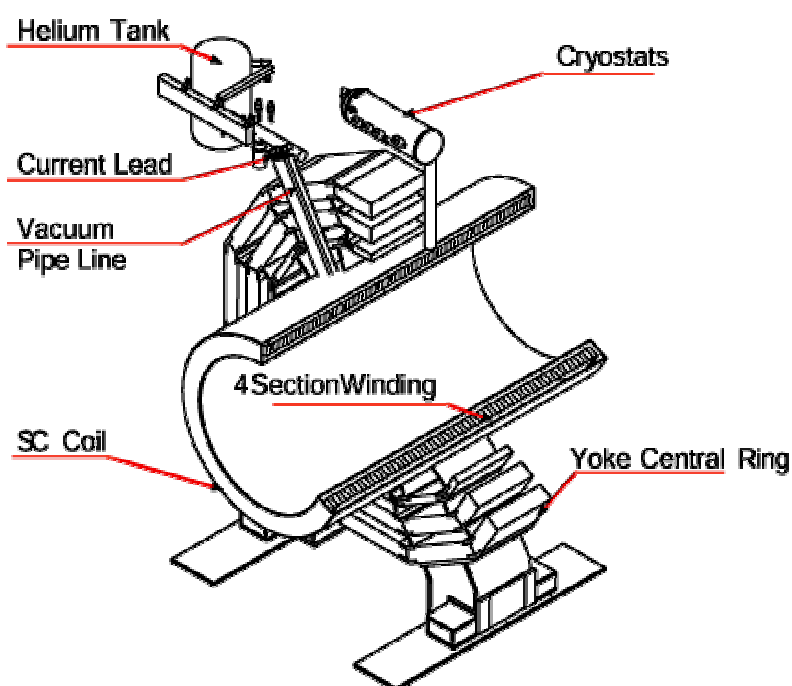


Figure 1.6: Diagram of the CMS superconducting magnet system.

A diagram of the magnet system, excluding most of the yoke, is shown in figure 1.6. The coil itself is built in four sections, each with four layers of winding, giving a total of 43 km of superconducting cable. The coil is contained within a vacuum tank, a 240 tonne stainless steel vessel, which also acts as a support structure for the barrel HCAL, ECAL, and tracker.

A cryogenic system, using liquid helium, keeps the coil at a working temperature of 4.5 K, with a maximum temperature difference of 0.1 K within the coil.

1.3.2 The Tracker

The tracker is designed to reconstruct tracks efficiently, giving accurate measurements of the vertex, the impact parameter, and any secondary vertices, whilst being as thin as possible to minimise multiple scattering and energy loss, which would have adverse effects on the calorimetry. It must have a high enough spatial resolution to isolate and identify isolated leptons and photons, in order to reduce backgrounds sufficiently for Higgs and SUSY searches. For a typical particle energy of 100 GeV, the tracker can measure the transverse momentum with a resolution of about 2 % up to $|\eta| < 1.6$ and about 6.5 % up to $|\eta| < 2.5$ [6].

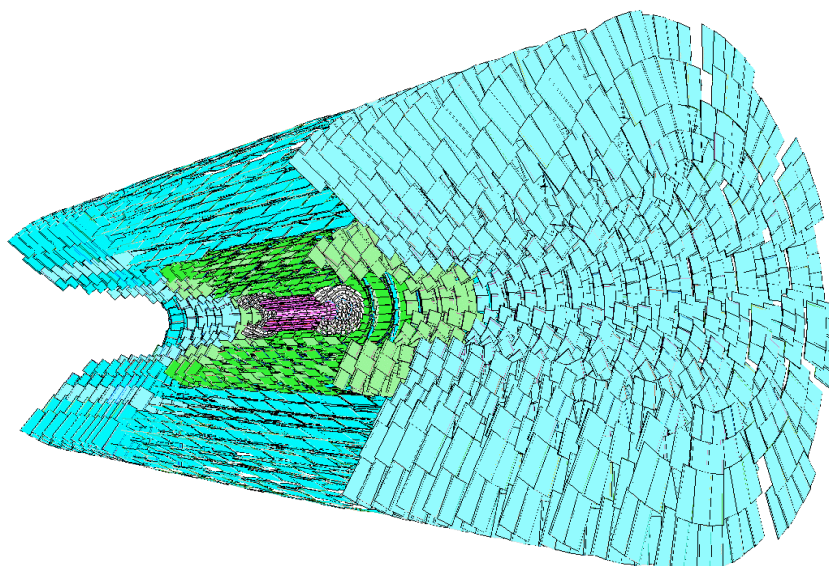


Figure 1.7: The CMS tracker.

The layout of the tracker is shown in figure 1.7. The central three layers are based on silicon pixel detectors. Surrounding this is the inner barrel, consisting of four layers of microstrip detectors, and the outer barrel, consisting of six layers. At each end of the cylinder are the pixel forward detector (2 layers, pixel), the inner disk (3 layers, microstrip) and the endcaps (9 layers). The original proposal had been to use microstrip gas chambers (MSGCs) for the outer layers of the tracker, but a review in December 1999 decided to move to an all-silicon design as this was just as viable and allowed more effort to be concentrated onto a smaller set of problems [7].

Pixel Detectors

The pixel detectors are located close to the interaction point, where the occupancies are highest, in three barrel-layers and two end-layers. Each pixel measures $150 \times 150 \mu\text{m}$, and by using charge sharing between pixels to interpolate the track positions, will provide a spatial resolution of about $10 \mu\text{m}$ in the $r\text{-}\phi$ direction and about $20 \mu\text{m}$ in the z direction [6]. The pixel detector will confirm or reject track segments proposed by the surrounding tracker layers.

Microstrip Detectors

The microstrip detectors are arranged in 10 layers around the pixel detectors. Their pitch varies from $80 \mu\text{m}$ in the inner layer to $205 \mu\text{m}$ in the outer layer. Typical spatial resolutions (for a $100 \mu\text{m}$ pitch detector) are $34 \mu\text{m}$ in $r\text{-}\phi$ and $320 \mu\text{m}$ in the z direction [6]. One of the prototype detector hybrid modules from the microstrip tracker is shown in figure 1.8. It consists of two microstrip detectors, bonded together at the centre. A pitch adaptor connects one end of the detector to the APV readout chips. There is space for six APV chips; each reading out 128 of the 768 detector strips, although in the prototype only three are mounted, and only half of the detector is read out. A kapton cable connects the outputs of the APVs to the opto-hybrid, where the signals are driven via optical fibres to the counting room.

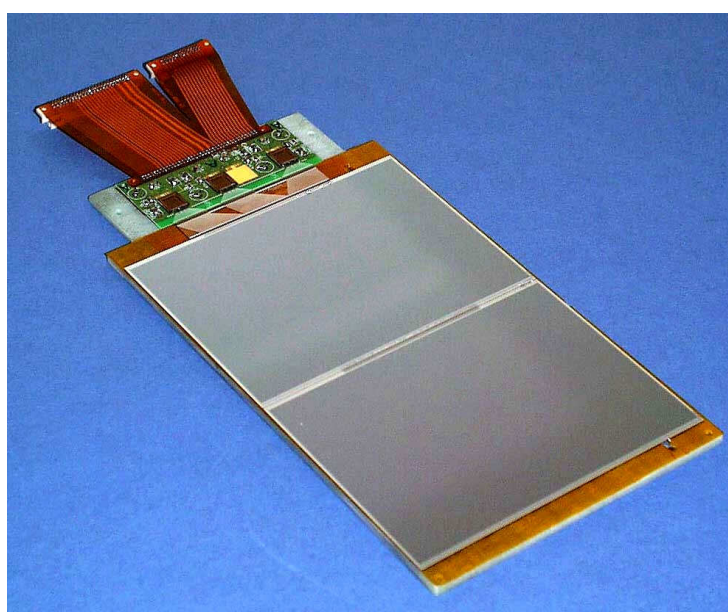


Figure 1.8: A prototype microstrip detector module from the tracker.

1.3.3 The Electronic Calorimeter (ECAL)

The electromagnetic calorimeter (ECAL) will consist of more than 80 000 lead tungstate (PbWO_4) crystals (see figure 1.9). Lead tungstate is extremely dense (more than eight times denser than water), and the whole collection of crystals will weigh more than 90 tonnes [8]. Lead tungstate has a very short radiation length of 0.89 cm, allowing a very compact detector, and a small Moliere radius of 2.19 cm, allowing a fine granularity. It has an interaction length of 22.4 cm, and each crystal has a length of 22 cm [8], so hadrons will on average only interact once in the ECAL.

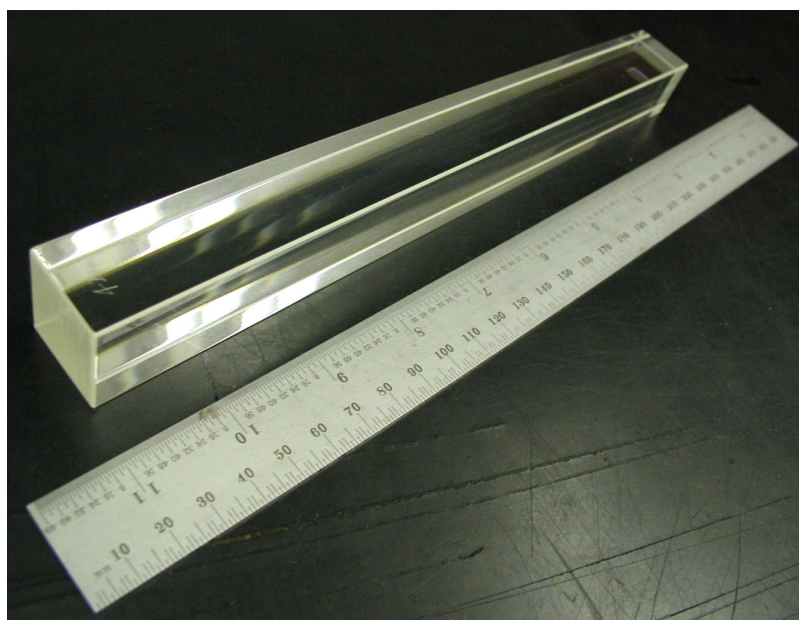


Figure 1.9: An ECAL crystal.

Particles are detected in the ECAL by the scintillation light they produce in the crystals. This is measured by avalanche photodiodes in the barrel section, and by vacuum phototriodes in the endcap regions, where the neutron flux is higher, and the photodiodes would suffer unacceptably high radiation damage. Vacuum phototriodes cannot be used in the barrel region due to the orientation of the magnetic field.

1.3.4 The Hadronic Calorimeter (HCAL)

The combined calorimeter system of CMS will measure the directions and energies of quarks, gluons, and neutrinos indirectly by measuring the direction and energy of particle jets and of the missing transverse energy [9]. Both the barrel and the endcap of the HCAL (see figure 1.10) will experience the 4 Tesla magnetic field of the CMS solenoid, and are therefore constructed from brass and stainless steel, which are non-magnetic. The central hadronic calorimeter consists of 4 mm thick plastic scintillator tiles inserted between copper absorber plates (5 cm thick in the barrel and 8 cm thick in the endcaps). The scintillator tiles are read out using wavelength-shifting plastic fibres. An additional layer of scintillator tiles is located outside of the solenoid to ensure adequate sampling depth for the whole $|\eta| < 3$ region. This is known as the outer hadronic calorimeter. The thickness of the HCAL system varies from 5.15 interaction lengths at $\eta = 0$ up to 5.82 interaction lengths [9].



Figure 1.10: An assembled half-barrel of the HCAL.

The HCAL also includes the forward calorimeter, located 6 m downstream from the HCAL endcaps, and extending the hermeticity of the hadronic calorimeter up to $|\eta| < 5$. It is constructed from quartz fibres embedded in a copper absorber matrix, and is necessary for an accurate measurement of missing transverse energy, and for forward jet detection.

1.3.5 The Muon Detectors

There are three different types of detector used for muons: Resistive Parallel Plate Chambers (RPCs), Drift Tubes (DTs), and Cathode Strip Chambers (CSCs). Together they measure the transverse momentum of the muons with an accuracy of better than 4 % up to $|\eta| < 2$, for muons with a typical energy of 100 GeV [10].

Drift Tubes

The drift tubes are located in the central barrel region of the detector, where the magnetic field is guided and almost fully trapped by the iron plates of the magnet yoke. They are located in four layers, or stations; two on the inner and outer face of the iron yoke, and two in slots inside it. The redundancy provided by four stations of twelve planes each means it is possible to cope with inefficiencies from dead zones caused by supporting ribs and longitudinal space caused by the joints between the rings of the CMS detector.

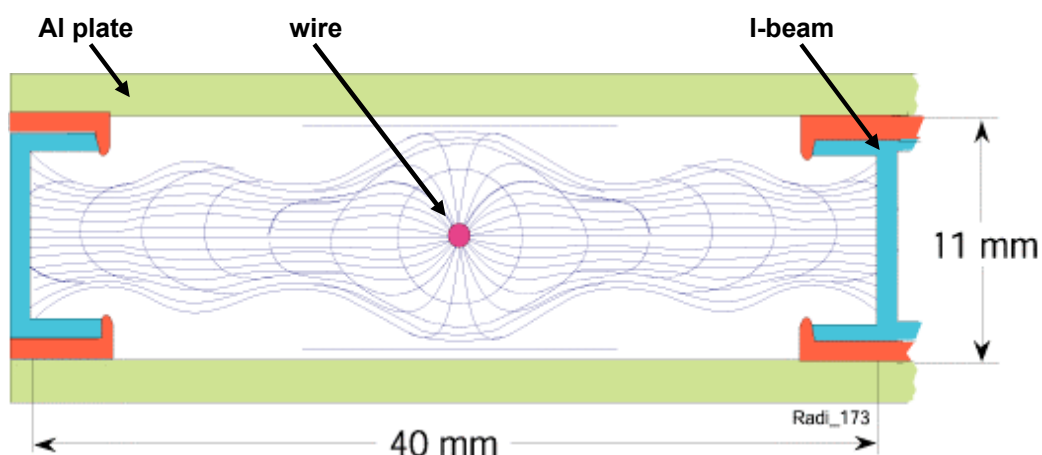


Figure 1.11: A Muon drift tube.

A diagram of a drift tube is shown in figure 1.11. It consists of parallel aluminium plates separated by aluminium I-beams, with a wire stretched along the centre. When an ionising particle passes through the tube, it liberates electrons, which then drift along the electric field lines towards the positively charged wire. The time taken for the ionisation electrons to drift to the wire is measured to within an accuracy of 1 ns, and as the drift velocity of the electrons is known, this gives a good measure of the distance of the original particle from the wire.

Cathode Strip Chambers

The cathode strip chambers (CSCs) are located in the endcap regions of the detector, where the magnetic field is vertical and contained within the iron yoke disks. There are four layers of CSCs sandwiched between the iron disks of the return yoke.

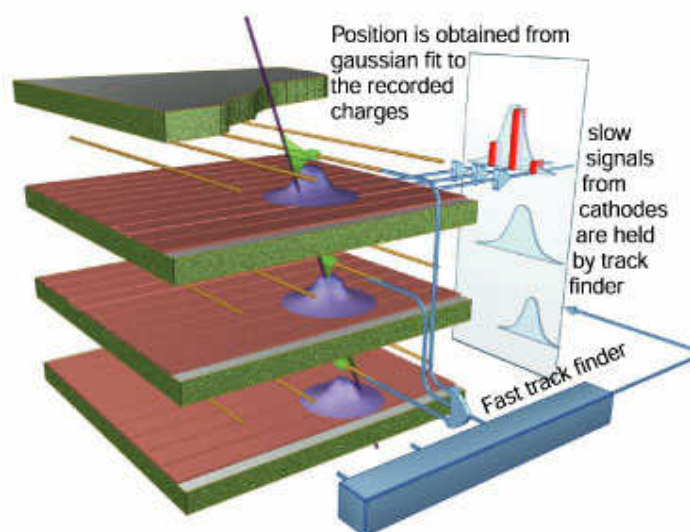


Figure 1.12: A Muon cathode strip chamber.

A CSC (see figure 1.12) consists of cathode planes segmented into strips, and interleaved with wires running perpendicular to the strips. A passing particle ionises atoms, and the freed electrons are collected by the wires, while the positive ions drift to the strips. This gives two coordinates, the wires measuring the radial coordinate, while the strips measure ϕ . The close spacing of the wires make the CSC a fast detector, particularly suitable for triggering.

Resistive Parallel Plate Chambers

The Resistive Plate Chambers (RPCs) are used in both the barrel and the endcap regions of the detector, and are used to provide an additional complementary trigger. They will cover approximately the same area as the DTs and CSCs, but will provide a faster timing signal and have a different sensitivity to background.

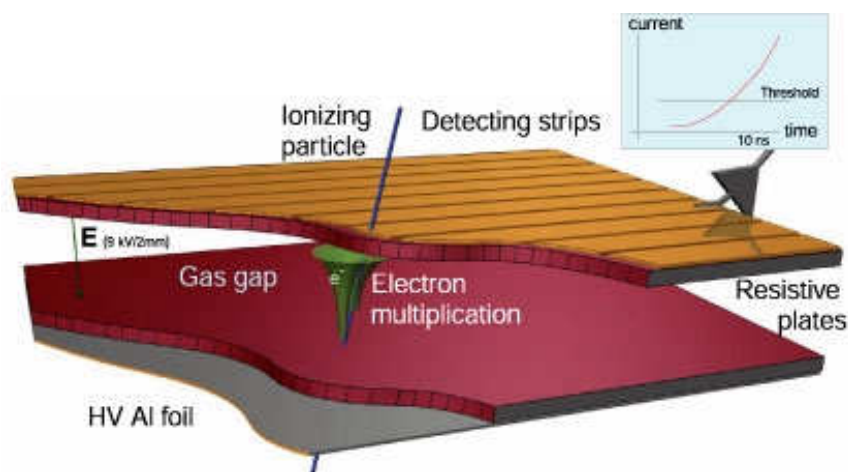


Figure 1.13: A Muon resistive plate chamber.

An RPC is shown in figure 1.13. It consists of two parallel plates of high-resistivity plastic material, separating a thin gap filled with gas. A passing ionising particle releases electrons, which accelerate towards the positively charged side of the chamber in an avalanche. The plastic is transparent to these electrical signals, which are then picked up by external metallic strips.

The signals from each of the three types of muon detectors proceed in parallel to the trigger logic. Every muon with enough energy to penetrate the detector material should traverse at least three of the muon stations.

1.3.6 The Trigger

In normal operation, the global trigger processor receives data from the calorimeters and the muon chambers. It can also use special signals for set-up, synchronisation, calibration and testing purposes. It contains logic for processing up to 128 different trigger algorithms in parallel, the results being delivered as a

128-bit word, with one bit per algorithm. This can be compared with a predefined input word that selects which particular triggers are of interest for the run.

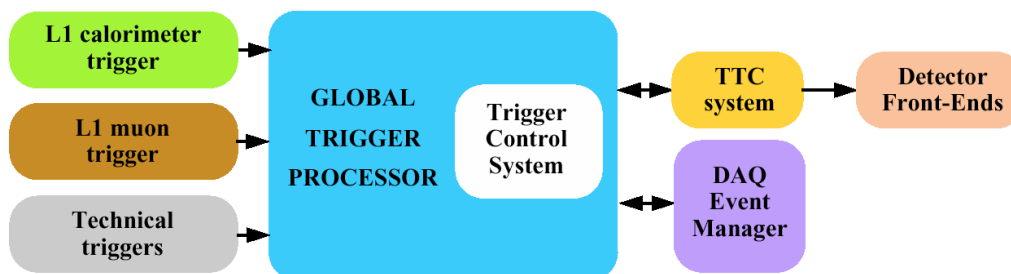


Figure 1.14: The CMS level-1 global trigger.

(Adapted from ref [11])

The level-1 accept trigger decision (L1A), along with the 40.08 MHz LHC machine clock, and other signals, such as bunch-crossing reset are distributed to the detector by the TTC system. The data for each 25 ns bunch-crossing period are stored in the detector front-end until the trigger decision is known. This period, known as the trigger latency, will be about 3 μ s.

1.4 Summary

The CMS detector and its readout system need to process huge volumes of data, and reduce it to a manageable amount before it can be stored and properly analysed. The LHC, at its full luminosity, will generate 20 interactions with a significant transverse energy for every bunch crossing, at a rate of 40.08 MHz. The first level trigger will reduce this to a rate of up to 100 kHz, with the raw data for each event being about 1 Mbyte. This means that the readout system still needs to process about 100 Gbyte of data every second. The tracker consists of about 10 million detector channels, and is expected to generate up to 70 % of the final data volume at CMS. These data rates are orders of magnitude higher than in any previous experiment and demand state-of-the-art technology as well as massively parallel processing if the experiment is to be successful.

Chapter 2: Field Programmable Devices

All digital logic circuits are made up of simple building blocks known as logic gates, which are in turn made of transistors. Two main technologies exist, known as transistor-transistor logic (TTL) and complementary metal oxide semiconductor (CMOS).

2.1 Digital Logic

The older of the two, TTL is made of bipolar transistors, which are sandwiches of n- and p-type semiconductor material in either npn or pnp configurations (see figure 2.1). The transistor consists of two p-n junctions, with the thin central section connected to the base terminal, and the two ends connected

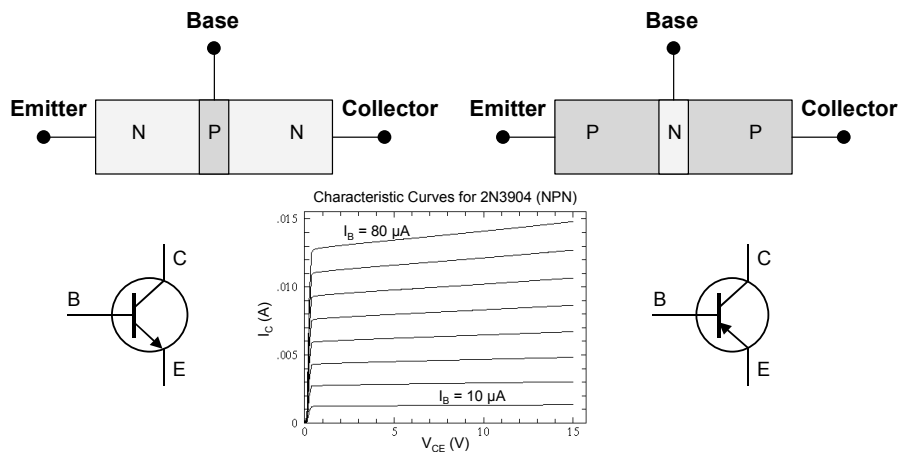


Figure 2.1: Bipolar transistors (nnp and pnp) and their symbols.

to the collector and the emitter. An npn transistor conducts current when its base is pulled high, and a pnp transistor conducts when its base is low. Bipolar transistors are current-amplifying devices: the amount of current flowing into the base controls the amount of current flowing in the collector circuit, but they can also be used in voltage amplification circuits. Bipolar transistors can operate at speeds in excess of a gigahertz, and can be designed to handle large currents up to several amps, but they have a relatively low input impedance of up to about 1 k Ω , and so are not suitable for applications requiring high circuit impedance.

Field effect transistors exist in two main types, Junction Field Effect Transistor (JFET) and Metal Oxide Semiconductor FET (MOSFET). In both types, current flows along a semiconductor channel (n-type or p-type) between the source at one end and the drain at the other. In a JFET, the gate is of the opposite type of semiconductor to the channel, creating a p-n junction (see figure 2.2). A DC voltage is connected to the gate so that the junction is normally reverse-biased, although under certain conditions a small current can flow during part of the signal cycle.

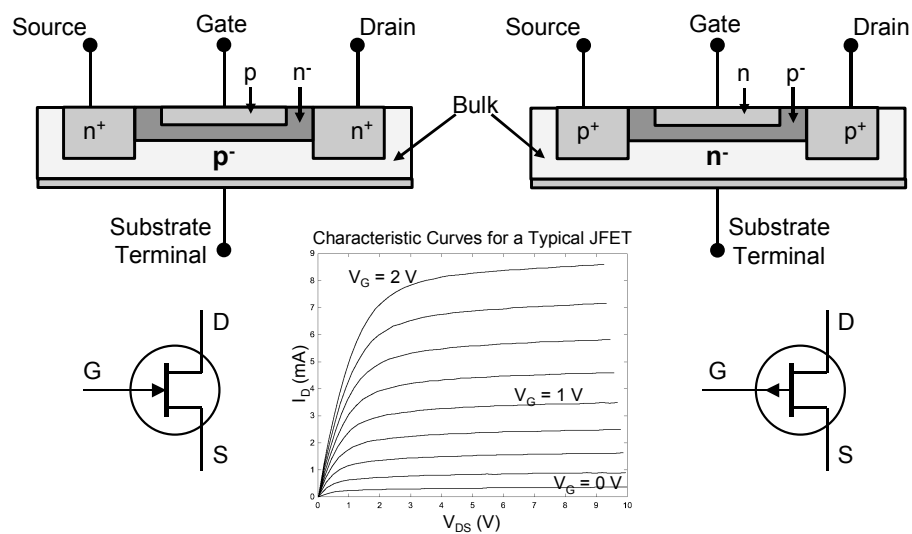


Figure 2.2: JFET transistors (n-channel and p-channel) and their symbols.

In MOSFETs the gate electrode is a piece of metal, separated from the semiconductor by a layer of oxidised silicon (see figure 2.3). This gate oxide acts as a dielectric and electrically insulates the gate from the junction. Because of this, the MOSFET has a very high input impedance of several megohms, and virtually no current flows during any part of the input cycle. However, the oxide layer is very thin, and is susceptible to damage from electrostatic discharge, so special precautions are necessary when handling MOS devices. A p-channel FET conducts when the gate voltage is low, and an n-channel FET conducts when the gate voltage is high.

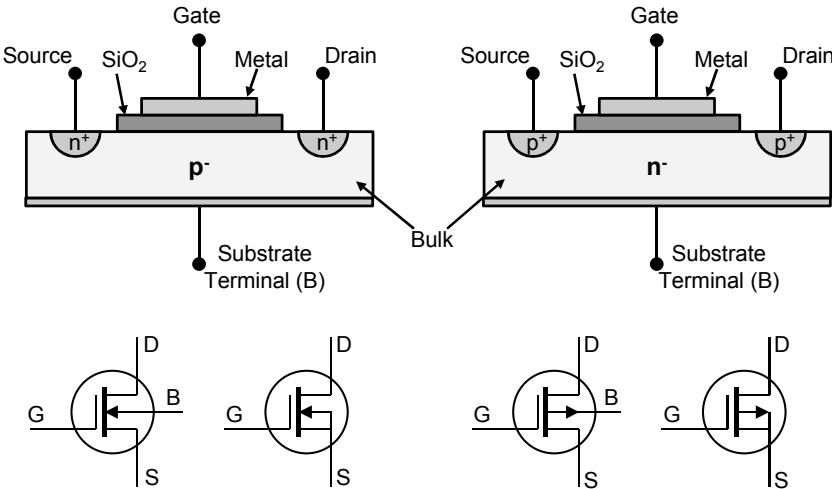


Figure 2.3: MOSFET transistors (n-channel and p-channel) and their symbols.

The dominant semiconductor technology is CMOS, which uses a combination of both n-channel and p-channel MOSFETS. The main advantage is its very low static power consumption; power is only dissipated when the circuit switches, allowing many gates to be integrated into each IC, resulting in higher performance than is possible with bipolar technology.

2.1.1 Combinatorial Logic

A CMOS inverter can be built with only two complementary MOSFET transistors (see figure 2.4). When the input voltage is high, the output is connected

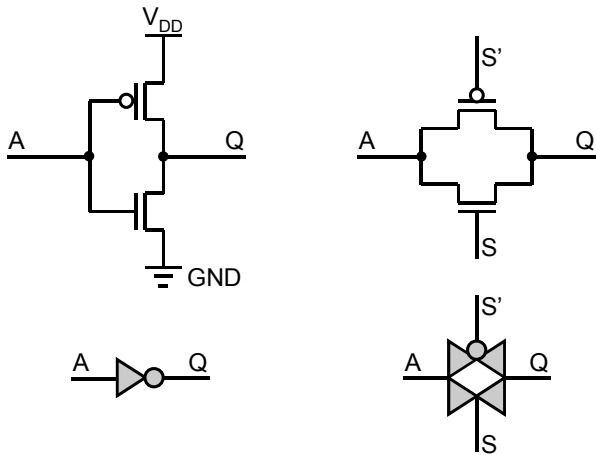


Figure 2.4: A CMOS inverter and transmission gate, and their symbols.

to ground, and when it is low, the output is connected to the drain voltage, V_{DD} (typically 1.8, 2.5, 3.3 or 5V). A transmission gate is used like a switch; when the input S is high (and S' is low), the input A appears at the output Q , and when S is low (and S' is high), the output is in a high impedance state, effectively disconnected.

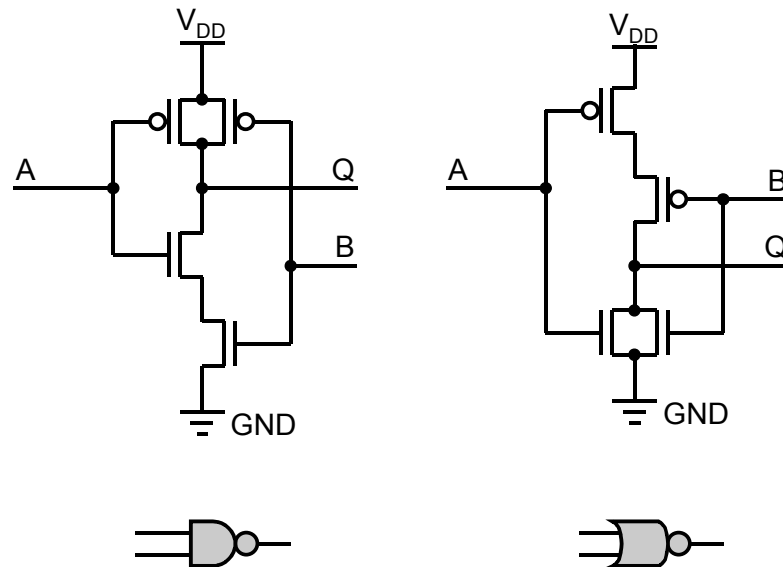


Figure 2.5: CMOS NAND and NOR gates and their symbols.

Two other combinatorial logic gates, the NAND and the NOR, are shown in figure 2.5, along with their truth tables in table 2.1. Other logic gates, such as AND and OR gates can be easily constructed by following the output of a NAND or NOR gate with an inverter.

A	B	Q
0	0	1
0	1	1
1	0	1
1	1	0

A	B	Q
0	0	1
0	1	0
1	0	0
1	1	0

Table 2.1: Truth tables for NAND and NOR gates.

2.1.2 Sequential Logic

In combinatorial logic circuits, the output is a function of only the current inputs. More complex circuits use sequential logic, with memory that is generated by feeding the output of a logic-block back in to the inputs. The output of a sequential logic circuit is a function not only of the current inputs, but also of past inputs. The simplest sequential logic block is the latch (see figure 2.6). When the clock input is high, the output follows the data input, but when the clock input is low, the output retains its current level no matter what appears on the data input. This is known as a level-triggered, or transparent, latch because it is triggered by the level of the clock input. However, most sequential logic is edge-triggered, meaning that the output only takes on the value at the input at the rising edge of the clock. This is achieved using two transparent latches in series, the second triggered by the inverse of the clock, producing what is known as a D-type flip-flop (see figure 2.6).

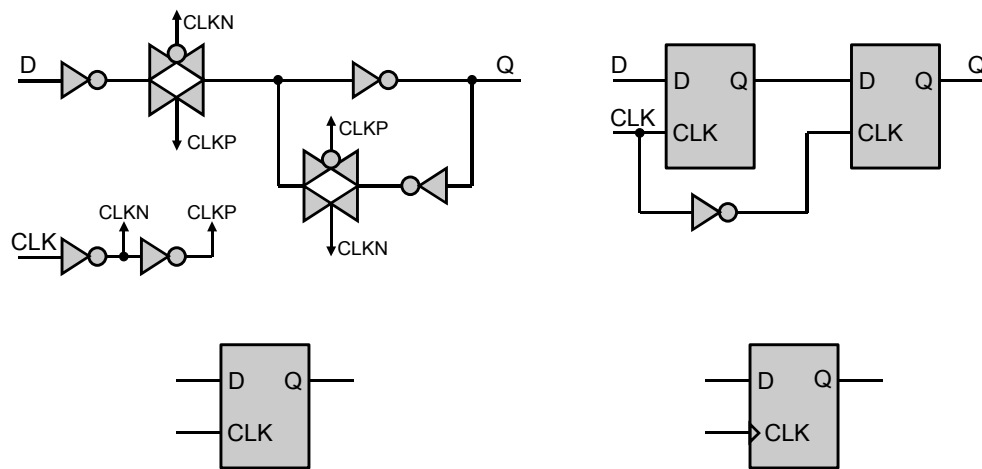


Figure 2.6: CMOS transparent latch and flip-flop and their symbols.

2.2 Programmable Logic

When custom logic devices are needed in a system, there are a number of different options available. Simple circuits can often be built out of discrete logic components, but many systems are more complex, consisting of the equivalent of tens of millions of logic gates, and this quickly becomes unfeasible. Another

option is to use a microprocessor, which offers great flexibility and is functionally very versatile, but due to its inherently serialised processing, for many tasks it is just too slow, when compared to the hugely parallel processing available in a dedicated logic circuit.

Application-specific integrated circuits (ASICs) are made up of successive layers, etched directly onto a silicon wafer using a photographic mask, and offer the highest level of complexity and speed. In full-custom ASICs, all mask layers are customised, and designing a new IC takes a huge amount of time and effort, as each individual transistor needs to be specified. In a standard-cell-based ASIC all layers are also customised, but a library of standard cells are available for higher-level functions, reducing the design effort to some extent. Another type of ASIC technology is the mask-programmable gate array (MPGA), which consists of an array of standard blocks, with only the interconnect layers being customised [12]. This reduces the manufacturing lead-time, but any design changes still require a complete new manufacturing run.

Field programmable logic devices have no custom mask layers or custom logic cells; they are programmed by the user. They have the advantage over custom-designed ASICs that the design and verification process is much faster, and (in technologies which are not one-time programmable) the configuration can be updated at a later time to fix errors, or simply to upgrade the firmware. For small to medium volumes they are also much cheaper. The disadvantage is that all the programming logic takes up space in the chip, leaving less space for the actual design. In a $0.18\mu\text{m}$ process an FPGA typically holds $1500\text{ gates}/\text{mm}^2$ compared to $60\,000\text{ gates}/\text{mm}^2$ for an ASIC, and runs at a maximum clock speed of 100 MHz, compared to 600 MHz in an ASIC. However, the density of these devices is increasing rapidly, and in many situations it is the speed of the input/output logic that limits the amount of processing that can be done, so FPGAs are becoming powerful enough to replace ASICs in more and more situations.

2.3 History of Programmable Logic

2.3.1 The PROM

The first type of user-programmable chip that could implement logic circuits was the PROM [13] (see figure 2.7). The n address lines represent the input to the logic function, the decoder translates each of the 2^n possible combinations to a logic signal on one of 2^n lines, and the m data lines are different functions of the inputs. Filling the memory appropriately allows any arbitrary logic function to be generated [12]. The 2^n lines generated by the decoder are known as product terms, and are logical ANDs of the input lines (or their inverses). If each product term is a function of all of the input lines (or their inverses), as is the case here, then they are known more specifically as minterms, and each will be active for only one possible input combination. Each function is simply a logical OR of all the minterms for which the corresponding bit in the memory is high. This method of representing a logic function is known as a sum of products (SOP).

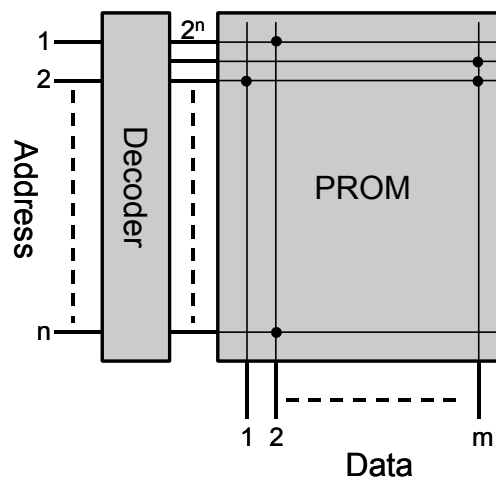


Figure 2.7: Memory used as programmable logic.

(Adapted from ref [13])

2.3.2 The PLA and PAL

Most logic functions require relatively few product terms, while a PROM contains a full decoder for its address inputs (generating all 2^n possible minterms for the n inputs). This makes it an inefficient architecture for implementing logic circuits, as a lot of the logic is never used. A Programmable Logic Array (PLA) is based on the same principle as the PROM device, but without the full decoding of the input variables (see figure 2.8). An array of programmable AND gates provide the product terms, and an array of programmable OR gates provide the sum of products. The number of product terms available is less than the total number of minterms (in this case 2 instead of 4), but most logic functions can be rewritten to use fewer product terms (e.g. using Karnaugh maps) and made to fit.

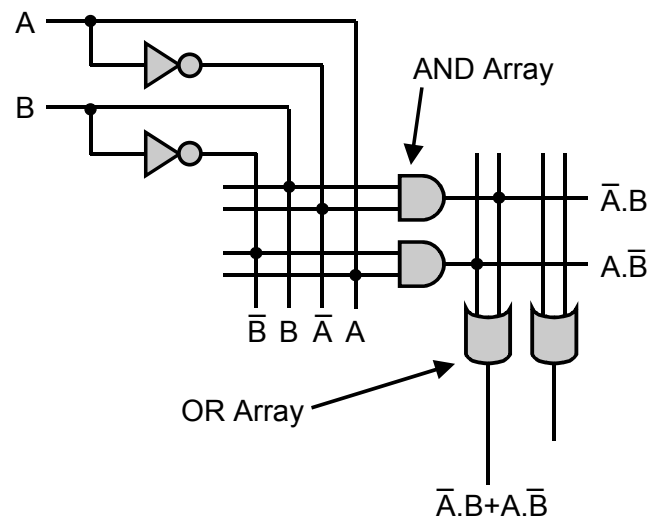


Figure 2.8: A very small PLA.

(Adapted from ref [13])

The two levels of configurable logic in a PLA make it relatively expensive to manufacture, and also affect the speed performance [12]. To overcome this, Programmable Array Logic (PAL[®]) devices were developed. They are similar to PLAs; with the OR array being fixed instead of programmable, and a number of improvements. The outputs of the OR gates are fed back to the inputs of the AND array, allowing a reduction in the number of terms in some functions at the expense of speed. At the outputs of the OR gates there are flip-flops, also with

their outputs fed back to the inputs of the AND array, allowing more complex systems to be built, such as state machines. The I/O pins are programmable, with tri-state outputs, allowing them to be used for input, output, or bi-directional signals.

2.3.3 The CPLD

Small programmable devices, including PLAs and PALs, are known collectively as Simple Programmable Logic Devices (SPLDs). As technology advanced, the capacity of SPLDs grew; but with these architectures, the structure of the logic planes grows very quickly as the number of inputs is increased, so the logic becomes less efficiently used. To get around this, Complex Programmable Logic Devices (CPLDs) were developed. These are effectively arrays of PAL-like blocks (known as macrocells) connected together with a programmable interconnect (see figure 2.9).

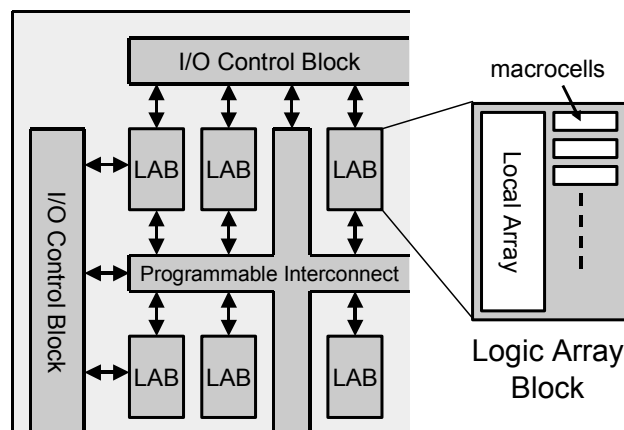


Figure 2.9: Architecture of a CPLD.

(Adapted from ref [13])

Blocks of 8 to 16 macrocells are grouped together with other logic into function blocks, or Logic Array Blocks (LABs), with the macrocells within each function block usually being fully interconnected [13]. Often the function blocks themselves will only be partially interconnected, as it makes the manufacturing process cheaper, but it means that complex designs will be harder to route, and design changes may force the pin layout to be changed. It also has the effect that

the delays between the function blocks are not fixed, whereas with full interconnect the delays are fixed and predictable.

CPLDs are generally CMOS devices, and use non-volatile memory cells (usually EEPROM or FLASH) to define their functionality. Typically, they are in-system programmable (ISP), meaning they can be programmed in-circuit, as opposed to needing to be plugged into a special CPLD-programming unit.

2.3.4 The FPGA

The architecture of CPLDs makes it difficult to increase the capacity beyond the equivalent of about 50 SPLD devices. The highest capacity devices, Field Programmable Gate Arrays (FPGAs), are based on a different architecture, similar to MPGAs. They are made up of an array of up to about 100 000 configurable logic blocks (CLBs), surrounded by programmable I/O blocks, and connected by a programmable interconnect network (see figure 2.10). The blocks are not fully interconnected, but sophisticated software is used to route the logic.

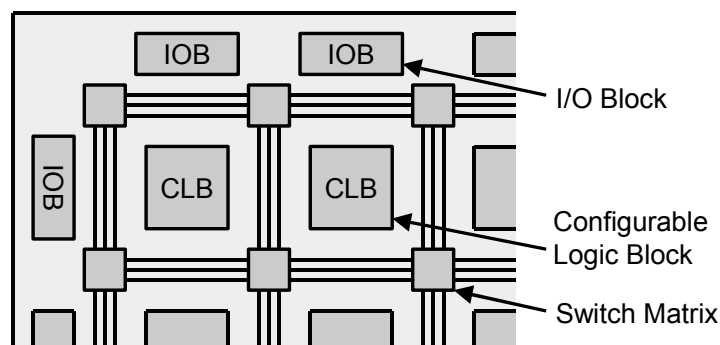


Figure 2.10: Architecture of an FPGA.

(Adapted from ref [13])

FPGAs can be either coarse-grained or fine-grained. Coarse-grained FPGAs contain large logic blocks containing two or more look-up tables, two or more flip-flops, and other logic such as multiplexers and fast-carry logic. Fine-grained FPGAs, on the other hand, contain a large number of simple logic blocks containing either a 2-input logic function or 4-to-1 multiplexer, and a flip-flop. They make more efficient use of the active components, but require greater

routing resources, and are generally slower and less dense. An example (from a Plessey device) is shown in figure 2.11.

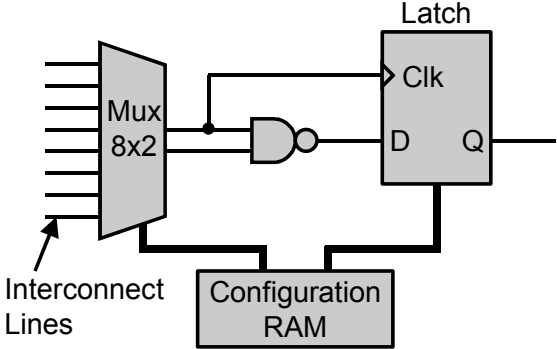


Figure 2.11: Example of a fine-grained logic cell.
(Adapted from ref [13])

2.4 Memory Technology

2.4.1 Fuses and Antifuses

Field programmable devices are programmed after the manufacturing process, and the configuration has to be stored in some form of memory. There are several technologies available for this, each with its own advantages and disadvantages. The original technology used was fuse technology. A metal link creates a normally closed connection, and the device is programmed by passing a relatively large current through the fuse, melting it and opening the connection.

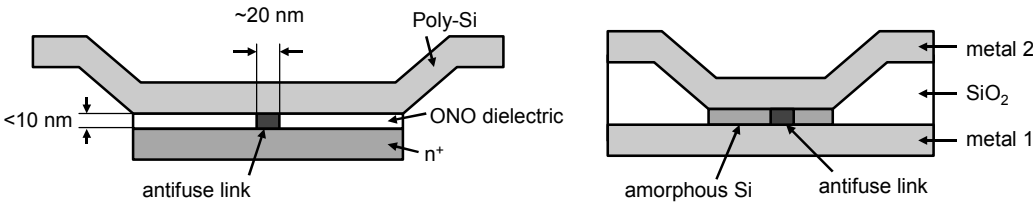


Figure 2.12: Antifuses: (a) ONO, (b) amorphous silicon.
(Adapted from ref [13])

A variation of this is antifuse technology; it is now much more widely employed as it uses a modified CMOS technology. An oxide-nitride-oxide (ONO) antifuse (see figure 2.12a) consists of an insulating ONO layer sandwiched between conductive polysilicon and n^+ diffusion layers [13, 14]. The device is programmed by applying a current of 5-15 mA, causing the thin dielectric to melt, and form a small antifuse link with a typical resistance of about 500Ω , and allowing current to flow through the device. The amorphous silicon (or metal-metal) antifuse (see figure 2.12b) is similar to the ONO variety, with the advantages that the connections are made directly to metal; they have a lower programmed resistance (typically about 80Ω), and have less parasitic capacitance. Antifuses are small and radiation hard, but they are slow to program, cannot be reprogrammed, and their properties can vary over time, creating reliability issues.

2.4.2 The EPROM and EEPROM

Another technology used is the EPROM, which is only slightly larger than an antifuse. It is similar to a standard n-channel MOSFET, with an extra *floating gate* (see figure 2.13a). In normal operation, the floating gate has no charge and the field effect transistor can be switched on or off by the gate voltage. To

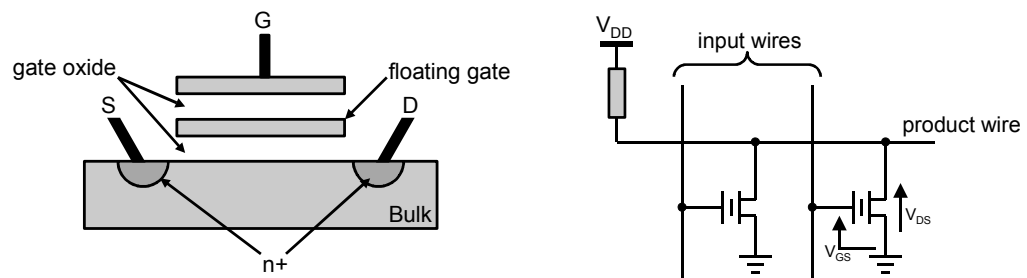


Figure 2.13: An EPROM memory cell: a) schematic, b) use in wired-AND.

(Adapted from ref [13] (a) and ref [12] (b))

program the device, V_{DS} is set to a large voltage (~ 12 V) creating energetic, or hot, electrons in the bulk. The gate voltage V_{GS} is set to a positive voltage, attracting some of the electrons, which tunnel through the gate oxide and are trapped in the floating gate, producing a negative charge. This increases the threshold voltage

enough so that the transistor is then permanently switched off, even with a positive gate voltage up to V_{DD} . An EPROM cell can be used in a programmable AND-plane (see figure 2.13b) where each input wire is connected to a separate EPROM cell and can be disabled by programming the relevant cell. If the device is built with a UV-transparent window, it can be erased by being exposed to UV light. This gives the trapped electrons enough energy to return to the substrate, therefore erasing the program; although it requires about an hour of exposure before the device is completely erased, and cannot be done in-circuit.

An EEPROM (or E²PROM) is similar to an EPROM, but uses an electric field to remove the trapped electrons, allowing this to be done in-circuit. Because of this, the cells are generally about twice as large as those in an EPROM. Some newer devices use FLASH memory, which is a type of EEPROM, but the electric field is applied to large areas of the memory at once so the erase time is much shorter, and the cells are smaller, being only slightly larger than in an EPROM.

2.4.3 SRAM

Many devices use static RAM (SRAM) technology (see figure 2.14). SRAM cells are relatively large, and are volatile, so any program will be lost when the power is removed. However, most SRAM devices are in-system programmable, and are designed to automatically boot at power-up from a PROM, which typically takes no more than a few hundred milliseconds. SRAM is widely used in FPGAs, where the function generators are often implemented as look-up tables. In this way, the tables can be made writeable and therefore used as memory blocks as well as function generators.

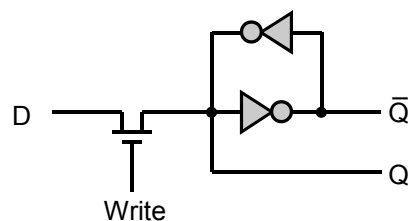


Figure 2.14: An SRAM memory cell.
(Adapted from refs [13, 15])

Static RAM is relatively expensive to produce, and a cheaper alternative, often used in computers, is dynamic RAM (DRAM). In DRAM, memory bits are stored on capacitors, and accessed through a transistor. However, the charge on the individual capacitors has a tendency to leak away, so DRAM has to be regularly refreshed every 50 ms or so. Because of this, DRAM is not suitable for use in programmable logic devices, since all the configuration data must be constantly available.

A summary of the different memory technologies and their main properties is given in table 2.2.

Name	Re-programmable	Volatile	Resistance (Ω)	Capacitance (fF)	Technology
Fuse	No	No	(Data not available)		Bipolar
Antifuse (ONO)	No	No	300-600	5	CMOS+
Antifuse (a-Si)	No	No	50-100	1.2	CMOS+
EPROM	Yes (out of circuit)	No	2k-4k	10-20	UVC MOS
EEPROM	Yes (in-circuit)	No	2k-4k	10-20	EECMOS
SRAM	Yes (in-circuit)	Yes	500-2k	10-20	CMOS

Table 2.2: Summary of Programming Technologies.

(Adapted from refs [12, 13])

2.5 The Xilinx Virtex-II Range of FPGAs

The Virtex-II range of FPGAs from Xilinx[®] is based on the previous Virtex and Virtex-E families, with sizes ranging from 40 K to 8 M system gates. It is SRAM based, and built on 0.15 μm technology, allowing clock speeds in excess of 300 MHz. The general layout consists of an array of configurable logic surrounded by programmable I/O (see figure 2.15). The configurable logic consists mainly of configurable logic blocks (CLBs, described in section 2.5.1), with some of the columns (from 2 to 6 depending on the size of the device) containing 18-kbit block RAMs and 18-by-18-bit multipliers in place of the CLBs, and a digital clock manager at the top and bottom of the column [16].

[®] The Xilinx name is a registered trademark. Virtex, Virtex-E and Virtex-II are trademarks of Xilinx Inc.

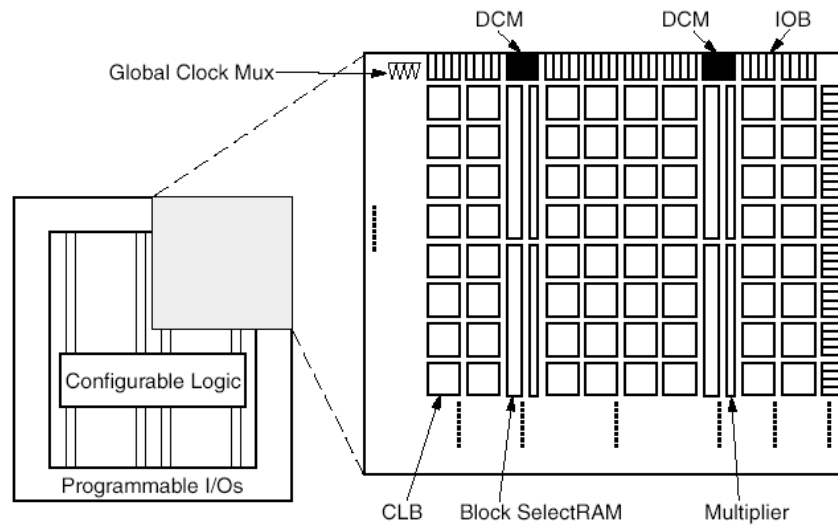


Figure 2.15: Xilinx Virtex-II Architecture.

(From ref [16])

The differences between the members of the Xilinx Virtex-II family are shown in table 2.3. The devices are named by their size, expressed in thousands of system gates (the number of NAND-gates needed to build an equivalent design in discrete logic), preceded by XC2V (Xilinx Virtex II). The table gives the width and height of the array of CLBs, and the number of slices (4 times the number of CLBs). Then the number of multipliers and block-RAMs are given (the same since they are paired together) and the total size of the block-RAMs (18 kbits times the number of BRAMs) followed by the number of Digital Clock Manager blocks, the number of tri-state buffers, and the maximum number of I/O blocks (which may be less, depending on the type of package). Finally the table gives the number of bits needed to configure the device.

Device	CLB Array	Slices	Multipliers/ BRAMs	BRAM (kbits)	DCMs	3-State Buffers	Max. IOBs	Config. Bits
XC2V40	8 x 8	256	4	72	4	128	88	338 208
XC2V80	16 x 8	512	8	144	4	256	120	597 408
XC2V250	24 x 16	1 536	24	432	8	768	200	1 591 584
XC2V500	32 x 24	3 072	32	576	8	1 536	264	2 557 856
XC2V1000	40 x 32	5 120	40	720	8	2 560	432	3 749 408
XC2V1500	48 x 40	7 680	48	864	8	3 840	528	5 166 240
XC2V2000	56 x 48	10 752	56	1 008	8	5 376	624	6 808 352
XC2V3000	64 x 56	14 336	96	1 728	12	7 168	720	9 589 408
XC2V4000	80 x 72	23 040	120	2 160	12	11 520	912	14 220 192
XC2V6000	96 x 88	33 792	144	2 592	12	16 896	1 104	19 752 096
XC2V8000	112 x 104	46 592	168	3 024	12	23 296	1 108	26 185 120
XC2V10000	128 x 120	61 440	192	3 456	12	30 720	1 108	33 519 264

Table 2.3: Virtex-II family members.

(Adapted from ref [17])

2.5.1 Logic Blocks

In the Xilinx Virtex-II FPGA family, each CLB contains four similar slices (see figure 2.16a) arranged in two columns with separate carry chains (used for implementing arithmetic functions and sum of products logic) and a single shift chain (used for implementing shift registers). There are also two tristate buffers

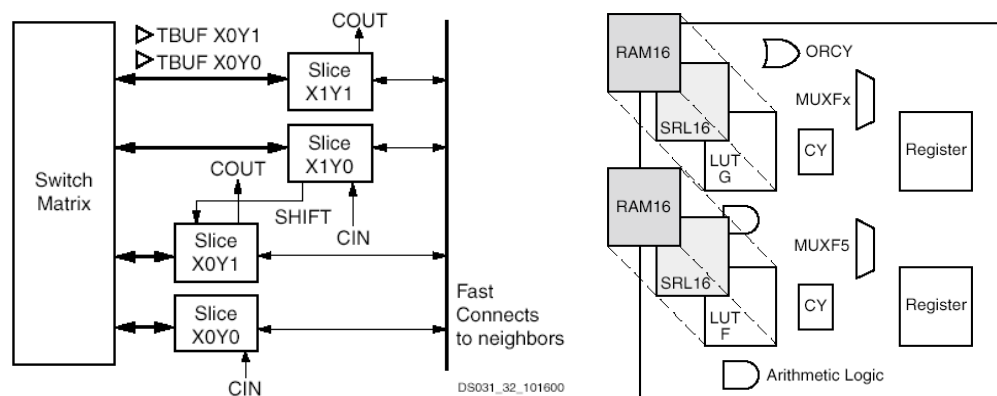


Figure 2.16: Virtex-II logic blocks: (a) CLB, (b) slice.

(From ref [17])

which are accessible to any of the slices via the switch matrix [17]. Each slice (see figure 2.16b) contains:

- Two independent function generators, implemented as 4-input look-up tables (LUT F and G), which can be reconfigured as 16x1-bit RAMs (RAM16) or 16-bit variable-tap shift registers (SRL16). If used as RAM, the look-up tables in a CLB can be combined into a larger memory blocks, from 16x8-bit to 128x1-bit. When used as shift-registers, the slices can be combined into one long 128-bit shift-register with dynamic access to any bit in the chain.
- Multiplexers (MUXF5 and MUXFx) to combine the outputs of the function generators and produce functions with larger numbers of inputs. Along with the function generators, MUXF5 can generate functions of five inputs, and MUXFx can generate functions of 6, 7 or 8 inputs, depending on the slice in the CLB.
- Logic for building fast carry chains (CY), used to build efficient addition and subtraction logic.
- A dedicated OR gate (ORCY) connecting carry logic with the output of the corresponding ORCY in the adjacent slice, allowing easy production of large sum of products chains.
- Logic for other arithmetic functions, such as efficient multiplier implementations.
- Two registers, configurable as either edge-triggered D-type flip-flops, or as level-sensitive latches.

Depending on its size, each Virtex-II FPGA can have between 64 and 11 648 CLBs. On top of that, it can have up to 168 18-kbit dual-port block RAMs. Each port of each block RAM can be individually configured for various widths (see table 2.4). In the 9, 18 and 36-bit widths the full 18 kbits are accessible with one bit per byte available for parity or for any other use. In the narrower configurations, the parity bits are not available and only 16 kbits are accessible.

Width (bits)	Depth (bits)	Addressable bits
36	512	18 k
18	1 k	18 k
9	2 k	18 k
4	4 k	16 k
2	8 k	16 k
1	16 k	16 k

Table 2.4: Virtex-II block-RAM configurations.

(Adapted from ref [17])

Associated with each block-RAM is an 18-bit twos-complement signed multiplier. The switch matrix is optimised to feed one input from an 18-bit wide block RAM, although they can be used separately. This is because many digital signal-processing applications use a multiplier-accumulator function for finite and infinite impulse response (FIR and IIR) digital filters.

Each FPGA has 16 clock inputs, and a number of global clock buffers used to distribute the clocks to the synchronous logic elements. There are also up to 12 Digital Clock Managers (DCMs), which are based on delay-locked loops (DLLs). Unlike phase-locked loops (PLLs) they are completely digital, meaning they are less affected by temperature and supply voltage variations. However, PLLs generally have lower jitter, as they tend to filter out higher frequency components. The DCMs are used to de-skew the clock signals, ensuring that they remain in phase over the whole device, and perform clock multiplication and division, generating a wide range of clock frequencies from a single clock source.

2.5.2 I/O Blocks

Connections to the outside world are made through programmable input/output blocks (IOBs). Each pin can be an input, an output, or bi-directional, and neighbouring pairs of IOBs can be combined to provide differential signalling [17]. Groups of IOBs are organised into eight banks (see figure 2.17a), each of which can operate at a range of voltages from 1.2 to 3.3 Volts, independently of the core voltage of 1.5 V; this allows a number of I/O signalling standards to be supported while maintaining a low core voltage. The increasing

density of FPGAs means that there is little space for termination resistors, especially with ball grid array packages. To help with this, each bank contains a digitally controlled impedance system, where a single pair of resistors provides a reference to set the series and/or parallel termination resistance of the entire bank.

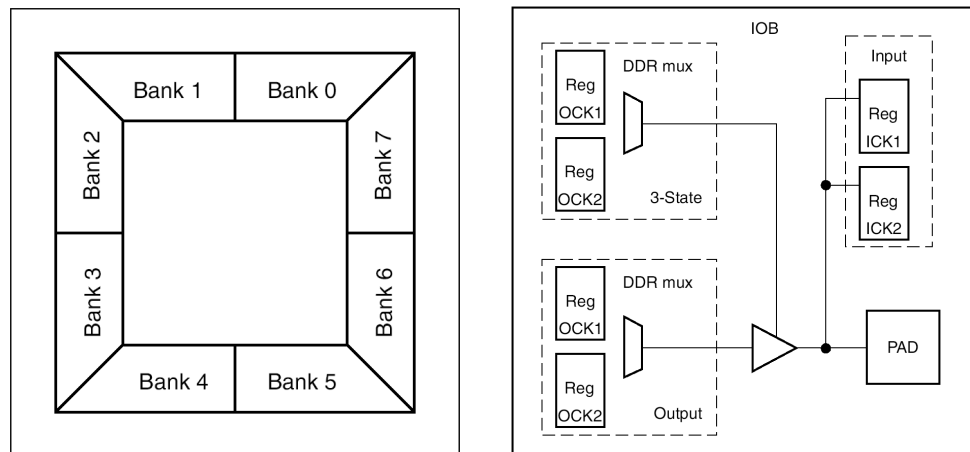


Figure 2.17: (a) I/O banks in Virtex-II flip-chip packages, (b) an I/O block.

(From ref [17])

Each IOB (see figure 2.17b) contains six registers, each of which can be configured as an edge-triggered D-type flip-flop or as a level-sensitive latch. Each path (input, output, and 3-state) contains two of these registers, allowing double data rate (DDR) input/output signals by clocking each register 180° out of phase with respect to the other.

2.5.3 Routing Resources

On top of the blocks mentioned, there are a number of local and global routing resources used to connect the blocks together and distribute signals across the device. Unlike previous architectures, the Virtex-II uses Active Interconnect technology, where the signals are fully buffered at each routing interconnect point. This means that signal delays are more precisely controlled and reasonably

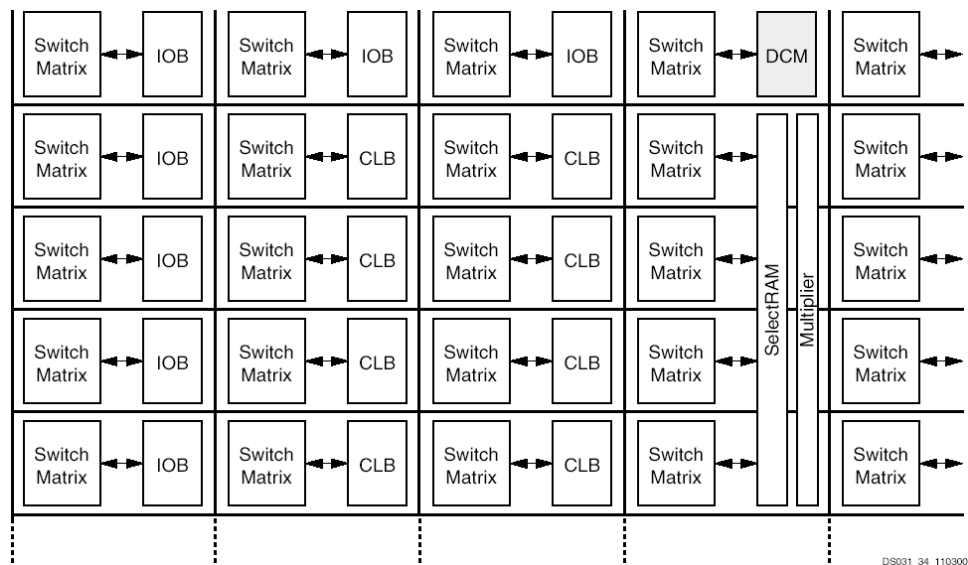


Figure 2.18: Virtex-II routing resources.

(From ref [17])

independent of signal fan-out, making it easier to route complex designs [17]. Each CLB, DCM and IOB is connected to a switch matrix, and each block RAM and multiplier share four switch matrices between them (see figure 2.18). Each switch matrix provides eight fast connections from the outputs of the associated block back to the inputs, and 16 direct connections to the eight neighbouring blocks. There are 40 horizontal and 40 vertical *double lines* providing connections to every first or second block away in all four directions, and 120 horizontal and 120 vertical *hex lines* providing connections to every third or sixth block. Finally there are 24 horizontal and 24 vertical *long lines* which are bi-directional wires spanning the width and height of the device. In addition to these routing resources

there are a number of dedicated signals such as the global clock nets, and the shift and carry chains.

The routing resources are segmented, allowing designs to be compiled hierarchically, i.e. small modules of the design can be compiled independently, and then moved around the device without affecting their internal timing characteristics. This allows faster compile times, and also permits the portable use of IP cores, which are precompiled modules that can be incorporated into designs and are available from both the device manufacturer and from other companies.

2.6 The Design Process

There are several steps to programming an FPGA (see figure 2.19) and a number of tools available for this.

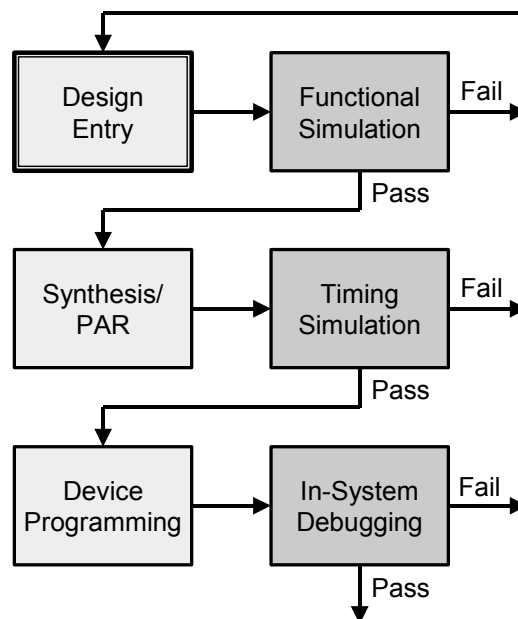


Figure 2.19: The FPGA Design Process.

2.6.1 Design Entry

The first step is the design entry. This can be done in either schematic form, using a hardware description language (HDL) such as VHDL or Verilog, or more often, using a combination of schematics and HDL. Schematics allow more control over the specific blocks used in the device, and their physical placement,

although for complex designs this is also more time-consuming. Language-based tools, on the other hand, allow quick design entry, especially for more sophisticated designs. In the past, this was often at the expense of lower performance or density; but logic synthesis tools have significantly improved over recent years, and are becoming better at inferring the correct blocks to use for different language constructs. Language-based tools also permit a higher level of abstraction, making designs easier to port to different devices, but they also pose dangers. For example, if a conditional statement (e.g. *if* or *case*) does not take into account all possible input states, it will be assumed that the output should remain unchanged in these cases. This implies memory (the signal must remember its previous value) and therefore a latch is needed. This is useful if a latch is actually required, but can often be unintentional, leading to code bloat (redundant logic that increases the size of a design without adding any functionality).

Libraries are available from the hardware vendors for blocks that cannot easily be inferred from an HDL. For example, in the Virtex-II, RAM is available in several block-RAMS, as well as distributed-RAM made from combining groups of look-up tables to generate larger RAM structures. By using an array of signals, the synthesis tools are able to infer that RAM is needed, but it is not obvious whether block-RAM or distributed-RAM should be used. If a block-RAM is needed (in order to conserve logic blocks for other functions), it is often better to use a block from the Xilinx-specific library and force the synthesis tools to use the correct type of RAM. This means that the design will not synthesise into devices which do not have the same block-RAMs, and for this reason it is nearly always necessary to decide on which family of FPGAs to use, before starting a design.

Many chip vendors also supply *cores*, which are common design building blocks, from distributed-RAM to PCI-bus interfaces and even microprocessors, implemented in programmable-logic elements. Some simpler cores are available free, whereas cores that are more complex generally have to be bought. They help to speed the development of logic systems, and are becoming an increasingly important design entry tool as FPGAs become denser and can implement ever-more complex designs.

There are two industry standard hardware description languages available: *VHDL* and *Verilog HDL* (usually referred to simply as Verilog). Both were originally designed for describing (and hence simulating) hardware, as opposed to design entry, and because of this, they allow certain constructs that it is not possible to synthesise. However, this is not considered a problem, as in any case different types of hardware have different capabilities, and there will always be constructs that cannot be synthesised in certain types of hardware. There are two main aspects to modelling hardware that HDLs facilitate: true abstract behaviour, and hardware structure. The hardware structure aspect (known as register transfer level, or RTL) is used to describe hardware in terms of registers and the logic joining them together, and is the most easily synthesizable. The true abstract behaviour is useful for higher-level descriptions of hardware systems, and for testing designs, where the test-bench will not be synthesised, and is therefore not described in terms of hardware. These aspects are harder to synthesise, and allow some constructs which are impossible to synthesise, although synthesis tools are getting better at understanding and synthesizing these higher-level descriptions.

2.6.2 Verilog

Verilog was designed in 1984 by the company Gateway Design Automation as an interpreted language for their logic simulator Verilog-XL [18, 19]. It takes features from HiLo, which was a popular HDL at the time, and the programming languages C and ADA. Verilog became popular after 1988, when Synopsis produced the first logic synthesiser using Verilog HDL as an input. Cadence Design Systems acquired Gateway Design Automation in 1989 and put the language in the public domain, where it is now maintained by the non-profit organisation Open Verilog International (OVI), which took the language through the IEEE standardisation procedure. In December 1995, Verilog HDL became IEEE standard 1364-1995, which is currently under review, with the purpose of adding analogue extensions.

2.6.3 VHDL

VHDL began life in 1981, when it was designed by the United States Department of Defence [18, 20]. From the beginning, it was designed as a

standard language, with participation being sought from industry, and the baseline language being published two years before standardization was complete, so that tool development could begin. In 1986, the rights to the language were given to the IEEE, in order to encourage industry acceptance and investment, and in 1987, IEEE standard 1076 was published. The standard is regularly reviewed, and the latest version for which tools are widely available is VHDL '93.

In terms of capabilities, VHDL and Verilog are very similar, and it is more a matter of personal preference and tool availability, than actual technical capability, as to which language should be chosen for a particular project. Nevertheless, VHDL does have more features useful in larger projects, such as libraries and packages, which facilitate code partitioning and design reusability; these are lacking in Verilog due to its roots as an interpreted as opposed to compiled language. However, Verilog is slightly better suited to low-level gate descriptions of hardware.

Data types in Verilog are very simple and are all defined by the language. VHDL allows a multitude of user-defined data types, which when used carefully can make models easier to write and clearer to read, but can also easily lead to clutter and confusion. VHDL is more strongly typed, meaning that there are strict rules about what types of variables can be used together, for example a variable of type *time* cannot be assigned to a variable of type *bit*, but the result of dividing a variable of type *length* by type *time* could be assigned to a variable of type *speed*. This means that many errors are caught at compile-time which in Verilog would not be caught until later, but this also means that VHDL is more verbose, with equivalent code usually being longer in VHDL than in Verilog.

Some design tools, for example Mentor Graphics[®] HDL Designer, allow design entry in other formats such as truth tables, flow charts, and finite-state machines. The design tools will automatically generate VHDL or Verilog code for these blocks, which is then compiled or synthesised like other HDL files.

[®] The Mentor Graphics name is a registered trademark. HDL Designer is a trademark of Mentor Graphics Corp.

2.6.4 Simulation and Synthesis

Throughout the process of entering a design, in HDL and/or schematic form, it is periodically compiled into a machine-dependent form, for simulation. Simulation packages allow the values of variables and signals to be monitored, and simulation time to be paused at any point, in order to verify the functionality of the design, and as an aid to debugging.

Once a design has been functionally verified, the next stage is to convert the source into a format that the family-specific implementation tools recognise. Usually this is a standard netlist format, in which the design is represented as simple logic blocks and the connections between them. The back-end tools perform design-checks and optimisations on the incoming netlist file, then partition it into the logic blocks available on the target device.

The next step is known as place-and-route (PAR), and is similar to printed circuit board placement and routing. The synthesis tools search for the best locations to place each block, in order to maximise the system performance, and to ensure that user-specified timing constraints are met. It is a very computationally intensive operation, particularly for large devices near their full capacity. It is generally recommended not to use more than about 85% of the capacity of an FPGA, in order to ensure that the place-and-route is successful, and to allow a small amount of space for later modifications.

The place-and-route step usually generates a file describing the timing delays in the circuit, often in Standard Delay Format (SDF), a spin-off from Verilog, but now an industry standard in its own right. This can be fed back into the simulator, allowing a full-timing simulation of the design.

2.6.5 Device Programming

The final stage is the generation of a file in the right format to download into the FPGA or PROM, known as a bit file. This is generated from the output of the place-and-route stage by vendor-specific software. The bit file can be downloaded into a device from a PC, often via the JTAG port in the case of in-system programmable devices, via a special cable that connects a serial, parallel, or USB port on the PC.

JTAG is a simple four-wire bus, and an associated set of rules, which allows access to the internals of JTAG-enabled devices. This enables in-system programming of Field Programmable Devices (FPDs) and flash memories, as well as testing and debugging. All JTAG devices in a system can be connected together in a single JTAG chain, allowing a large number of devices to be programmed or tested from a single JTAG port. JTAG includes a mode called boundary scan, where all I/O pins of a device are connected together as a shift register; a system can be tested for open or short circuits by shifting in values to the pins and reading back the values on other pins. JTAG also allows the configuration memory to be read back for verification, as well as the values of all flip-flops/registers and distributed/block RAM for real-time debugging.

In most systems the configuration data for the FPGAs will be stored in some form of non-volatile memory, and automatically uploaded to the FPGAs on power-up. For simpler systems this usually consists of a serial PROM for each FPGA. They are connected by either a serial link, or an 8-bit parallel link (which is faster, but requires more interconnections). The PROMs may also be in-system programmable, and connected to the JTAG chain, allowing them to be easily programmed via a JTAG cable.

For more complex systems, with many FPGAs, a more powerful configuration system may be needed. This could be a dedicated circuit using a microprocessor to retrieve the configuration data from memory, and upload it to all the FPGAs. However, this adds a significant amount of extra complexity to the system, leading to increased design and debugging time, and therefore cost. An alternative is to use a pre-engineered system-level FPGA configuration solution such as the Xilinx System ACE (Advanced Configuration Environment) [21]. This consists of three different products with slightly different capabilities. System ACE CF (CompactFlash) uses CompactFlash, or one-inch Microdrive disk drive technology, to store up to 8 Gbit of configuration data. It has a built-in microprocessor to manage the uploading of bitstreams to the FPGAs via the JTAG port, and can communicate with an on-board microprocessor. The large memory capability allows multiple configurations to be stored and easily selected, and

unused space may be used as extra system memory, or even to store other information, such as user manuals or technical schematics.

System ACE MPM (Multi-Package Module) and SC (Soft Controller) both use AMD flash memory to store from 16 to 64 Mbit of configuration data, which can be uploaded to up to 4 FPGAs in parallel mode, or 8 FPGA chains in serial mode. The MPM version is a single module containing the microprocessor and flash memory, while the SC version is a software version with the same functionality implemented in an FPGA.

2.7 Summary

Semiconductor technology is constantly advancing, with logic density increasing exponentially. Although custom ASICs will always be more powerful than programmable logic such as FPGAs, more and more problems are becoming solvable with programmable logic. FPGAs provide highly parallel processing close to that available in ASICs, while providing a turnaround time not quite as short as programming a microprocessor, but significantly shorter than designing a custom ASIC. The availability of high-level programming, modelling and synthesis tools make this technology accessible to a wide range of applications. All of these points mean that the use of FPGAs is rapidly increasing, and they are particularly suited to many high-throughput systems.

Chapter 3: The CMS Tracker Readout System

3.1 Overview

An overview of the CMS microstrip tracker readout system is shown in figure 3.1; the solid lines represent the flow of readout data, and the dashed lines represent control and monitoring signals. The tracker is made up of a number of detector- and opto-hybrids, with optical cables delivering the signals to the counting room. The detector hybrids contain silicon microstrip detectors, APV front-end readout chips, and APV multiplexers. The outputs are sent to the opto-hybrids, where the electrical signals are converted to optical. In the counting room, the FEDs convert the signals back to electrical form, digitise them, and process them, reducing the volume of data by a factor of more than 20, and then send them to the DAQ. The data from all sub-detectors are then combined, and finally sent to a processor farm where higher-level processing takes place, and eventually a small proportion of the bunch crossings (~ 100 out of 40 000 000 every second) are written to archival storage.

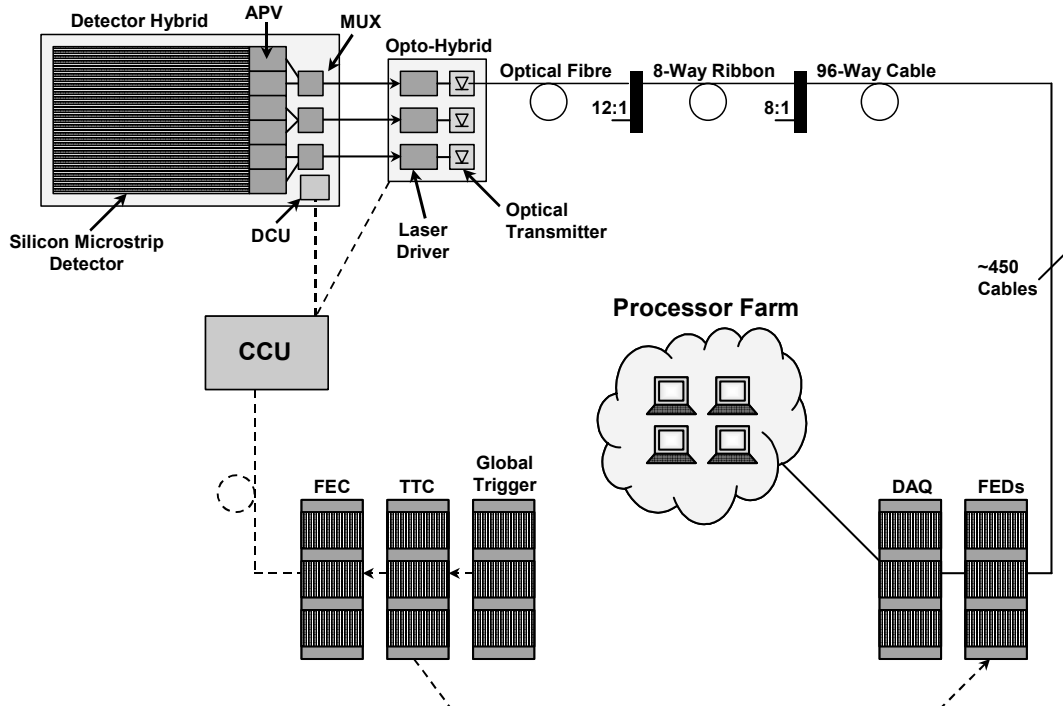


Figure 3.1: An overview of the tracker readout system.

3.2 The Silicon Detectors

The CMS tracker is based on silicon pixel detectors close to the interaction point, surrounded by several layers of silicon microstrip detectors, both of which detect ionising particles. Electromagnetically interacting particles traversing the detecting medium interact with electrons in the detecting medium, and can transfer energy to them. This transferred energy can excite the atoms or molecules, or even detach electrons from their atoms [22]. In a bubble chamber, the energy is redistributed as heat, causing boiling and hence bubble formation along the path of the particle. In a scintillation detector, the excited atoms release their energy as ultraviolet or visible photons, which are in turn usually detected by photomultiplier tubes or photodiodes. In a silicon detector, the energy creates electron-hole pairs, which then drift in an electric field, and when collected generate an electrical signal which can be amplified and measured.

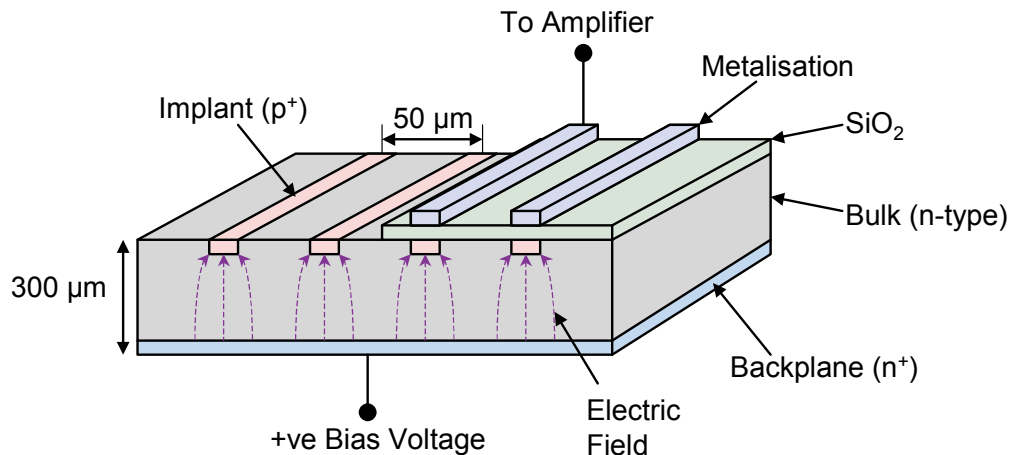


Figure 3.2: A silicon microstrip detector.

A silicon microstrip detector (see figure 3.2) is built on a wafer of n-type silicon. One side of the wafer has strips made of implanted p^+ silicon, which are isolated from the metallic strips by a layer of silicon dioxide (SiO_2). In a single-sided detector, the opposite side of the wafer forms a backplane of n^+ silicon, to which is connected a positive bias voltage. The p-n junctions in the detector are therefore reverse-biased and virtually no current flows, and the voltage difference creates an electric field across the detector. When an ionising particle crosses the

detector, the deposited energy generates electron-hole pairs. These drift in opposite directions because of the electric field, the electrons towards the positively charged backplane, and the holes toward the nearest strip. When the holes reach a strip, a pulse of current is generated, which can be amplified and measured by the readout electronics.

The energy deposited in the detector by a charged particle is described by the Bethe-Bloch equation. It is approximately proportional to the electron density in the detecting medium and to the square of the charge of the projectile particle. It also depends on the energy of the particle; at low energy decreasing rapidly to a minimum around $\beta\gamma = 3-4$, then rising logarithmically with higher energies, and finally levelling off at a constant value. A particle near the minimum is known as a minimum ionising particle (MIP). In a 300 μm silicon detector, this corresponds to a charge deposition of about 25 000 electrons.

3.3 The APV Readout Chip

The APV readout chip (see figure 3.3) processes and buffers the signals from the detectors. The chip reads out 128 strips of the microstrip detectors in parallel, amplifying and shaping the pulses, then storing them in an analogue pipeline. When ready, the signals are read out, further processed, and then multiplexed out.

As it is located inside the detector, it must be able to withstand the huge radiation levels that are present. Particle fluxes in the tracker are expected to be about $10^{14} \text{ cm}^{-2}\text{yr}^{-1}$ and the total radiation dose over the lifetime of the experiment up to 10 Mrad.

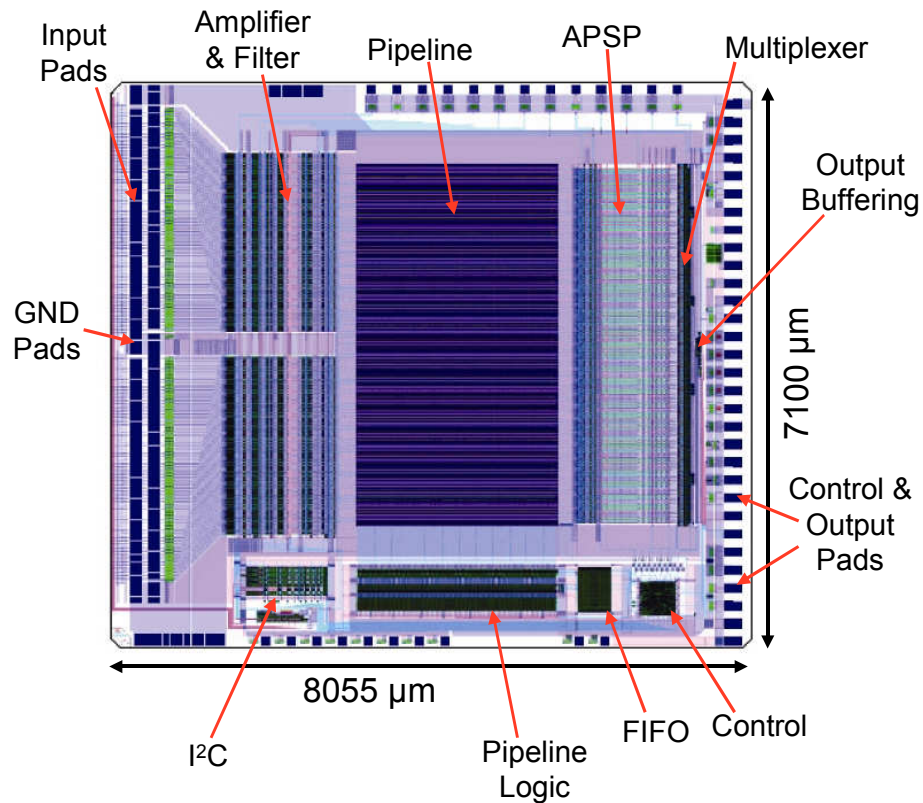


Figure 3.3: The APV25-S1.
(Adapted from refs [23, 24])

The APV was originally developed in a radiation-hard $1.2\ \mu\text{m}$ process, with the APV6 intended for silicon microstrip detectors, and the APVM intended for microstrip gas chamber (MSGC) detectors. Recent developments in deep sub-micron processes make it possible to design radiation-hard circuits using processes that are not intrinsically radiation-hard. A new prototype, the APV25-S0 was designed in a $0.25\ \mu\text{m}$ 3-layer metal process [25], based on the APV6 but with slight modifications to take into account the smaller feature-size and lower operating voltage. The APV25-S0 was successfully fabricated and tested and met the operating requirements of CMS, and so a new version, the APV25-S1 was designed, with slight modifications to reduce the input resistance and hence reduce noise and increase the amplification. Both versions of the APV25 had much higher yields than the previous APV6 [24], with up to 85 % of all chips on each wafer passing all tests. In total, about 80 000 APV chips will be needed for the tracker readout system.

3.3.1 Preamplifier

The first stage in the APV is the preamplifier. It reads the signals and amplifies them to a level of 18.7 mV per MIP (25 000 electrons). A switchable unity-gain inverter allows the signal to be inverted if detectors of the opposite polarity are used.

3.3.2 Shaping Filter

The output of the preamplifier is shaped by a CR-RC filter into a 50 ns wide voltage pulse and further amplified. The combined amplification of the preamplifier and filtering stages produce a pulse height of 100 mV per MIP.

3.3.3 Pipeline and FIFO

The output of the filter circuit is sampled at a rate of 40 MHz, and stored in an analogue pipeline for the 3.2 μ s latency until a level 1 trigger decision is made. The pipeline is made up of 128 channels by 192 columns of switched capacitor elements. The capacitors are made using the gates of 7 μ m x 7 μ m nFETs, which have a capacitance of 0.28 pF. One side of the capacitor is connected to VSS, and the other end to both the output of the shaper via a write switch, and the input of the APSP via a read switch [26].

A write pointer circulates the pipeline, sampling the output of the shaper every 25 ns. A trigger pointer follows it, separated by the trigger latency. When a trigger is received, one or three columns, depending on the mode, are marked and reserved for reading out. These will not be overwritten by any triggers until they have been read out; the pointers instead skip over them to the next empty column.

A FIFO of depth 32 stores the column addresses of the marked data in the pipeline, so that they are read out in the right order.

3.3.4 APSP

The APV has two main modes of operation, *peak* mode and *deconvolution* mode. In peak mode, one sample is reserved in the pipeline for each trigger received, corresponding to the peak of the CR-RC shaped pulse. This maximises the signal-to-noise ratio and minimises the non-linearity of the system, and is used when the data occupancy in the tracker is expected to be relatively low. When

occupancy is higher, the incoming pulses get closer together, and can start getting superimposed on one another. This is known as *pile-up*, and if it becomes significant, then the APV can be run in deconvolution mode. In this case, three samples are stored in the pipeline for every trigger, and these are then deconvoluted by the Analogue Pulse Shape Processor (APSP).

The APSP is a three-weight Finite Impulse Response (FIR) filter, consisting of a charge amplifier and a switched capacitor network. The filter performs a deconvolution of the input data by producing a weighted sum of the three inputs (corresponding to three samples of the input signal at different times). This technique can be easily implemented in CMOS technology, and has low power consumption [27].

The operation of the APSP is shown in figure 3.4. The three pipeline columns are sampled into three capacitors, one after the other, by *ri1* ①, *ri2* ②, and *ri3* ③. The feedback capacitor is then increased by *last_cycle*, the charges on the three capacitors summed by *ro1*, *ro2*, and *ro3*, and the resulting signal stored on the hold capacitor by *store* ④. The DC output level can be adjusted by the signal *Vadj*. The effect of the filter is to reduce the width of the output pulse to fit within one 25 ns bunch-crossing period.

The chip actually has a third mode of operation, called *multi* mode, where three consecutive samples are made on each trigger (as in deconvolution mode), but all three are output as consecutive frames by the multiplexer, each processed by the APSP as in peak mode. This is useful when calibrating the timing, as consecutive triggers to the APV must be separated by at least two clock cycles, so this mode allows a run of frames from consecutive clock cycles to be read out.

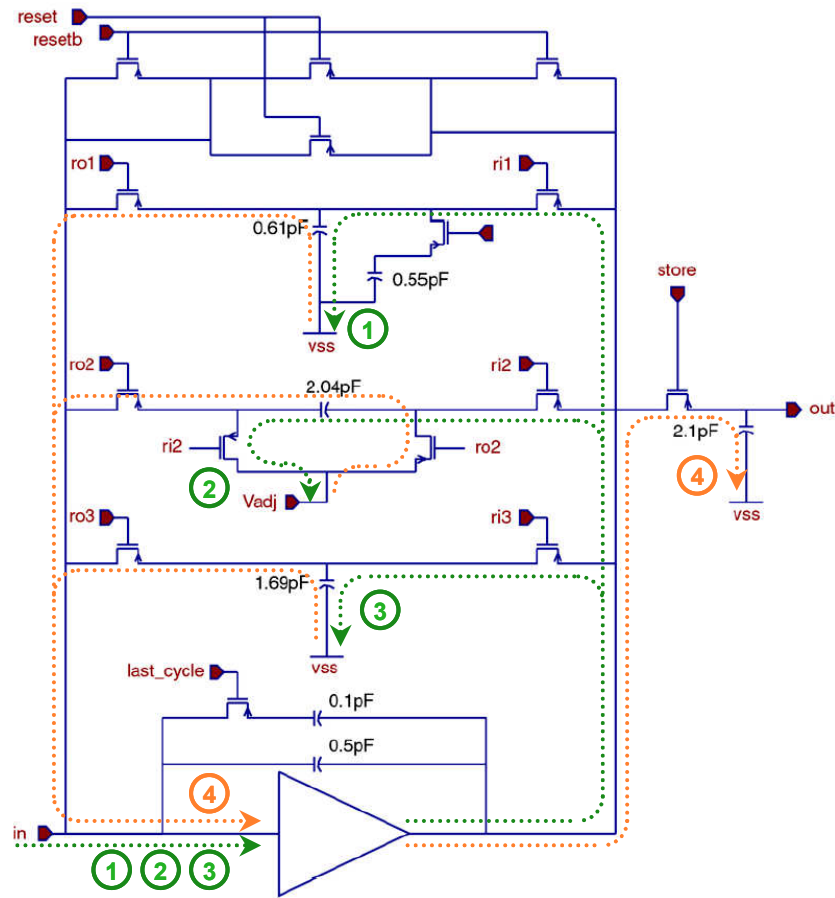


Figure 3.4: The APV25 APSP circuit.

(Adapted from ref [26])

3.3.5 Analogue Multiplexer

The outputs from the 128 channels of the APSP are read out by a 128-channel analogue multiplexer and driven off the chip as a differential current. Due to the way the multiplexer is implemented, in three levels, the order in which the data are transmitted does not correspond to the physical order in the detector; but this reordering can be easily undone at a later stage in the readout chain. The outputs of the APSP are converted to a current by a resistor, which has five programmable values, allowing the gain of the multiplexer to be trimmed. The output of the multiplexer is a current of magnitude $100 \mu\text{A}$ per MIP. This is then converted to a differential signal, linearised, and amplified by a factor of 10, generating an output current of $\pm 1 \text{ mA}$ per MIP.

In addition to the three operational modes, the APV has two readout modes. The data can be read out at either 20 MHz or 40 MHz. If read out at 20 MHz, then pairs of APV outputs can be multiplexed together to generate a 40 MHz signal.

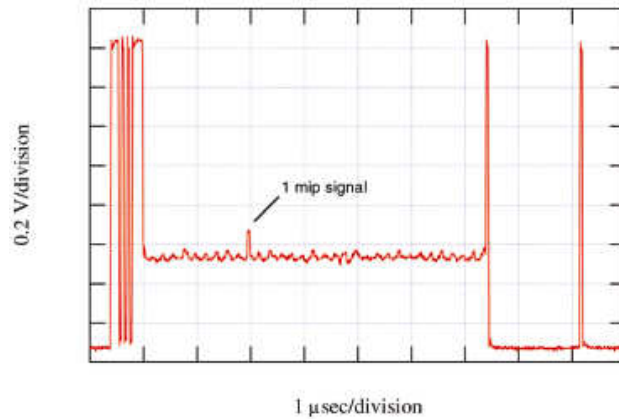


Figure 3.5: A typical APV output frame

A typical APV output frame is shown in figure 3.5. The APV continuously outputs pulses (every 70 clock cycles in 20 MHz mode, and 35 clock cycles in 40 MHz mode) known as tick-marks, which are used to synchronise to the APV output when no data are being transmitted. When an event is ready to be sent, the tick-mark is lengthened to three clock cycles, enabling the start of the event to be easily detected. It is followed by an 8-bit value representing the column address of the sample within the pipeline (used to verify that multiple APVs are synchronised) and an error bit (used to signal that an error has been detected in the chip). Finally, the 128 analogue samples are sent, immediately followed by the next tick-mark.

3.3.6 Slow Control

As well as the clock and trigger inputs (fast control), the APV also has a slow control system, based on the I²C protocol. This is a simple two-wire bus developed by Philips about 20 years ago. The original version allowed data transfer rates of up to 100 kbits/s with 7-bit addressing, and more recent versions of the standard allow fast mode (400 kbits/s), high-speed mode (3.4 Mbits/s), and 10-bit addressing [28], although in the APV the original mode is used since fast

data rates are not needed. The APV has a number of internal registers, which control internal voltage and current biases, set the mode of operation and the programmable latency, and hold error flags. These can be written and read back via the I²C bus.

3.4 The APVMUX

The outputs from pairs of APVs (each driven at 20 MHz) are multiplexed together by APV multiplexer (APVMUX) chips, each of which contains two 2-to-1 multiplexers. The differential current output of the APV is converted to a voltage by internal resistors connected to a reference voltage pad [29]. The value of these resistors can be switched to a range of values between 50 and 200 Ω by a register controlled by an I²C connection.

3.5 The Optical Link

The output of the APVMUX is sent to the optical hybrid, where the electrical signals are converted into optical signals. Each opto-hybrid contains either two or three (depending on its geometrical position in the detector) laser drivers and laser diodes [30]. The laser drivers bias the laser diodes at their working point, and modulate them with a signal proportional to the input signal. The laser diodes convert the signals from electrical to optical, and transmit them in analogue form over optical fibres. At patch-panels inside the detector, groups of 12 fibres are bundled together in ribbons, and then 8 ribbons are grouped together into cables. These then take the signals out to the counting room where they are processed further.

3.6 The Front-End Driver

The front-end drivers (FEDs) are located in the counting room, and receive the analogue optical signals from the front-end of the detector. The tracker has a

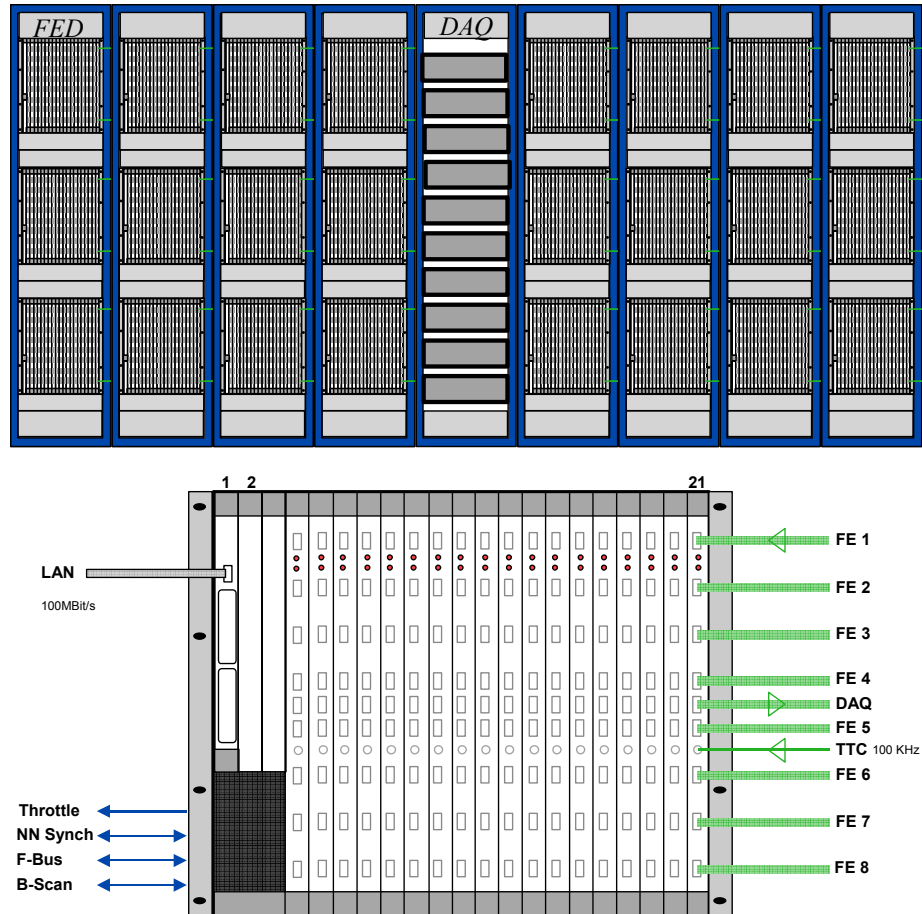


Figure 3.6: The FED and DAQ racks (top) and a FED crate (bottom).
(Adapted from ref [31])

total of about 440 FEDs, located in 24 crates, in 8 racks (see figure 3.6). Each crate holds 18 FEDs, along with a crate controller with a 100 Mbps Ethernet connection, and two spare slots for possible other cards. The 440 FEDs work in parallel to process data from all 10 million channels in the tracker. This involves converting the optical signals into electrical form, amplifying and digitising them, then subtracting unwanted components of the signal and performing cluster finding and zero suppression to reduce the volume of data sent to the DAQ. The internal operation of the FED is described in more detail in the next chapter.

3.7 The S-LINK64

The data produced by the FED are transmitted to the DAQ over a fast data link known as S-LINK64, which is an extension of the S-LINK specification. S-LINK is a simple link interface that can be used to connect a layer of the front-end electronics to the next level of readout. In addition to transferring data, it provides error detection, and optional return signals providing two-way communication. The physical medium of the link is not specified by the standard, and could be implemented as an optical fibre, copper wires, or any other medium that meets the required transmission speeds. Since the FED crates will be close to the DAQ system, in this case it is likely to use copper wires; for distances in excess of about 15 meters [32] it would be necessary to use optical fibres. With S-LINK, data can be 8, 16 or 32-bits wide, and can be transmitted up to a maximum clock frequency of 40 MHz [33]. The S-LINK64 standard extends this to 64 bits, and up to a maximum clock frequency of 100 MHz [34], corresponding to 800 Mbyte/s.

3.8 The DAQ

An overview of the DAQ architecture is shown in figure 3.7. It receives the signals from the FEDs of the various subdetectors via the S-LINK64 fast copper links. The builder network is a large switching fabric, providing interconnections between the FED readout systems and the filter systems, and is capable of sustaining a data transfer rate of 800 Gbyte/s [35]. For each event, the fragments from the different subdetectors are combined, and sent to one of the filter systems.

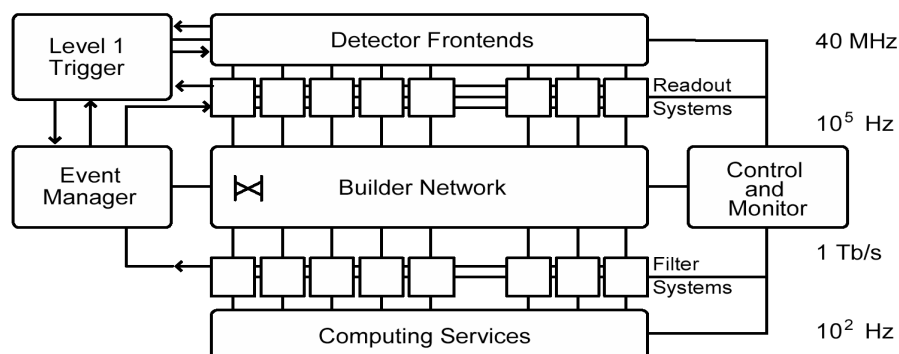


Figure 3.7: Overview of the CMS DAQ system.

(From ref [35])

The filter systems consist of a network of processors that verify the integrity of the received data, and execute the high-level trigger algorithms that select the events to be stored for offline analysis. These are then sent to the computing services, where they are forwarded to mass storage. The computing services also perform monitoring of the high-level trigger system and of the detector itself.

3.9 Control and Monitoring

As well as reading out and processing data from the tracker, it is necessary to distribute signals, such as clock, level-1 accept and reset commands, to all the readout electronics and to monitor their state (e.g. temperature) to ensure that everything is working properly.

3.9.1 Timing, Trigger and Control (TTC)

The TTC information is broadcast to the detector over optical fibres, using Time Division Multiplexing (TDM) and BiPhase Mark (BPM) encoding to encode two channels (A and B) onto a single fibre [36]. Channel A is dedicated to transmitting the level 1 accept decisions, a one-bit decision being transmitted on every bunch crossing. Channel B transmits the trigger number reset and bunch counter reset commands, as well as individually addressed commands and data, which transmit user-defined information over the network, and allow the TTC receivers to be controlled centrally. The 40.08 MHz LHC clock is not explicitly encoded, but due to the regular transitions at well defined times in the BPM-encoded signal, it can be easily recovered.

The TTC signals are received and decoded by the TTCrx chip, which is a custom ASIC developed at CERN. It contains a number of registers controlled by the incoming TTC signals, and also accessible via an I²C interface. The bunch counter register is a free-running 12-bit counter incremented by the 40.08 MHz clock, and the 24-bit event number counter is incremented by the level 1 accept signal. Both counters can be reset by commands sent over the TTC system.

3.9.2 The Tracker Control System (TCS)

An overview of the TCS is shown in figure 3.8. It consists of Front-End Controllers (FECs) in the control room, connected to CCU modules in the tracker by digital optical fibres. Groups of CCU modules are connected in loops, with two connections. One of them links all of the modules in a continuous loop, and the other connects alternative modules, allowing a closed loop to be sustained in the case of failure of one of the modules.

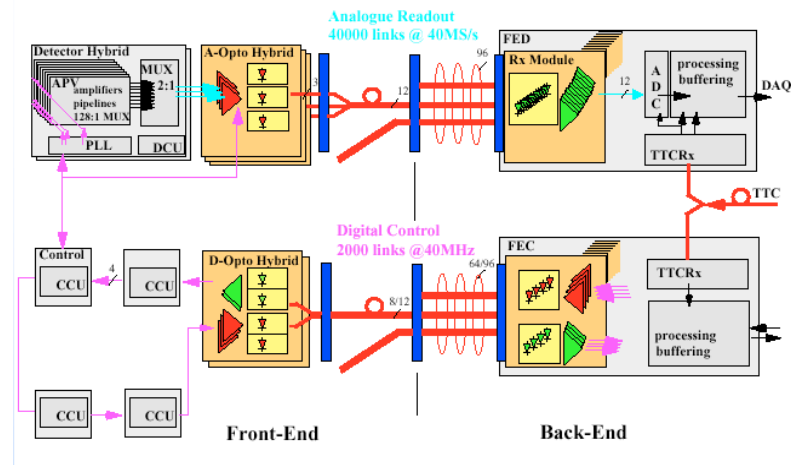


Figure 3.8: Schematic of the tracker control system.

CCU modules communicate with components on the detector and opto-hybrids, such as the APVs, APVMUX, laser driver, and the DCU modules. The DCU modules perform generic monitoring of variables such as temperature, voltage, and current, using a 12-bit ADC.

This system allows the overall state of the tracker to be continuously monitored, to ensure the proper functioning of the detector.

3.10 Summary

The tracker readout system samples 10 million silicon detector channels at the LHC bunch-crossing rate of 40 MHz. The data are stored in the APV readout chips, in the detector, until an L1A trigger decision has been made. The signals are then sent over optical fibres to the counting room, where they are processed by an array of 440 FEDs. The volume of data is reduced by a factor of 20 using zero-suppression, and the results sent over a fast link to the DAQ. Here they are further processed, and a small proportion of the events are written to archival storage.

Chapter 4: The Front-End Driver

The FED design is based on a VME64x 9U x 400 mm card. It receives the analogue optical signals from the tracker, digitises and processes them, and then transmits the resulting data to the CMS DAQ using S-LINK64 fast copper links. The S-LINK64 transmitter (a PCI Mezzanine card) is plugged onto a transition card, which is in turn plugged onto the back of the FED. In this way it is not necessary to bring the S-LINK cable out through the front-panel of the FED, which is already highly populated.

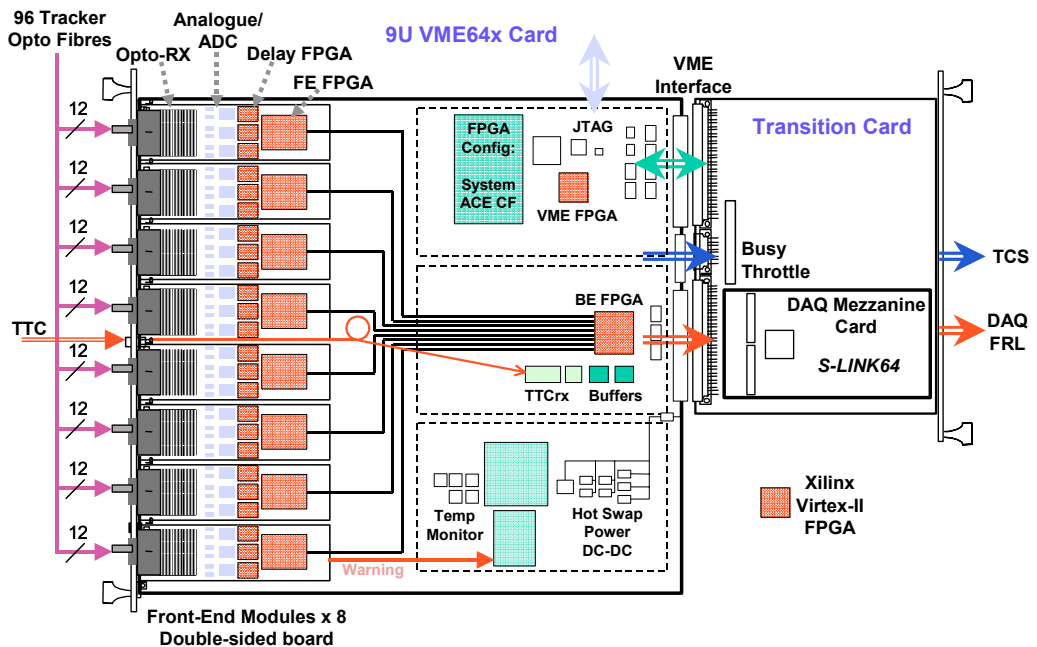


Figure 4.1: Schematic of the Front-end driver.

(Adapted from ref [31])

Each FED (see figure 4.1) has eight identical sections at the front of the PCB known as front-end modules, each of which processes data from twelve channels (one ribbon, corresponding to 24 APVs) via an optical connector on the front-panel. Each module contains six dual-ADCs, three delay FPGAs to tune the timing of the individual channels, and a front-end FPGA, which processes the data. The data produced by the front-end modules are combined and buffered by the back-end FPGA prior to being sent to the DAQ system via a transition card

which plugs onto the back of the FED. The back-end FPGA also receives TTC information such as the clock, L1A and reset signals, via a separate optical connection on the front-panel. A separate FPGA, which is configured separately from the others via its own PROM, provides the connection to the VME bus. In this way, the other FPGAs can be reconfigured via VME without risk of losing the VME connection if a bad configuration is loaded.

All FPGAs on the board are from the Xilinx Virtex-II range, with speed grade -4 and fine-pitch ball grid array packages. The 24 delay FPGAs are XC2V40 parts with 144-pin packages, the 8 front-end FPGAs and the back-end FPGA are XC2V2000 parts with 676-pin packages, and the VME FPGA is a XC2V1000 part with a 456-pin package.

4.1 The FED Front-End Modules

Each front-end module processes twelve channels in parallel. It contains a photodiode array, six high-bandwidth dual-ADCs, three delay FPGAs and a front-end FPGA (see figure 4.2). The optical ribbon is connected to an opto-receiver package consisting of 12 p-i-n photodiodes and an amplifier, producing twelve single-ended current outputs [37].

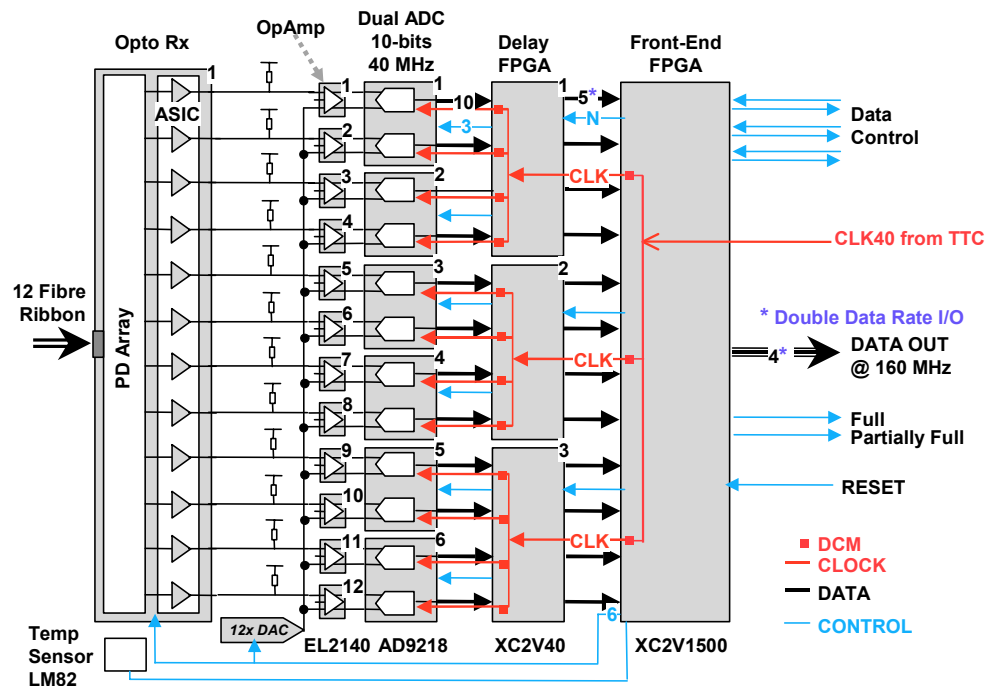


Figure 4.2: Schematic of a FED front-end module.

(Adapted from ref [31])

The individual fibres connected to the FED are unlikely to be all exactly of the same length, and therefore the signals will all arrive at slightly different times. To compensate for this, each ADC has a separate clock input (generated by the delay FPGAs, and controlled by the front-end FPGAs) that can be individually skewed relative to the main clock, allowing the sampling point to be controlled at the level of $1/32$ of a clock cycle, or 781 ps [39]. The outputs of the ADCs are then sampled, using the main clock, by the delay FPGA, bringing them all into the main clock domain. In addition, the delay FPGA contains a variable length pipeline, allowing the data to be delayed by up to 16 clock cycles. The values of the clock skew settings will be calculated by software, outside of the FED, and stored in a database to be loaded during the setting up of the FEDs.

By looking for the regular tick-marks sent by the APVs, the FED is able to adjust the timing automatically, so that the signals from all fibres arrive at the same time to within the level of about $1/32$ of a clock cycle (781 ps) [40]. This can be done by scanning over a 70-clock cycle range (the distance between two tick marks), in 781 ps steps, and looking for the rising edge of the tick-mark.

4.2 The Front-End FPGA

Once the twelve channels of data in a front-end module have been digitised and de-skewed, they are processed by the front-end FPGA (see figure 4.5). There are twelve double data rate (DDR) 5-bit inputs, which are latched on both the rising and falling clock edges, thus reducing the number of connections needed between the delay FPGAs and the front-end FPGAs [39].

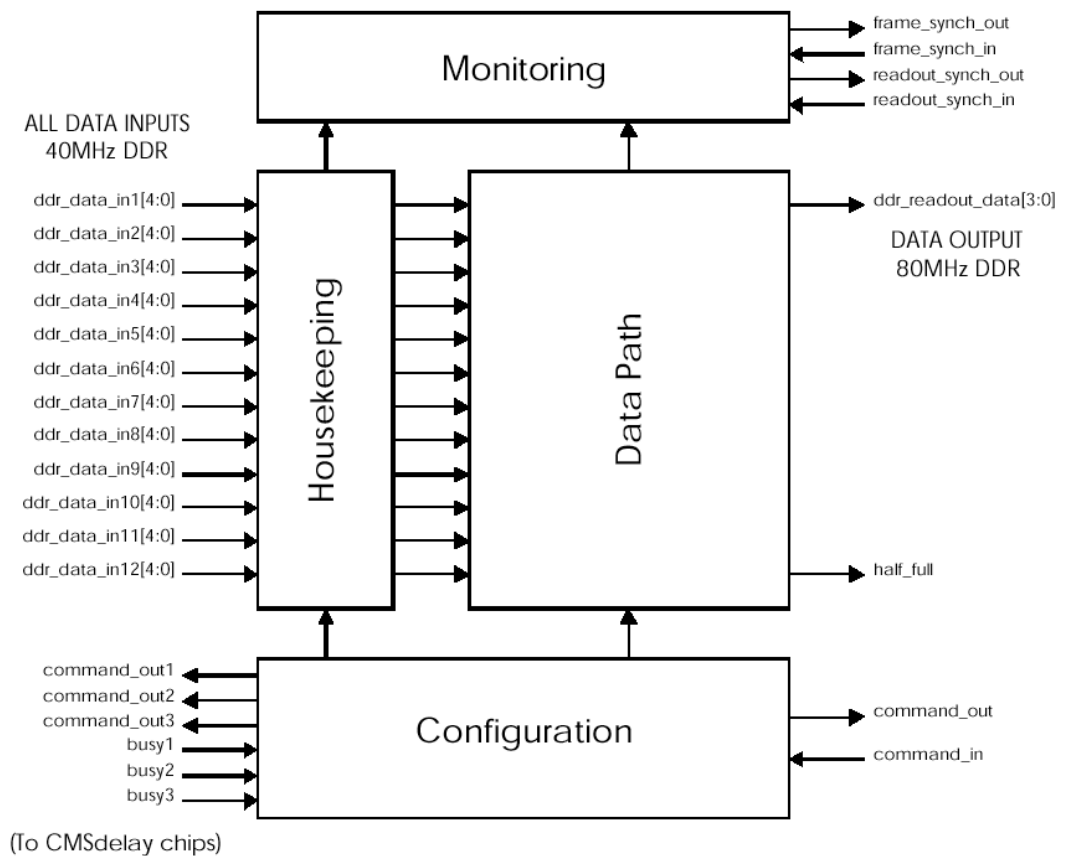


Figure 4.5: Schematic of the FED front-end FPGA.

(From ref [39])

4.2.1 Housekeeping

The *housekeeping* block in the front-end FPGA monitors the incoming data, and looks for the tick marks and the headers that signal the beginning of an event, as well as detecting any faults that develop. It also contains functionality to adjust automatically the delays of the individual fibres to their optimal values, and calculate the threshold for the detection of the header bits, although these values

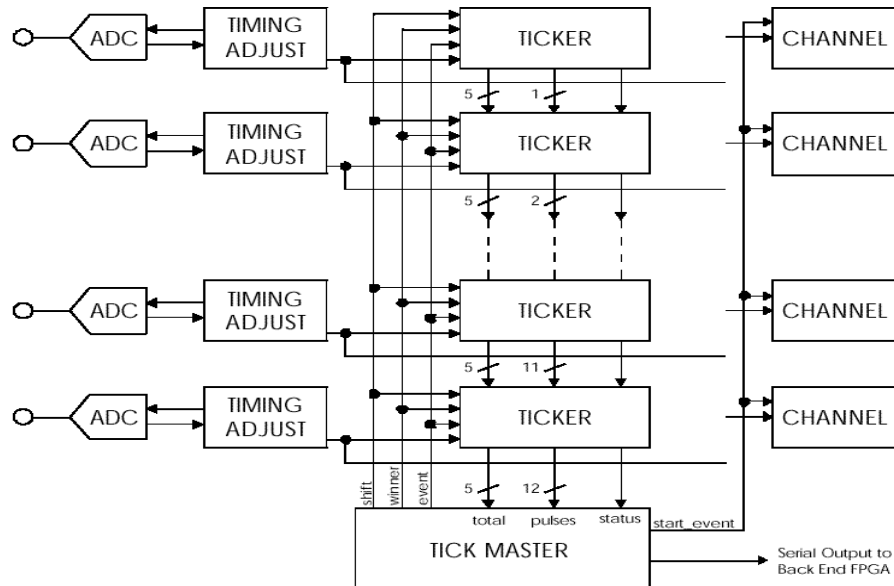


Figure 4.6: Basic schematic of the housekeeping block.

(From ref [39])

can also be loaded from an external source, if necessary. As the signal levels can vary from channel to channel, each channel has a separate digital threshold register, which stores the value above which a header bit is considered a logic 1. The *ticker* block monitors the incoming data, comparing it to this threshold value, and when a tick mark or event header is detected, sends a pulse to the *tick master* in the *monitoring* block (see figure 4.6). A header is detected by the presence of another high bit after the two initial bits of the tick mark. The *ticker* block also

checks that a tick mark is received every 70 clock cycles (except during a data frame), hence verifying that the FED remains in synchronisation.

4.2.2 Monitoring

The *tick master* monitors the signals from the *tickers*. If a clear majority (more than 50%) of channels detect a frame on the same clock cycle, an event-start signal is sent to all channels, and any that did not trigger can set their status bits accordingly. Once a frame has been recognised, the digital header has to be extracted. If all is well, then all 12 headers should be identical, but it is possible that some APVs may be out of synchronisation and therefore be sending the wrong headers. In this case the header is calculated as the bit-by-bit majority value of all the received headers, i.e. for each bit, the majority (1 or 0) is calculated, independent of the other bits. As long as the majority of APVs remain in synchronisation, then this will always be the correct value. The number of APVs out of synchronisation is transmitted with the data, so if too many APVs lose synchronisation a reset signal can be sent. The monitoring block then sends a *frame_synch_out* signal to the back-end FPGA with the majority header, and the status bits for each channel. The status bits indicate whether the channel has locked on to a signal (i.e. it is detecting tick-marks at the expected time every 70 clock-cycles), whether it is in synchronisation with the other channels, whether either APV sent the wrong header (compared to the majority header), and whether either APV had the error bit set in its header.

The *monitoring* block also checks regularly the state of the *datapath* block. Once a frame has been processed by the data path and stored in the front-end buffer, a second signal, *readout_synch_out*, containing a 14-bit number with the length of the zero-suppressed event in the buffer, is sent to the back-end FPGA. In the normal zero-suppression mode this will always occur 559 clock cycles (at 40 MHz) after the first bit of the *frame_synch_out* signal.

4.2.3 Configuration

The *configuration* block controls the loading and reading back of all the various parameters of the front-end modules. These include the delay and digital threshold values for each fibre, the enable/disable bits for each APV, the pedestal

data, and the mode of operation. It can also set the control bits for the opto-receivers, the ADCs, and the reference-voltage DACs, as well as passing control signals back to the delay FPGAs.

4.2.4 Data Path

The main processing takes place in the front-end FPGA *data path* block. This contains twelve almost-identical channels (some of the memory blocks are shared between pairs of channels), each processing data from one pair of APVs.

Each channel contains a number of blocks, which subtract unwanted components of the signal, find clusters of hits, and buffer the data. The raw signal can be decomposed into several different components in addition to the useful data, namely the pedestal, common-mode, and random noise. The pedestal is the component of the signal that is constant from event to event, but is different for each strip. It can be calculated by averaging the data from the APVs in the absence of any hits, and the result can then be stored in a look-up table for later use. The common-mode is a DC level that varies from event to event, but is assumed to be constant for the duration of a single event. It is estimated by averaging all of the strips except those containing hits. If hits are present in the

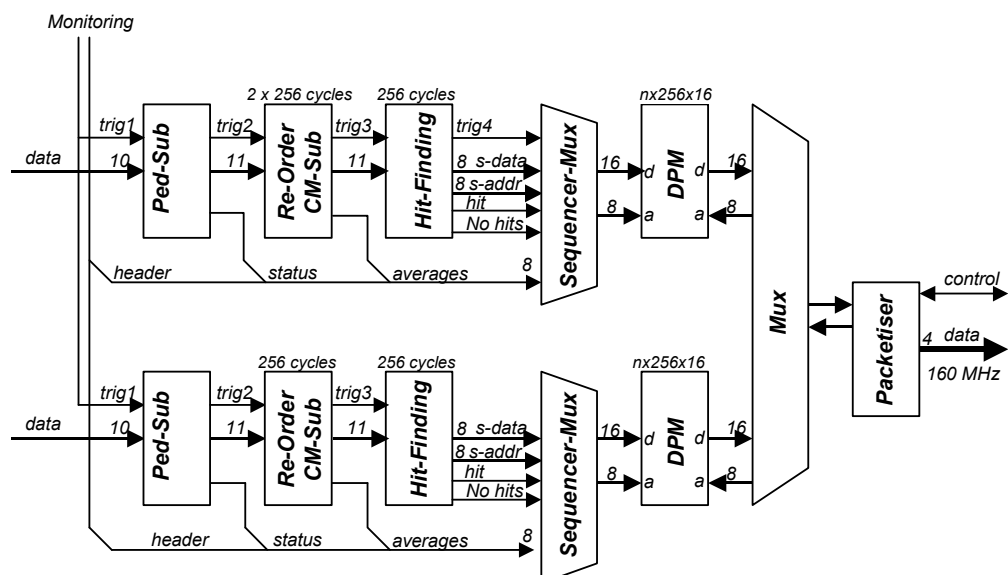


Figure 4.7: A pair of channels from the datapath block.

(Adapted from ref [39])

data, this requires at least two passes, first to calculate an average, then to exclude strips significantly higher than this average and calculate a better estimate ignoring these strips. It turns out to be better to calculate the median of all the strips, which still needs two passes over the data, but is less prone to bias from the hits. The random noise component varies from strip to strip and from frame to frame, and is therefore impossible to remove.

A pair of channels from the *datapath* block is shown in see figure 4.7; the individual blocks are described below.

Ped-Sub

The first block receives the raw data from the ADC. It contains a look-up table with the 256 pedestal values for the two APVs. The pedestal values are subtracted from the raw data, and this is then sent to the next block for further processing.

Re-order / CM-Sub

The second block performs the common-mode subtraction and reorders the data. The common mode is calculated using a two-pass median technique, where the first pass histograms the most significant five bits, and the second pass histograms the least significant five bits. As the data arrive, they are written into the re-ordering RAM and stored there while the median calculation takes place. Once the median is ready, the data are read out of the reordering RAM in a different order, so that the re-ordering of the APV multiplexer is undone, and at the same time, the common mode is subtracted.

Hit-Finding

The reordered data are then searched for hits above threshold, which are grouped into clusters. The FED uses one threshold for groups of more than one contiguous strip, and a higher threshold for single strips, as these are more likely to be caused by noise in the signal. The clustering block outputs the starting address and length of each cluster, followed by the data for each strip in the cluster, meaning that two words have to be output before each cluster. One word is sent per clock cycle, so there must be two empty clock cycles before each

cluster. To ensure that this is always the case, clusters that are only separated by a single strip are merged together into a single cluster, including the intervening strip. The algorithm is shown graphically in figure 4.8. The data flows from top to bottom along the left-hand side, and *word n* represents the current strip, which is examined along with the neighbouring two strips on each side. Each strip is compared to the two thresholds, and the results of these comparisons are then masked by different patterns. There are a number of pattern masks, representing the different conditions for which any particular strip should be included in a cluster. A 1 in the pattern means that the corresponding strip must be above the multi-strip threshold, a 2 means that the strip must be above the single-strip threshold, and an *x* means *don't care*. The first two patterns check whether the strip is part of a multi-strip cluster, the third checks whether it is a single-strip cluster, and the remaining four patterns check if the strip is in the middle of two clusters.

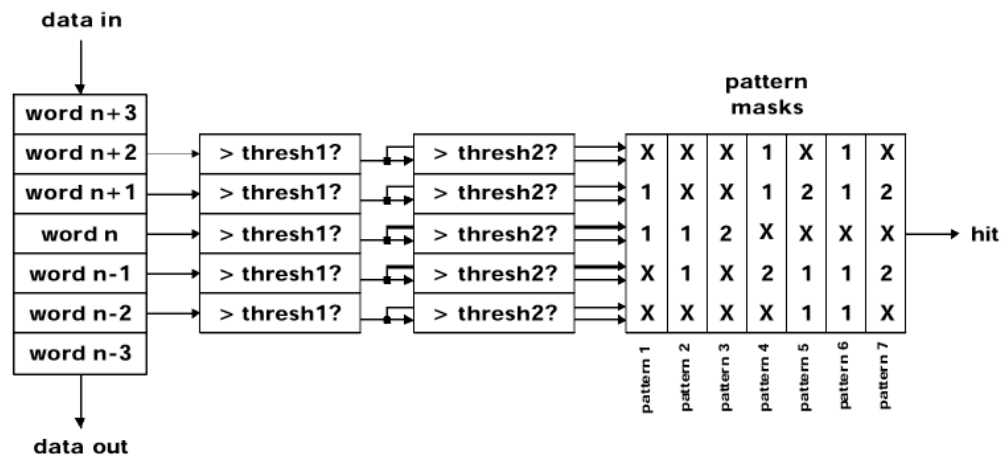


Figure 4.8: Graphical representation of the clustering algorithm.

(From ref [39])

If none of the patterns are matched, then the corresponding strip is discarded, as it contains no useful data. This is known as zero-suppression; it significantly reduces the volume of the data, as only a minority of the strips contain hits.

At the output of the *hit-finding* block, the data are reduced to eight bits according to the scheme in table 4.1. An output of 255 represents a value that was off the scale of the ADC, and 254 represents any other overflow value (from 254 up to 1022). Normal physics data up to 6 MIPs will be in the range 0-253, and negative values, which can only occur due to noise, are truncated to 0.

Input	Output
1023	255
254-1022	254
0-253	0-253
< 0	0

Table 4.1: Rules for data size reduction in the FED.

(Adapted from ref [39])

Truncating the data from ten to eight bits (thus throwing away $3/4$ of the available range) does not have a significant effect on the performance of the tracker [41]. The majority of the signals are within the 8-bit range anyway, and for track reconstruction, the positional information is more important than the absolute amount of charge in the detector. An ADC range of 9 bits is still needed, because there can be large offsets in the data (common mode), which are only subtracted later; a 10-bit ADC was used due to the unavailability of 9-bit devices.

Sequencer-Mux & DPM

The *Sequencer-Mux* block combines the physics data with other information, such as the majority APV header (from the *monitoring* block), the common-mode, and the status bits for the event, and writes it into a dual-port memory (DPM) buffer. Once the data are stored in the buffer, a signal is sent to the back-end FPGA by the *monitoring* block, and if there is free space in the back-end buffer, it will subsequently be read out.

Mux & Packetiser

Once the back-end FPGA is ready to receive the data, it sends back a signal, and the *Mux* block reads the data, for one event, from each channel in turn, sending it via the *Packetiser* to the back-end FPGA. The *Packetiser* receives 8-bit

A DCM receives the main 40 MHz clock, using it to generate 80 MHz and 160 MHz clocks, which are then distributed throughout the FPGA and to other parts of the FED.

The *address generator* block receives the lengths of the events in each front-end FPGA before the data arrive. In this way, the amount of memory needed, and the start-address in the RAM for each front-end FPGA's data, can be calculated. Then, as the data arrive, they are assembled into 64-bit words, and each channel is in turn written into the appropriate address in the buffer.

As long as there are data in the buffer and the link to the DAQ is not busy, the data are constantly read out and sent to the transition card at the back of the FED, from where they are sent to the DAQ.

4.3.1 Common Data Format

The data are stored and sent to the DAQ as 64-bit words, along with an extra flag bit (*K* or *D*), indicating whether each word is control information or data. Each event is preceded by a header word (or possibly two), and followed by a trailer word (see figure 4.10), that are common to all of the sub-detectors.

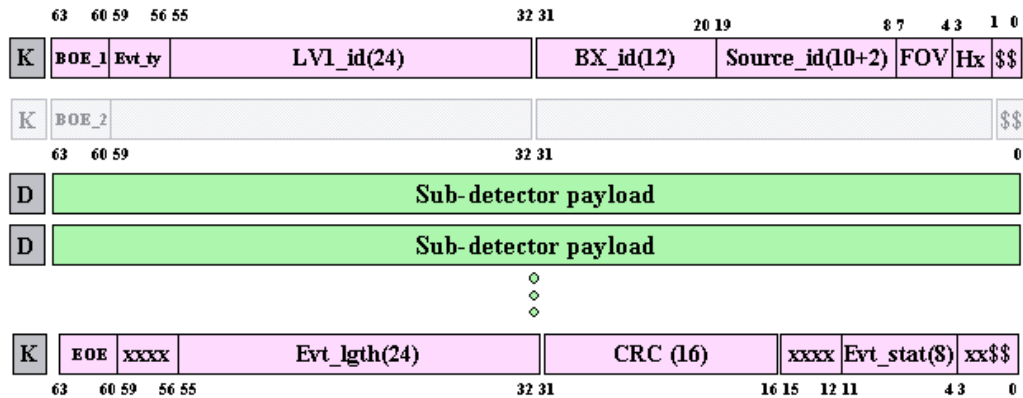


Figure 4.10: Common data format header and trailer.

(From ref [42]).

The header contains the event type, event number, bunch crossing number and source identifier, and the trailer contains the event length, a CRC (for error detection) and some status bits. The individual fields are described in table 4.2.

The control/data bit that accompanies each word determines how the S-LINK64 handles the data. In control words, the two least-significant bits are ignored, because the S-LINK64 uses these for its own error detection [33]. The possibility of adding a second header word is left open; if used, this would hold error-correction data for the first header word.

Field	Size (bits)	Description
K	1	Indicates control word
D	1	Indicates data word
H	1	Indicates final header word
x	-	Reserved
\$\$	2	Ignored
BOE_1	4	Beginning of event (word 1)
BOE_2	4	Beginning of event (word 2)
EOE	4	End of event
Evt_ty	4	Event type (data/calibration etc)
LVI_id	24	Level 1 trigger number
BX_id	12	Bunch crossing number
Source_id	12	Source identifier
FOV	4	Format version
Evt_lgth	24	Event length (in 64-bit words)
Evt_stat	8	Event status bits
CRC	16	Cyclic Redundancy Check
Sub-detector payload	64 x N	Detector dependent data

Table 4.2: Common data format header and trailer fields.

4.3.2 CRC

The Cyclic Redundancy Check (CRC) bits in the trailer are used to detect errors in the data. The CRC algorithm is well adapted to implementation in hardware as it consists mostly of XOR logic operations. It generates a number from a stream of bits, in such a way that the value obtained is completely different if even a minor error is introduced into the data. In order to check the data, the receiving end simply calculates the CRC for the data, and compares the calculated and the received CRCs. If there has been any error in the transmission of the data, it is highly likely that the CRCs will no longer match, and the error will be detected. There are certain types of errors that the CRC is guaranteed to detect; for

other errors its effectiveness depends on its length, N . The probability of an error going undetected is 2^{-N} ; for a 16-bit CRC this is 1 in 65536.

The CRC algorithm effectively treats the message as one huge binary number, which it divides by another number and returns the remainder [43]. However, instead of using normal arithmetic, it uses what is known as polynomial arithmetic modulo 2. This means that no carries are performed between adjacent digits of the numbers, and each digit is only stored modulo 2 (i.e. can only be 0 or 1). It turns out that in this system addition and subtraction are the same, and are both equivalent to the XOR logic operation. Therefore, as division is effectively repeated subtraction, the algorithm becomes a series of XORs.

The number by which the data is divided is known as the polynomial of the CRC. For any given length CRC, there are a number of possible polynomials, with the highest term being the length of the polynomial. For example, the standard 32-bit CRC (CRC-32) uses the polynomial $1 + x^1 + x^2 + x^4 + x^5 + x^7 + x^8 + x^{10} + x^{11} + x^{12} + x^{16} + x^{22} + x^{23} + x^{26} + x^{32}$, often written as (0, 1, 2, 4, 5, 7, 8, 10, 11, 12, 16, 22, 23, 26, 32). A graphical representation of the algorithm is shown in figure 4.11, for the polynomial (0, 1, 2, 8). As this is an 8-bit CRC, an 8-bit register is used. The data is fed into this register one bit at a time, and the register is shifted to the left. The bit that ‘falls off’ the left of the register is then fed back in, by XORing it with several bits in the register. Which bits are affected depends on the polynomial used, in this case bits 0, 1, and 2.

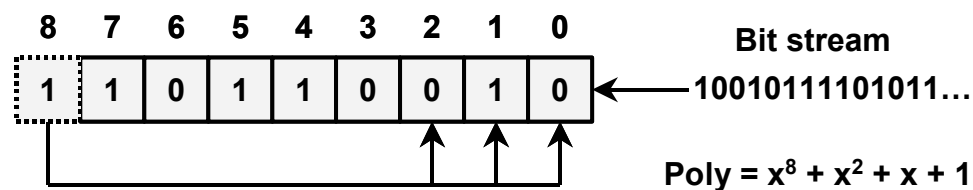


Figure 4.11: Graphical representation of the CRC algorithm (for CRC-8).

In practice, it is not necessary to process the data only one bit at a time. Many implementations process 8 bits at a time, using a 256-location look-up table, which stores the effect of any 8-bit sequence on the CRC. In hardware,

many logic operations can take place in parallel, and a look-up table is not needed to create efficient implementations that process many bits at a time.

Some polynomials are better than others at detecting various types of errors. For example, a CRC is guaranteed to detect all single-bit errors if the polynomial has at least two bits set (i.e. two terms). If the polynomial has an even number of bits set, then it will also catch all errors that modify an odd number of bits (in fact, a parity bit is a trivial example of one such CRC, with length 1). Additionally, if the lowest bit of the polynomial is set, then the CRC is guaranteed to detect all burst errors with lengths up to that of the CRC. However, choosing a good polynomial is extremely difficult and involves a large amount of complex mathematics. In practice, there are a number of standard polynomials, already proven and in widespread use, and it is usual to use one of these.

The initial value of the CRC, before any data are processed, can be chosen arbitrarily. However, a value of zero will mean that any initial zeros in the data stream would have no effect on the CRC, and therefore, any inserted zeros or dropped bits in this region would go unnoticed. For this reason, a non-zero starting value is often used.

An interesting characteristic of the CRC is that if the calculated CRC is appended to the data, and the CRC is taken of this *augmented data*, the resulting CRC will be zero. However, in most situations, it is just as easy to compare the CRC of the data to the transmitted CRC, as it is to compare the CRC of the augmented data to zero.

4.4 Implementation of Common Data Format

Code was developed in VHDL to implement this header format in the back-end FPGA of the FED. The different blocks that make it up are shown in figure 4.12, and the VHDL code for each block is listed in appendix A. The main processing, including the actual construction of the header and trailer words, takes place in the *builder* block. It is notified when all the necessary information, such as the trigger number and event length, is available for a new event by control logic in the back-end FPGA, which sends a pulse to the *prepare* input. The header and trailer are then assembled by the *builder* (apart from the CRC, which cannot

be known before the event data are available), and sent to the *FIFO* block to be stored until needed.

When the event data are ready to be read out, the control logic will notify the *builder* block with a pulse on the start input. The *builder* then sends the header word out to the *MUX* block, making a note of the length of the event. The control logic can then start sending the data to the *data_in* input. With each word of data sent, the CRC is updated, and the counter of the event length is decremented by the *builder* block. When the entire event has been sent, the *builder* block sends the trailer word, with the newly calculated CRC inserted in the appropriate place, to the *MUX* block, which sends the resulting word to the output.

Package List

```
LIBRARY ieee;
USE ieee.std_logic_1164.ALL;
```

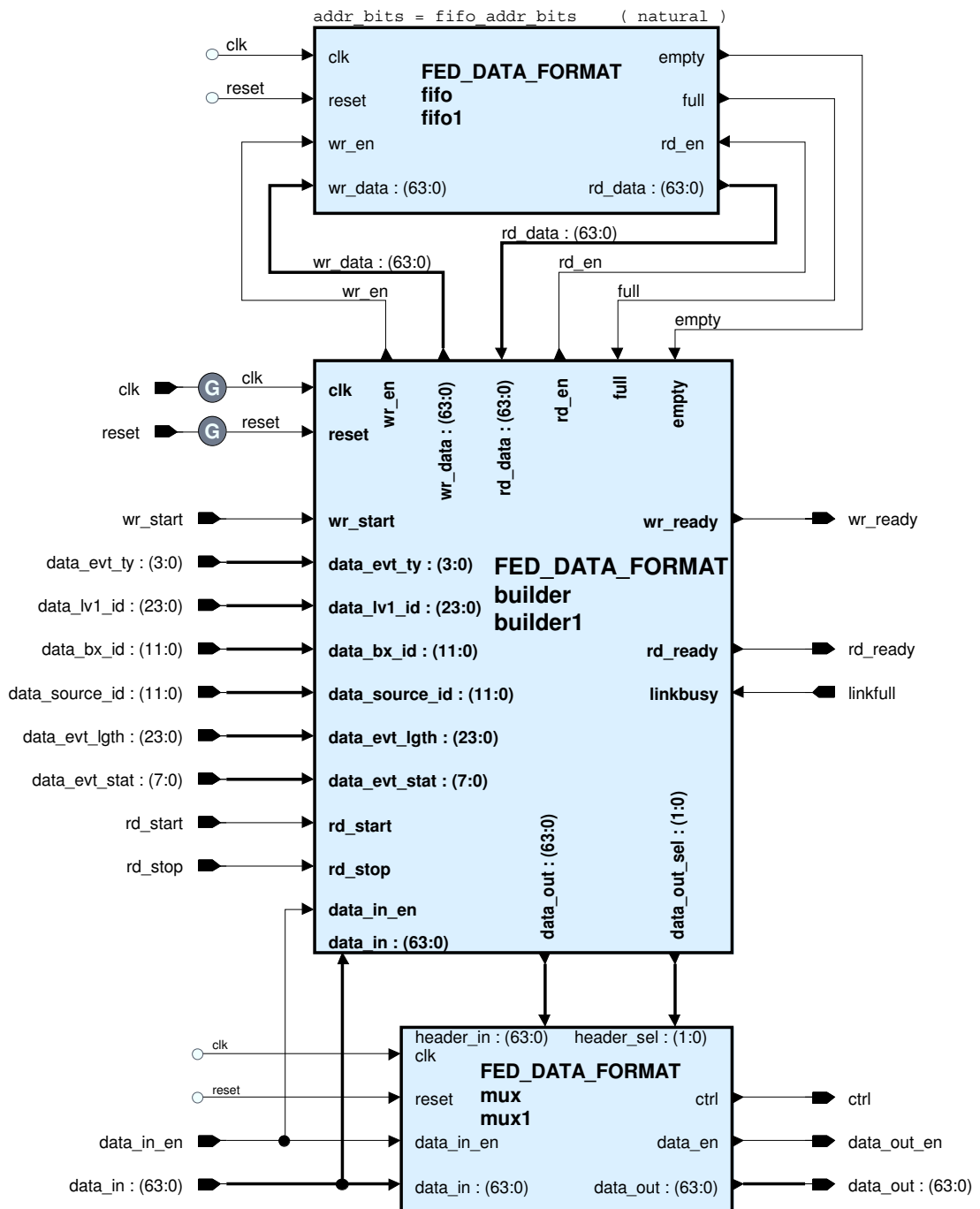


Figure 4.12: Block diagram of the header formatting block.

The *mux* block simply switches between the incoming data and the header/trailer sent by the *builder* block. The *header_sel* input specifies whether the *mux* should be outputting header, data, trailer or nothing. This allows the *mux* to issue a warning during simulation if data is sent at the wrong time.

The *fifo* block buffers the header and trailer words until they are needed. Internally it contains a 64-bit wide memory block (*mem64*) for storage, and it has two pointers into this memory that define where data should be written, and from where data should be read. Two outputs (*full* and *empty*) are also provided, which allow detection of overflows and underflows during simulation.

The *mem64* block (inside the *fifo*) provides a block of memory 64 bits wide, and of variable depth, specified by a generic value. Three different implementations were written, one using pairs of 32-bit wide Virtex II 16-kbit block RAMs, one using Spartan II/Virtex 4-kbit block RAMs, and one general implementation using an array of signals, which, when synthesised with Leonardo Spectrum, uses distributed RAM.

The VHDL code for the actual CRC function (used in the *builder* block) was generated with the Easics CRC Tool [44]. As the polynomial to be used in the CRC of the trailer has not yet been decided, two different versions were generated, corresponding to the two standard 16-bit CRC polynomials currently in widespread use: the CCITT standard CRC-16, and the X.25 standard.

A testbench was written to verify the operation of the VHDL code. It sends a range of typical signals to the header building block, using a pseudorandom number generator to create the data for each event, and writes the output to a text file. A short period of the simulation is shown in figure 4.13, following various signals over a period of 1 μ s. Each horizontal line represents a different signal, with simulation time running from left to right. The top signal represents the 40 MHz system clock, followed by various other internal signals. The bottom three signals represent the *data_out_enable* signal, the data/control bit and the 64-bit wide data bus respectively, and the first event can be seen being transmitted over these lines. A program was written in C to verify the output data, and both the VHDL testbench and this C program are listed in appendix B.

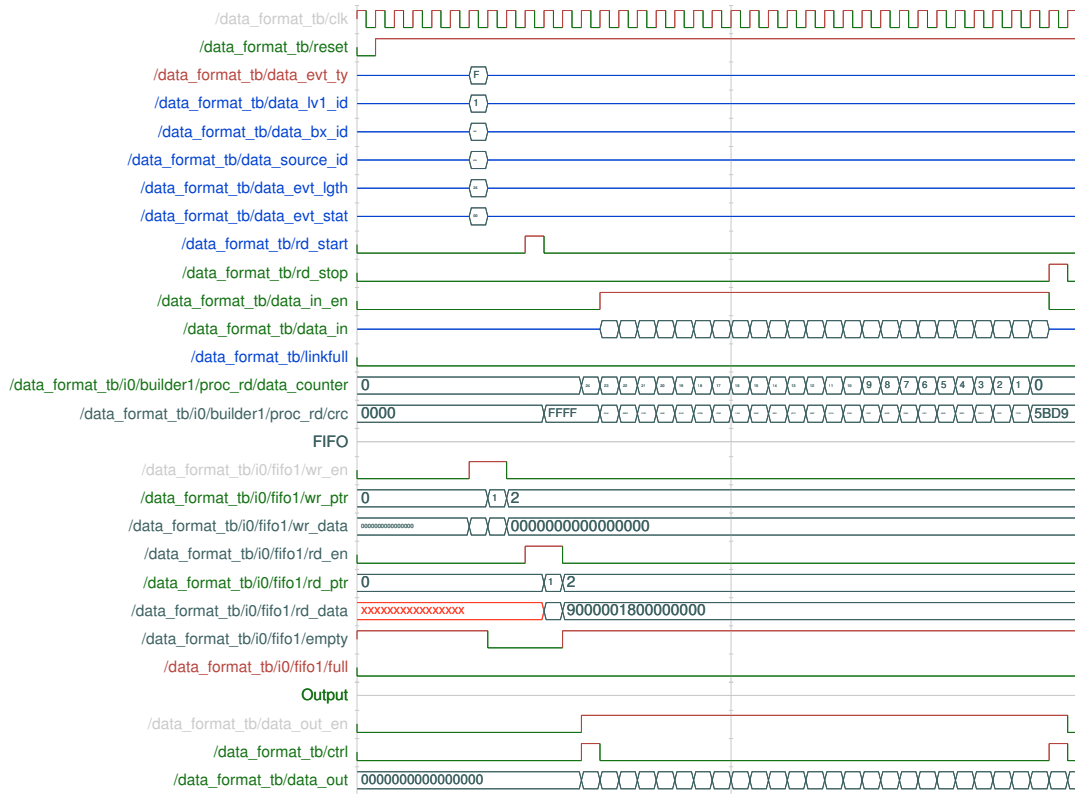


Figure 4.13: A short period of the simulation.

To test the generated CRC code, the verification code contains a reference CRC implementation [43]. The parameters used for the reference CRC are shown in table 4.3. The two values for the polynomial correspond to the standard CRC-16 and X.25 CRCs, respectively. The highest bit is not included as this is already implicit in the width of the polynomial. The `cm_init` value is what the CRC is set to at the start of a calculation, and `cm_xorot` is XORed with the CRC at the end of a calculation. The `cm_refin` and `cm_refot` parameters specify whether the input (data) and output (CRC) should be reflected; if false, the data are processed most-significant-bit first, and if true the data are processed least-significant-bit first.

Parameter	Value	Description
cm_width	16	Width of polynomial
cm_poly	0x8005 / 0x1021	Polynomial
cm_init	0xFFFF	Initial value
cm_refin	FALSE	Reflect input
cm_refot	FALSE	Reflect output
cm_xorot	0x0000	XOR Output

Table 4.3: Parameters for the reference CRC.

Once verified, the header generation code was synthesised for a Xilinx Virtex-II FPGA (speed grade -4), using Leonardo Spectrum. Three different versions were synthesised, corresponding to the two possible CRC polynomials, and a version that did not calculate a CRC (as a reference). The results of the synthesis are given in table 4.4. For each version, the area of the implementation (in slices, and as a percentage of a 1 million gate FPGA), and the maximum clock speed, are given. The CRC-16 polynomial is slightly slower, but uses slightly less area of the FPGA. In the X.25 version, the CRC calculation is no longer a bottleneck, it being just as fast as the reference version with no CRC calculation. In fact, in these versions, the bottleneck is an adder in the *builder* block, where the event length is incremented by two, to account for the two extra words (header and trailer). It may be possible to optimise this adder at the expense of a small amount of area, although the speed increase is likely to be small, and is probably unnecessary.

Name	Polynomial	Slices	Fraction	Speed (MHz)
Reference	-	166	3.3%	86.6
CRC-16	(0, 2, 15, 16)	223	4.4%	85.8
X.25	(0, 5, 12, 16)	240	4.7%	86.6

Table 4.4: Synthesis results for the header building code.

Neither of the CRC implementations reaches the 100 MHz maximum clock speed of the S-LINK64. However, the link has to be driven by one of the FED's on-board clocks, which are all multiples of 40 MHz, and so in practice it would be

driven at 80 MHz. Therefore both possible polynomials are fast enough to be implemented in the back-end FPGA.

4.5 Summary

The FED has to process huge volumes of data, using zero suppression to reduce this for the later stages of processing. To be able to cope, it must use highly parallel processing, to which FPGAs are very well suited. The code for these FPGAs is being developed in Verilog (front-end FPGA) and VHDL (back-end FPGA).

Each event sent to the DAQ is wrapped in a common data format header/trailer, which are common to all sub-detectors. They contain information such as the level-1 trigger number and the bunch crossing number, to help identify the event, along with the event length, status bits, and error detection information. This is implemented as a CRC, which is a reliable and proven method of error detection.

I have developed VHDL code for the generation of the common data format header and trailer, except for the CRC code, for which a publicly available tool was used. For reasons of consistency the same code will be used throughout the whole of the CMS readout system.

Chapter 5: Analysis of Data Flow and Buffering in the FED

The tracker readout system has to handle huge volumes of data, from about 10 million channels. Level-1 triggers arrive randomly at an average frequency of 100 kHz, and the tracker occupancy can vary, leading to unpredictable fluctuations in the data rates. There are a number of buffers distributed along the readout chain, which help to de-randomise the flow of data, but they also introduce the risk of overflows. In such a complex system, even a very small risk of overflow in individual buffers can easily lead to disastrous results for the physics data, as all the small probabilities quickly add up to affect a significant

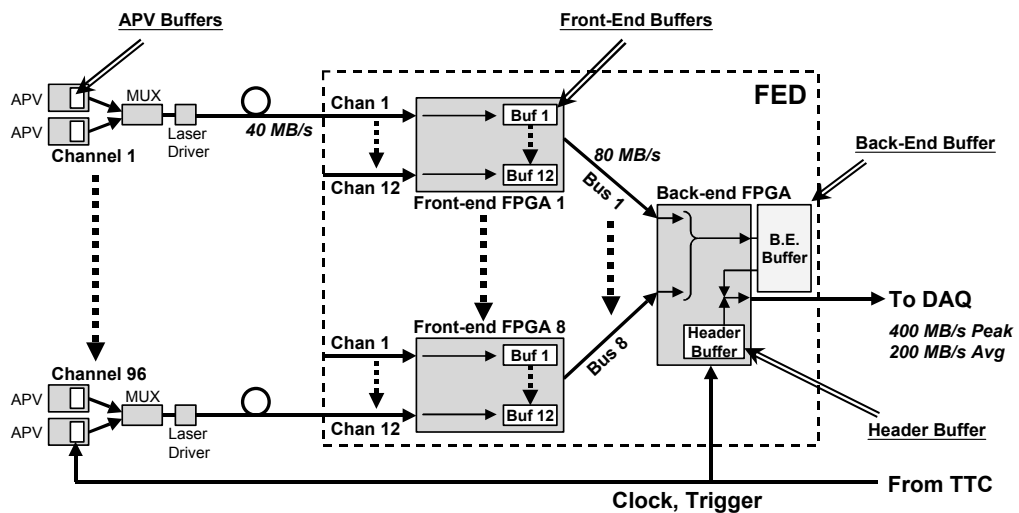


Figure 5.1: Data flow and buffers in the tracker readout system.

proportion of events.

An overview of the flow of data and the buffers in the readout system is shown in figure 5.1. Each FED contains a back-end buffer, a header buffer, and a total of 96 front-end buffers (one for each channel). In addition, each of the 192 APVs per FED (~80 000 in total) contains its own buffer.

5.1 The APV Buffers

Each APV contains a 192-location pipeline that stores the analogue data from the detector until a level-1 trigger is received. Individual triggers may arrive only 3 clock cycles (75 ns) apart, but the APV takes 7 μ s to transmit the data for the 128 channels. The APV can buffer up to 32 samples without overflowing (in deconvolution mode, this corresponds to 10 triggers, as each trigger requires 3 samples). It is important that the APVs should never overflow, as, if they do, they are left in an undefined state. This could be handled by pausing the triggers for a short time and sending a reset signal, but it would be preferable to prevent this situation if possible. However, since the APVs all receive trigger and reset signals at the same time, and the events are all a fixed size at this stage, they are completely synchronous and behave predictably.

5.1.1 The APV Emulator

The trigger system will have an APV emulator (APVE), which will monitor the L1A signal being sent to the front-end, keeping track of the number of events stored in the APV, and veto any triggers that would cause the APVs to overflow. Therefore, the APV buffers will never overflow, as any trigger that would have caused this to happen will simply not be sent.

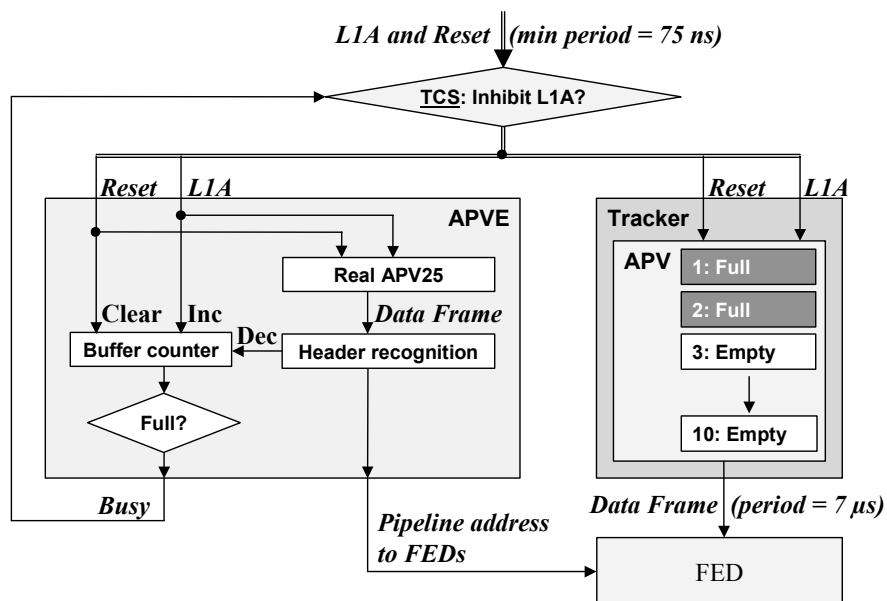


Figure 5.2: The APV Emulator System.

(Adapted from ref [45]).

An overview of the APVE is shown in figure 5.2. It receives the same L1A and reset signals that are sent to the detector front-end. It contains a real APV25, logic to recognise an output frame, and a counter that keeps track of the number of events stored in the APV buffers [45]. On receipt of a level-1 trigger, the buffer counter is incremented, and when a frame is recognised on the output from the APV, the counter is decremented. When the buffer counter reaches the maximum level (10 in deconvolution mode, 32 in peak mode), the *busy* signal is asserted, which blocks any further triggers until the buffer levels decrease. If a trigger causes the buffer to become full, the trigger crate must receive the *busy* signal before the next trigger can be sent, and since consecutive triggers can be as close as three clock cycles (75 ns) apart, the APVE has to be extremely fast. For this reason it will be located in the trigger crate to keep the wiring distances as short as possible.

A useful side effect of using a real APV in the APVE is that the correct pipeline address in the APV header can be known. If this *golden header* is transmitted to the FEDs, then the received APV headers can be crosschecked with this header – on loss of synchronisation an error can be flagged. If the single APV fails, the APVE could block all CMS triggers indefinitely. To prevent the APV being a single point of failure, it may be possible to use three APVs with majority logic for added security.

5.2 Modelling the FED

The data flow in the FED is not so simple, because of the zero-suppression that takes place. The amount by which the data can be compressed depends on the occupancy, which varies over the different channels, and from event to event.

A program was written in C++ to model the flow of data within the FED. Several assumptions were made, in order to keep the simulation simple and fast enough to generate a useful amount of data in a reasonable time. Only one channel of a front-end FPGA is simulated. There is no need to simulate all eight front-end FPGAs, as they are all doing the same thing in parallel, and each is connected to the back end FPGA individually via a point-to-point link. Similarly, the 12 channels within a front-end FPGA all behave alike. The only difference

here is that the buffers are read out sequentially, so the twelfth channel, which for any particular event is always the last to be read out, is the most likely to overflow. For this reason, only the twelfth channel is simulated. For simplicity, it was assumed that for each event, all twelve channels receive the same sized frames. This means that only one frame needs to be generated per event, and used for all channels, which speeds up the simulation.

Only the sizes of the events were generated, not the actual hit strips, as the actual values of the hit strips are irrelevant to the flow of data. This means that many parts of the FED do not need to be simulated, such as the pedestal and common mode subtraction, the zero suppression, and the clustering. This provides a significant increase in speed, and makes the model more general, allowing it to be easily adapted to the back-end buffers. The number generators for the event sizes and L1A trigger times can be selected at run-time from a constant value, or random numbers generated from one of several possible distributions, including uniform, Gaussian, Poisson and exponential, as well as an arbitrary distribution from a user-supplied histogram.

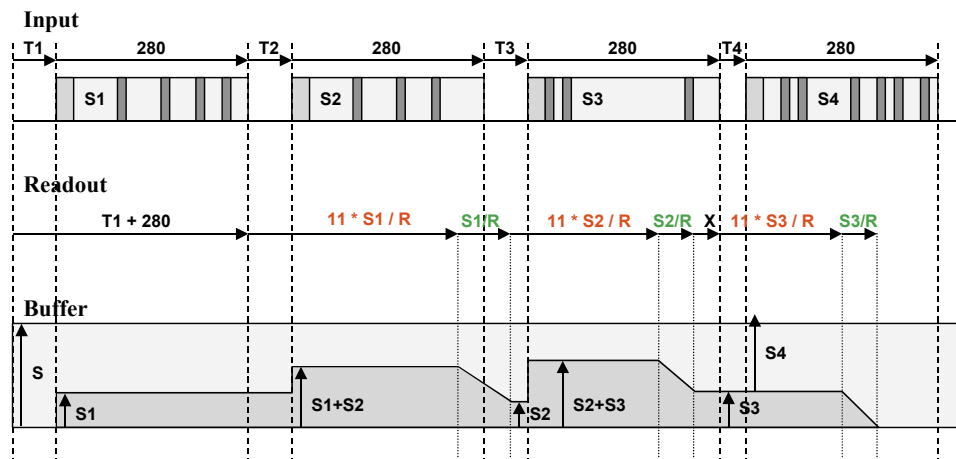


Figure 5.3: Graphical representation of the FED buffer model.

The operation of the model is shown in figure 5.3. The input line represents the APV data frames, with length 280 clock cycles, of variable size S_n , and separated by time T_n . The buffer line represents the fill level of the buffer. Since the distribution of hits within each frame is unknown, the whole of the data are

stored in the buffer at the start of the event, and the buffer level jumps up by the size of the event. Only once the whole of the event is stored in the buffer, at the end of the frame, can the data start being read out. However, since we are looking at the last of the twelve channels, the eleven other channels must be read out first. The status of the readout link is represented by the readout line. After the end of the first event, the first eleven channels are read out, taking a time per channel equal to the size of the event divided by the output rate of the link. Only after this can the twelfth channel be read out, and during this time, the buffer level falls linearly.

If an event is too large to fit in the remaining buffer capacity (as in event 4 in the diagram), the whole event is discarded. A counter keeps track of the number of lost events, and at the end of the run, this is displayed and saved to a file for later analysis.

5.2.1 Source Data

In order for the simulation to be useful, the generated event sizes should be similar to the actual distribution of event sizes in the tracker, so a histogram of event sizes was obtained from Monte-Carlo simulation [46] (see figure 5.4). The graph shows the frequency of event sizes per 768-strip detector (read out by 6 APVs) in the inner layer of the tracker, where the occupancy is highest. As only the total number of hit strips per event is known, but not the distribution of the strips within each event, it is not possible to obtain the exact distribution per APV.

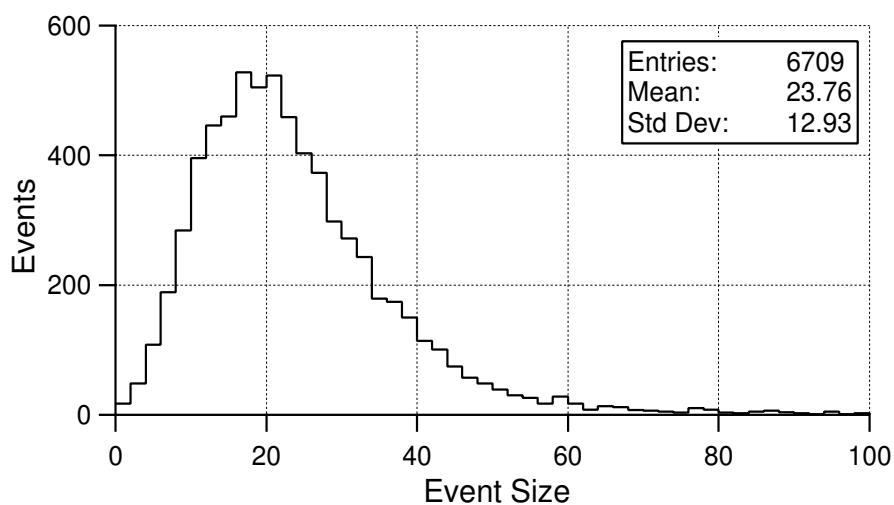


Figure 5.4: Distribution of event sizes in strips per detector, from Monte-Carlo.

(Adapted from ref [46])

For example, an event with 18 hit strips may consist of one APV with 18 hits and 5 with none, or all 6 APVs having three hits each. Therefore, an estimate was obtained by scaling down the event sizes by a factor of six, which unfortunately results in an underestimation of the spread of event sizes, but the average event size is correct, and should be good enough for the purposes of this simulation. The resulting distribution is shown in figure 5.5 (solid line) along with a fitted Poisson (dashed line).

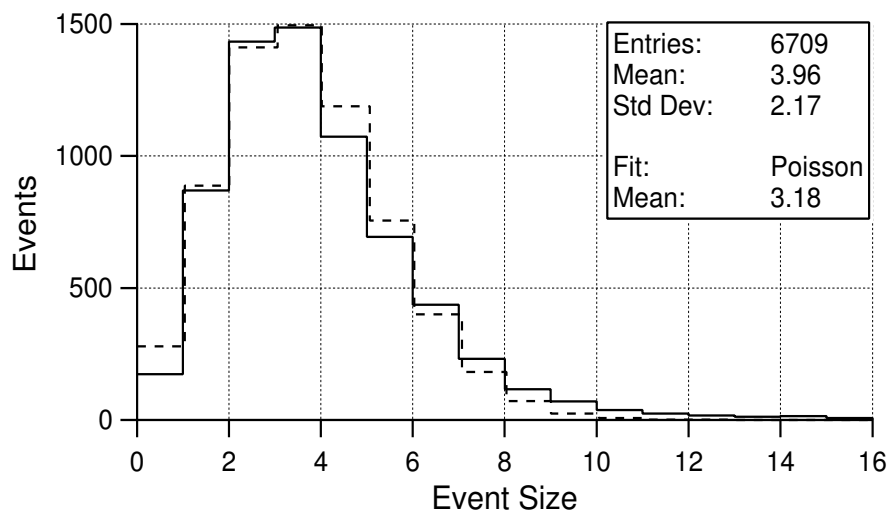


Figure 5.5: Estimated distribution of event sizes in strips per APV.

The Monte-Carlo simulation contains only minimum-bias events [47], whereas the real data will contain a small fraction of other events, containing interesting physics data. These events will tend to have a higher occupancy than the minimum bias events, due to features such as jets, and may therefore have some impact on the buffer overflow rates. In order to account for these and any other effects, a fraction of the events (0.1 %) were given an occupancy of 100%. This should be enough to account for any unforeseen fluctuations in the tracker occupancy.

The mean event size is about 4 hits per APV, and the simulation was performed either with this histogram, or with Poisson distributed event sizes in the cases where other values of occupancy were required. In both cases, the 0.1 % of events with high occupancy were included.

Only the front-end buffer is modelled. However, by suitable changes to the parameters of the simulation, i.e. data rates and buffer size, it is possible to obtain a reasonable simulation of the back-end data buffer. The header buffer can be modelled by counting the number of events in the back-end data buffer (including ‘lost’ events, which are still stored, but given a size of 0), as opposed to the total volume of data, because the data stored in the header buffer have a fixed size per event. The actual number of events in the header buffer could be greater than the number of events in the data buffer, if L1A signals have been received but the frames from the APVs have not yet arrived at the FED, so the peak level of the header buffer may be underestimated. However, this difference will be limited by the number of events that can be buffered by the APV, which is 10 in deconvolution mode, or 32 in peak mode, and is negligible when compared to the total buffer size.

5.3 Simulation Results

5.3.1 Zero-Suppression Mode

In normal FED operation, the zero-suppression mode is used. Level-1 triggers are sent at a maximum average rate of 100 kHz with a Poisson distribution, and the sizes of the events transmitted to the DAQ depend on their occupancy.

Front-End Buffer

The fraction of events lost due to overflow in the front-end buffer is shown in figure 5.6, for several buffer sizes, and as a function of the data rate of the link to the back-end FPGA, assuming that this rate can be sustained, i.e. the back-end buffer is not getting full. The event sizes are all generated from the histogram of Monte Carlo events, and the trigger rate is assumed to be a worst-case 140 kHz, corresponding to back-to-back events from the APV. The results for three different buffer sizes are plotted; the actual buffer size is about 4 kbytes (the solid line), corresponding to about 250 events in the highest occupancy inner tracker layer.

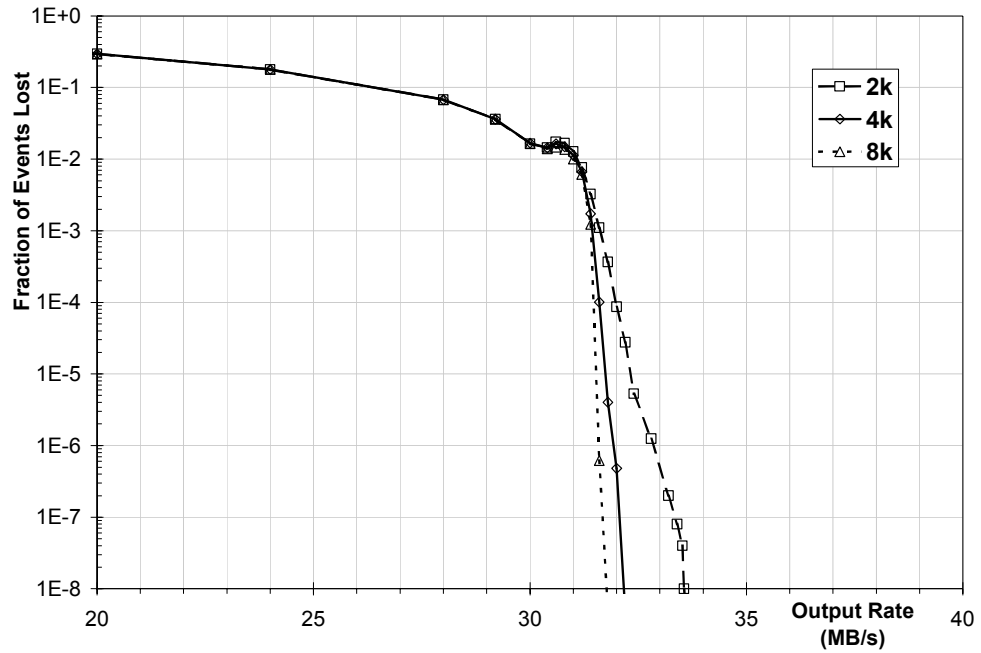


Figure 5.6: Zero-suppression, front-end: events lost vs. output rate.

The actual data rate between the front and back-end FPGAs is 80 Mbyte/s, which is well off the end of the x-axis of the graph. The curves fall extremely quickly, and at 80 Mbyte/s there is effectively a zero probability of buffer overflow.

If we fix the readout rate at 80 Mbyte/s, and instead vary the occupancy, we get the results shown in figure 5.7. Again, for the worst-case inner-tracker occupancy of 4%, there is a virtually zero probability of buffer overflow. Obviously this still assumes that the readout rate of 80 Mbyte/s can be sustained indefinitely; to verify under what conditions this is true, we need to look more closely at the back-end buffer.

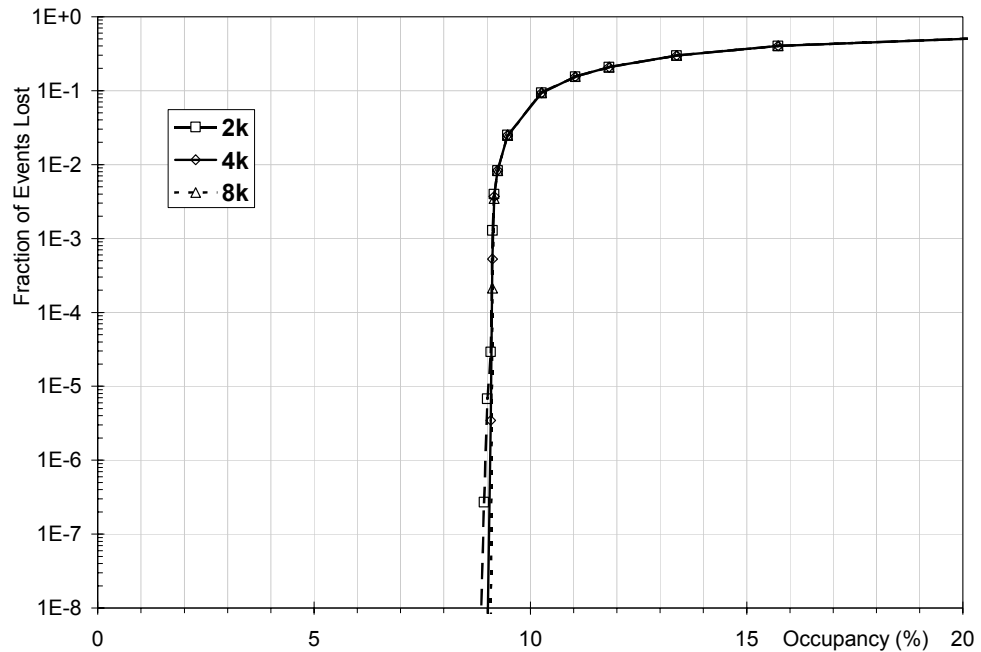


Figure 5.7: Zero-suppression, front-end: events lost vs. occupancy.

Back-End Buffer

The maximum data rate between the front-end and back-end FPGAs is so high, relative to the average data rate, that the front-end buffers will effectively never overflow, as long as there is space in the back-end data buffer. If some of the parameters of the simulation are changed, i.e. the buffer size and data output rate, reasonably good results may be obtained for the back-end data buffer, as well as for the front-end buffers.

The results were calculated for buffer sizes of 1 Mbyte and 100 kbyte (see figure 5.8). The buffer was originally planned to be 1 Mbyte, but was later increased to 2 Mbyte because two external 1 Mbyte RAM chips were used in order to reduce the data transfer rate to each chip and simplify the design. It can be seen that there is virtually no difference between the two buffer sizes, indicating that any further increase in buffer size should have no significant effect, and the 1 Mbyte (and therefore also 2 Mbyte) buffer is large enough.

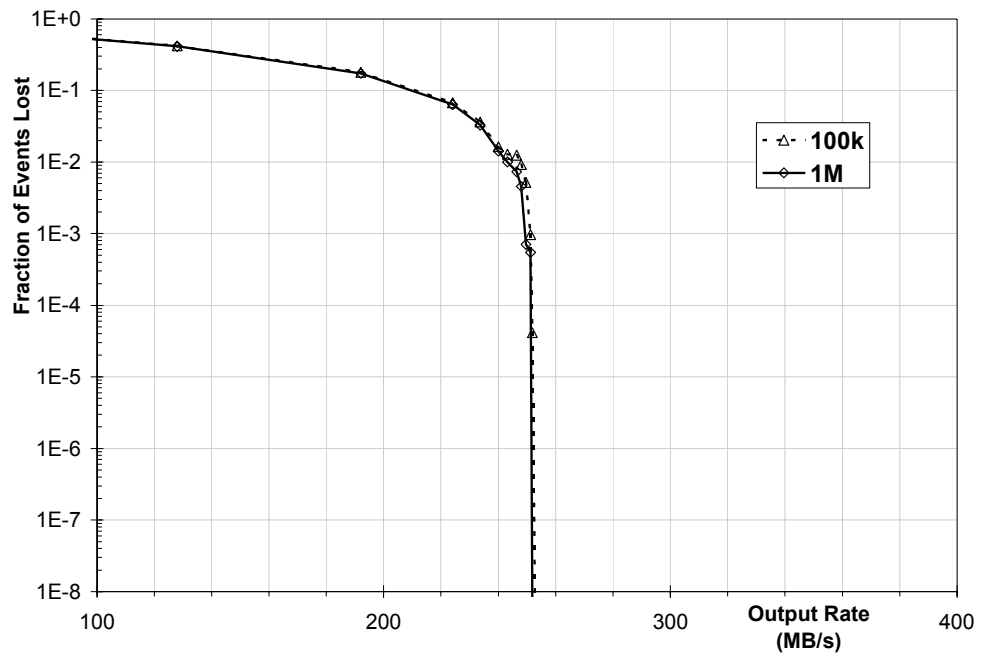


Figure 5.8: Zero-suppression, back-end: events lost vs. output rate.

In order to handle a tracker occupancy of 4 %, it is necessary that the DAQ link can sustain a data rate of at least 260 Mbyte/s, which is higher than the specified maximum average rate of 200 Mbyte/s. However, this was using back-to-back frames at 140 kHz; when 100 kHz Poisson level-1 triggers are used this rate falls to 185 Mbyte/s, which is within the specified range. Also the average occupancy over any individual FED should be lower than 4 %, as each FED will handle a mixture of high-occupancy (inner barrel) and lower occupancy layers.

In figure 5.9, the overflow rate of the back-end buffer is plotted as a function of the tracker occupancy, for three different output rates, and using back-to-back (140 kHz) frames. It can be seen that the maximum occupancy before the back-end buffer starts overflowing depends strongly on the output data rate.

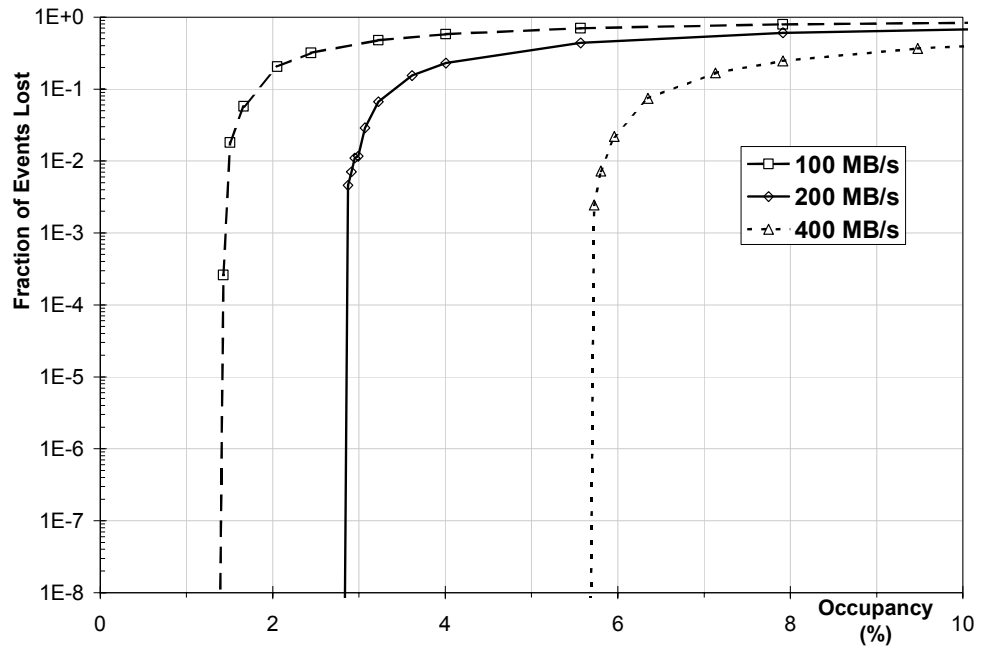


Figure 5.9: Zero-suppression, back-end: events lost vs. occupancy.

The maximum occupancy was found for several output rates, both for back-to-back frames (140 kHz) and for 100 kHz Poisson triggers, and the results are shown in figure 5.10. The maximum occupancy was found to the nearest 0.1 %, such that no events were lost in a total run of 10^8 events. At a data output rate of 200 Mbyte/s and with 100 kHz Poisson level-1 triggers the FED can just cope with an occupancy of 4 %. However, as mentioned earlier, the actual occupancy will be less than this, since each FED will handle a mixture of high and low-occupancy layers.

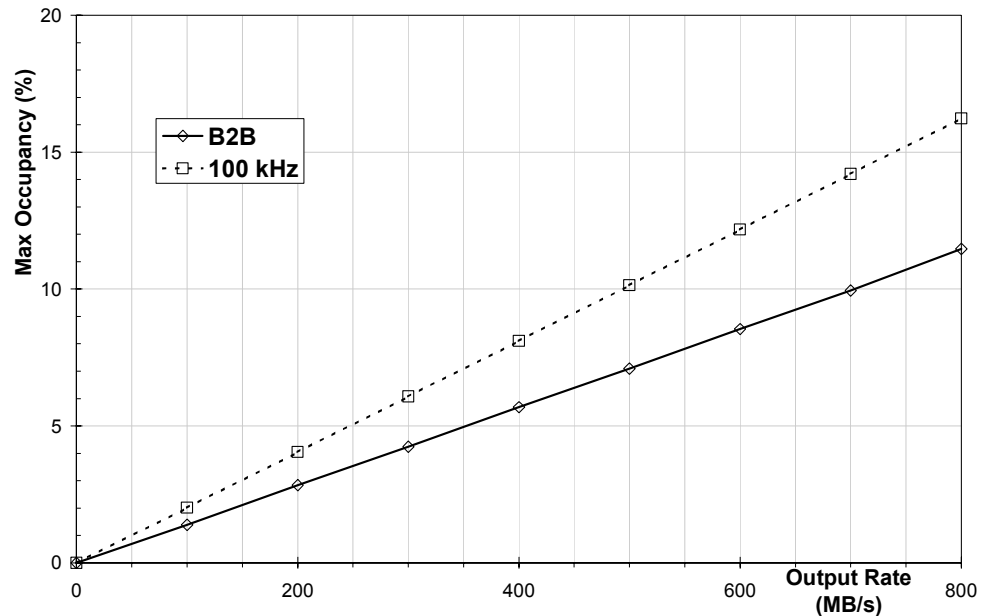


Figure 5.10: Zero-suppression, back-end: maximum occupancy vs. output rate.

Header Buffer

The FED also has a header buffer, which contains the common-data-format header and trailer, which is used to identify each event. It was shown in the previous sections that under normal conditions the data buffer will rarely, if ever, overflow. However there may be pathological cases, such as some form of hardware or software failure, that cause the occupancy and/or trigger rate to increase, causing the data buffer to overflow. In this case, the FED will send just the header and trailer without the data (an empty event) to the DAQ. This allows the DAQ to stay in synchronisation, but reduces the data rate to the DAQ allowing the buffers to recover without the system having to be reset. However, it is important that the header buffer does not overflow if this is to be effective.

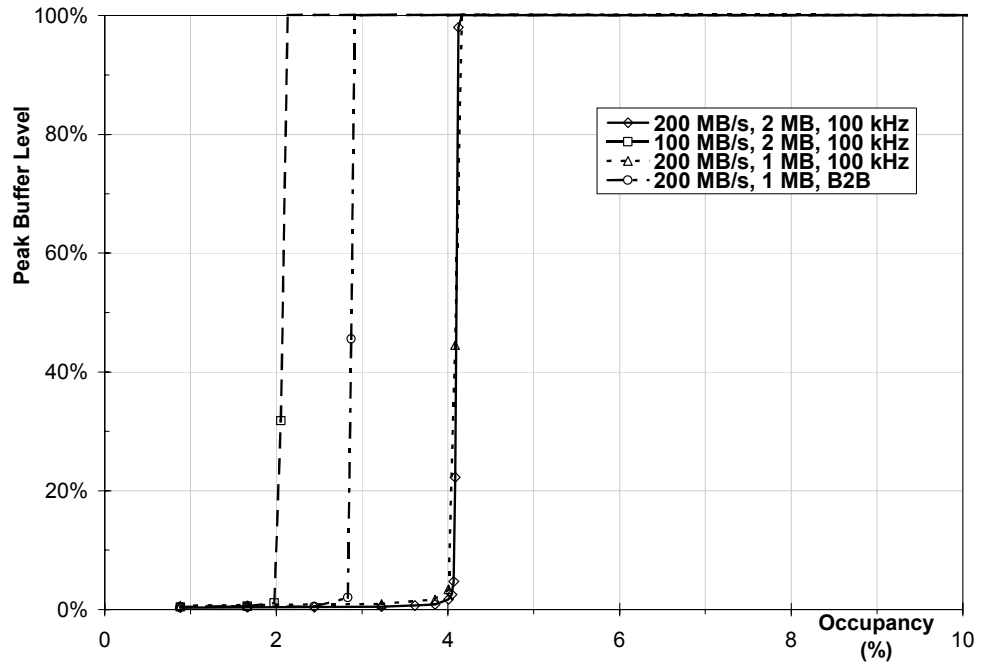


Figure 5.11: Zero-suppression: peak level of data buffer vs. occupancy.

The peak level of the back-end data buffer is shown in figure 5.11, as a function of tracker occupancy. The peak level was calculated as the maximum fill level of the buffer during a run of 10^6 events. It can be seen that in normal operation, the buffer level stays very low, at the level of a few percent. At the point when the buffer starts overflowing, the peak level very quickly reaches 100%. The occupancy at which this happens depends on the output rate and the trigger rate, but not on the buffer size (as is expected, since there was virtually no difference between the overflow rates of the different buffer sizes in figure 5.8).

If we now look at the number of events in the buffer, as opposed to the volume of data, this gives us the level of the header buffer, as in this buffer each event is a fixed size. The results for various parameters are shown in figure 5.12. It can be seen that at low occupancy the peak level of the header buffer is also very low. However, as the occupancy increases, and the data buffer starts overflowing, the header buffer reaches a constant level, independent of the occupancy.

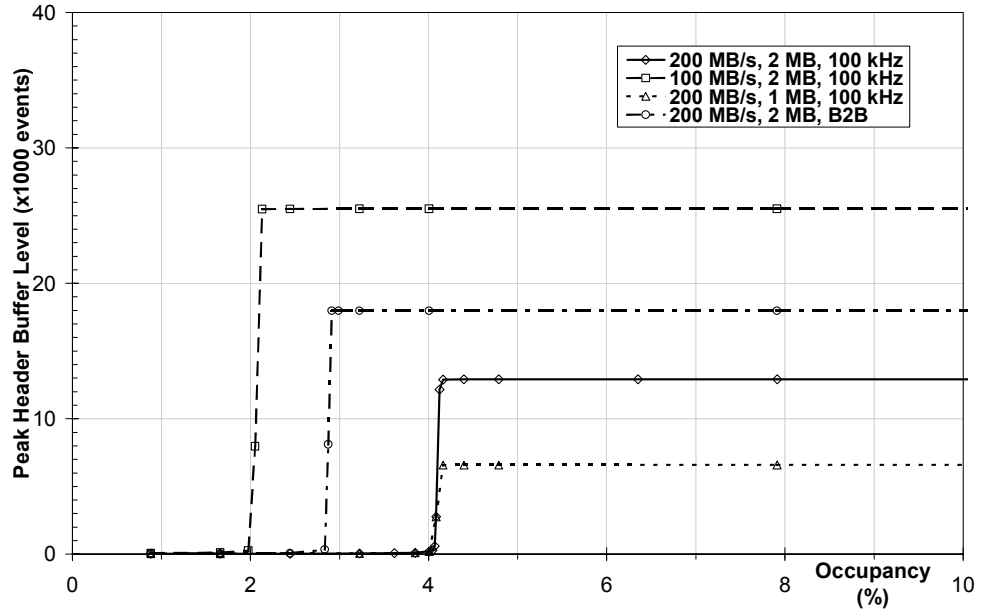


Figure 5.12: Zero suppression: peak level of header buffer vs. occupancy.

The header buffer reaches its peak level when the data buffer is overflowing, i.e. the rate of data entering the buffer is greater than the output link can cope with. The number of events stored in the data buffer, N_d , is given by the formula:

$$N_d = \frac{S_d}{S_e} \quad \text{Equation 5.1}$$

where S_d is the size of the data buffer, and S_e is the average event size. The average frequency of events leaving the header buffer, F_h , is equal to the frequency of events entering it, i.e. the trigger frequency, T . The frequency of events leaving the data buffer, F_d , is given by the formula:

$$F_d = \frac{R}{S_e} \quad \text{Equation 5.2}$$

where R is the readout rate, and S_e is the average event size, as before. Since the header buffer also includes the lost events that didn't fit in the data buffer, the number of events it holds will be greater, by a factor of F_h / F_d . Combining this

with equation 5.1 and equation 5.2 we can see that the number of events in the header buffer is given by the formula:

$$\begin{aligned}
 N_h &= N_d \cdot \frac{F_h}{F_d} = \frac{S_d}{S_e} \cdot T \cdot \frac{S_e}{R} \\
 &= \frac{S_d \cdot T}{R}
 \end{aligned}
 \tag{Equation 5.3}$$

i.e. it is proportional to the size of the data buffer and to the trigger rate, and inversely proportional to the output data rate. It is also independent of the size of the events.

The peak level of the header buffer (from figure 5.12) is compared with the predicted values (from equation 5.3) in table 5.1. It can be seen that the formula gives a reasonably good estimate of the peak header buffer level, although it does underestimate the actual values by up to 10 %. This is probably due to statistical variation in the flow of data.

O/P Rate (MB/s)	Data Buffer (MB)	Trig Rate (kHz)	Peak Headers (1000 events)	Calculated (1000 events)
200	2	100	12.9	12
100	2	100	25.5	24
200	1	100	6.6	6
200	2	140	18.0	16.8

Table 5.1: Peak header buffer levels.

Using this result, it may be possible to provide a header buffer large enough so that it can never overflow, even in pathological situations with very high occupancy that cause the data buffer to overflow. This assumes that the output data rate can be sustained; if the DAQ fails, then there is obviously nothing that can be done to prevent the eventual loss of data. The header buffer sizes needed are reasonably large, being in the region of 10 000 events or more, and it may not be possible to provide such a large header buffer memory. To overcome this, a limit could be imposed on the size of the data buffer, meaning data would be lost sooner, but ensuring that the headers are always available for every event.

5.3.2 Raw-Data Mode

In certain conditions, such as the early detector study and calibration runs, and during heavy-ion runs, the FED will be run in raw data mode. In this mode, zero-suppression of the data will not be performed, and the entire events will be sent to the DAQ. The events will therefore all be the same size, and much larger than in normal operation. In order for the readout system to be able to cope with this, the level-1 trigger rate will have to be much lower than in normal operation.

Front-End Buffer

The results for the front-end buffer are shown in figure 5.13, as a function of the average level-1 accept rate, for three different buffer sizes. The actual buffer size is 4 kbyte, corresponding to 16 raw events. It can be seen that up to a trigger rate of 10 kHz, and with a 4 kbyte buffer, less than one event is lost per 10^8 .

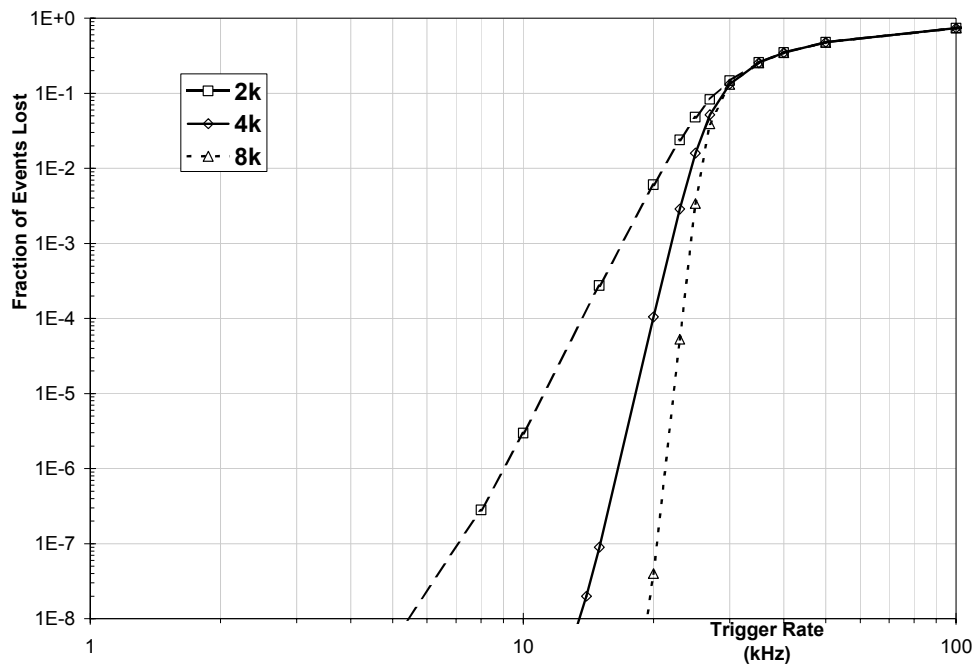


Figure 5.13: Raw data, front-end: events lost vs. trigger rate.

Back-End Buffer

The results for the back-end buffer are shown in figure 5.14, as a function of the level-1 accept rate, and for three output rates.

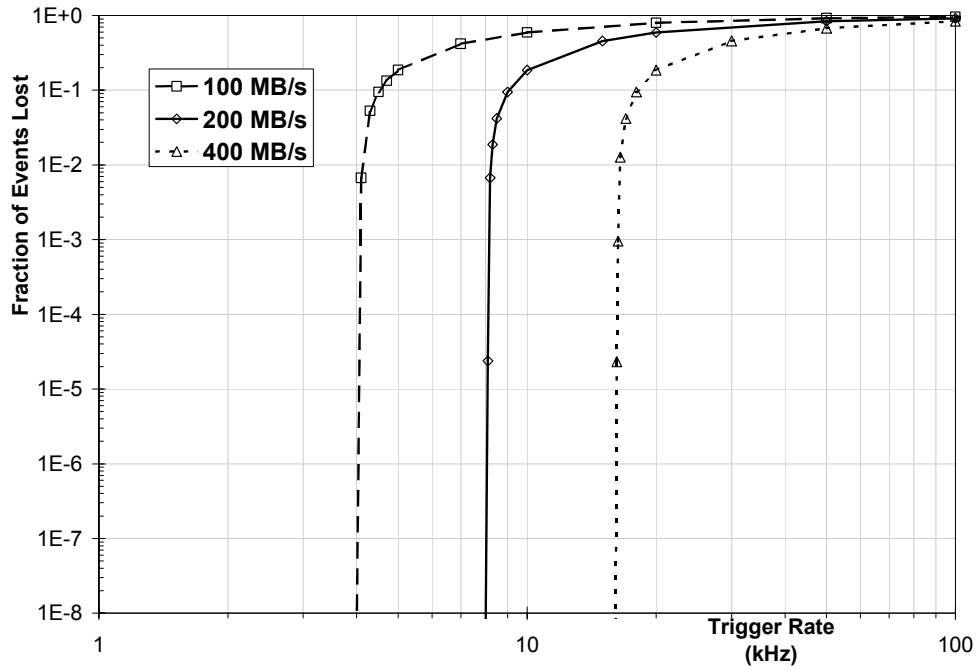


Figure 5.14: Raw data, back-end: events lost vs. trigger rate.

The maximum level-1 trigger rate depends on the output rate, and at 200 Mbyte/s, the FED can cope with trigger rates up to just under 8 kHz. The graph in figure 5.15 shows the maximum level-1 accept rate as a function of the data output rate.

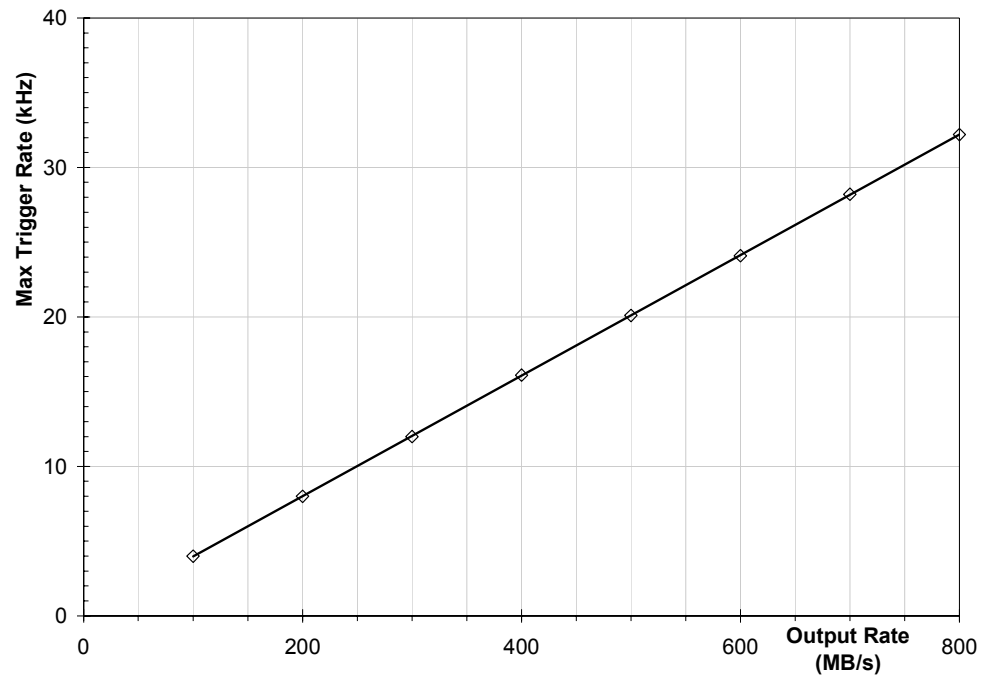


Figure 5.15: Raw data: maximum trigger rate vs. output rate.

5.4 Summary

There are a large number of buffers throughout the tracker readout system, and it is impossible to guarantee that none of them can ever overflow. However, by using high data transfer rates, compared to the average data transfer rate, the levels of the buffers can be kept low. A software model of the flow of data through the FED and the levels of its buffers was developed. The results showed that with the expected conditions, the FED buffers should never overflow. It was shown that even in exceptional conditions, when the data buffers start to overflow, the level of the header buffer will never exceed a certain level that depends on the data buffer size, the level-1 trigger rate, and the output data rate. If the header buffer is chosen to be larger than this size, then even in pathological cases, the FED will be able to send empty events to the DAQ, allowing it to remain in synchronisation.

Chapter 6: Perspectives

6.1 FED Schedule

The LHC is due to start operating in 2007 and the 440 FEDs must be ready by then. A first batch of 2 FEDs is currently under construction. The board level routing is in its final stages, and the PCB manufacture and board assembly are expected to be completed by the end of 2002. The prototype FEDs will then be thoroughly tested at RAL and Imperial College over the following months. After preliminary tests are completed, the optical receivers will be mounted on the boards, and also tested. By mid 2003 there will be a design review, and any necessary design changes will then be implemented.

The construction of a second batch of 10 FEDs will start following the review of the previous batch. These are expected to be assembled, production tested, and delivered to CERN by the end of 2003. Field tests of these FEDs will then be carried out until the end of 2004.

By this time, the procurement and production of the remaining FEDs will have started. FED assembly is scheduled for completion by mid 2005. From that point onwards, field tests at CERN will run until mid 2006, and the installation at CMS will start in parallel with these tests and should be completed by the end of 2006, in time for the first LHC collisions, scheduled for mid 2007. This is a reasonably tight schedule, and may have to adapt to external circumstances, so effort will be needed to ensure it stays on track.

6.2 FED Testing

The testing of the FEDs will consist of a number of stages. The PCB manufacturer should perform bare-board tests, and on delivery of the PCBs to RAL they will be visually inspected and simple tests for short-circuits will be performed. The boards will then be assembled, and should be visually inspected by the assembly company. On delivery to RAL, each FED will be given a unique 3-digit serial number, with each board labelled and programmed electronically, allowing them to be traced individually. The first pair of FEDs will also be thoroughly inspected visually for missing or incorrect components, solder bridges,

and other general visible damage, as well as the power rails being tested for short circuits.

6.2.1 JTAG and Boundary Scan Testing

The boards will then be ready to be powered-up for the first time, and voltages will be measured at specific points and the results recorded. The next step will be to verify that the JTAG chain is operational, and all the correct devices are present in this chain. A boundary scan test can then be performed, which will verify the connections between all devices in the JTAG chain. The FPGAs themselves will then be configured with simple designs, via the JTAG chain, to verify their basic functionality. During large-scale production runs, these JTAG tests will be performed by the assembly company.

6.2.2 Basic Analogue Tests

The analogue and digital parts of the FEDs will be tested using Xilinx Chipscope Integrated Logic Analyzer (ILA). This tool embeds logic analysis cores inside the FPGAs, allowing external ports and internal signals of the FPGA to be monitored via the JTAG port. The FPGAs will be configured with logic to distribute the relevant clocks across the board, and the delay FPGAs will additionally contain a Chipscope ILA on the ADC inputs. Signals can then be injected into the analogue circuitry, and the results read out via the JTAG port. At this point, one of the first two FEDs may be sent to Imperial College so that the remaining tests may be carried out in parallel.

6.2.3 Basic Digital Tests

Once the functionality of the board has been verified, then tests can begin on the firmware. The first FPGAs to be tested will be the delay FPGAs. They will be configured with their standard firmware, and the front-end FPGAs will be loaded with a Chipscope ILA connected to the raw data input. APV frame-like data will then be injected into the analogue section, allowing the verification of both the delay FPGA firmware, and the double data rate connection between the FPGAs. The front-end FPGAs will then be loaded with their standard firmware

and the back-end FPGA configured with a Chipscope ILA so that the front-end FPGA firmware can be verified.

The next step will be to load a basic VME interface into the VME FPGA, and plug the board into a VME crate. A simple program will be run on the crate controller to test the writing and reading of internal registers, using a VME bus analyser to verify signals on the VME bus. The interface between the VME and the other (delay, front-end and back-end) FPGAs can then be tested.

6.2.4 More Advanced Tests

A FED testing system is being developed at Imperial College. This will provide realistic input signals, in optical form, including the TTC clock and L1A signals. The output from the FED will be sent back to the testing system, allowing this to be compared to expected output data. The testing system is based around a PC, with a PCI-64 bus for the S-LINK64 receiver. This will eventually allow the testing process to be semi-automated, which will be necessary when testing large numbers of production FEDs.

6.3 Conclusions

Firmware code for the FED was developed in VHDL, including a testbench for verifying its functionality. It was designed with the back-end FPGA of the tracker FED in mind, but is general enough to be included in other systems. In this way, the same VHDL code will be used in the front-end drivers of all the CMS subdetectors, thus ensuring uniformity across the readout system.

The study into the data flow and buffering in the FED showed that in normal operating conditions, the FED will never overflow. The maximum tracker occupancy before overflow occurs was calculated as a function of output data rate, using both 100 kHz random triggers, and 140 kHz back-to-back triggers. At an output rate of 200 Mbyte/s these results were 4 % and 2.5 % respectively. For raw data mode, the maximum trigger rate was calculated as a function of the output data rate, and at 200 Mbyte/s this was found to be just under 8 kHz.

It was shown that the speed of the links between the front and back-end FPGAs was more important than the buffer sizes in preventing overflows in the

front-end buffers. Because of this, a link speed of 80 Mbyte/s was chosen over the other possibility of 40 Mbyte/s.

In addition, the header buffer was investigated. It was found that for any given trigger rate, buffer size, and output data rate, a maximum trigger buffer level could be calculated. The firmware for the back-end FPGA of the FED is still under development, and if enough memory is available for the necessary header buffer size, this may be exploited to provide a header buffer that can never overflow, no matter how high the occupancy, as long as the DAQ continues to accept data.

Appendix A: Common Data Format Implementation

The VHDL source code for the common data format header and trailer building block from the FED back-end FPGA is listed. It was developed using Mentor Graphics *FPGA Advantage*, which includes *HDL Designer* (previously called *Renoir*) for code entry, *ModelSim* for simulation, and *Leonardo Spectrum* for synthesis. All of the modules are written in VHDL, apart from the top-level *FED_DATA_FORMAT* block, which is a block-diagram (shown in figure 4.12), and therefore the listing for this block contains the generated VHDL code.

A.1 fed_data_format.vhd

```
-- hds header_start
--
-- VHDL Entity FED_DATA_FORMAT.data_format.symbol
--
-- Created:
--   by - corrinep.UNKNOWN (EMLYN)
--   at - 10:58:39 10/26/02
--
-- Generated by Mentor Graphics' HDL Designer(TM) 2002.1a (Build 22)
--
-- hds header_end
LIBRARY ieee;
USE ieee.std_logic_1164.ALL;

ENTITY data_format IS
  GENERIC(
    fifo_addr_bits : natural := 9;
    length_at_start : boolean := true
  );
  PORT(
    clk           : IN      std_logic;
    data_bx_id    : IN      std_logic_vector (11 DOWNTO 0);
    data_evt_lgth : IN      std_logic_vector (23 DOWNTO 0);
    data_evt_stat : IN      std_logic_vector (7 DOWNTO 0);
    data_evt_ty   : IN      std_logic_vector (3 DOWNTO 0);
    data_in       : IN      std_logic_vector (63 DOWNTO 0);
    data_in_en    : IN      std_logic;
    data_lvl_id   : IN      std_logic_vector (23 DOWNTO 0);
    data_source_id : IN      std_logic_vector (11 DOWNTO 0);
    linkfull      : IN      std_logic;
    rd_start      : IN      std_logic;
    rd_stop       : IN      std_logic;
    reset         : IN      std_logic;
    wr_start      : IN      std_logic;
    ctrl          : OUT     std_logic;
    data_out      : OUT     std_logic_vector (63 DOWNTO 0);
    data_out_en   : OUT     std_logic;
    rd_ready      : OUT     std_logic;
    wr_ready      : OUT     std_logic
  );
END data_format;
```

```

);

-- Declarations

END data_format ;

-- hds interface_end
--
-- VHDL Architecture FED_DATA_FORMAT.data_format.fed_data_format
--
-- Created:
--       by - corrinep.UNKNOWN (EMLYN)
--       at - 10:58:41 10/26/02
--
-- Generated by Mentor Graphics' HDL Designer(TM) 2002.1a (Build 22)
--
LIBRARY ieee;
USE ieee.std_logic_1164.ALL;

LIBRARY FED_DATA_FORMAT;

ARCHITECTURE fed_data_format OF data_format IS

    -- Architecture declarations

    -- Internal signal declarations
    SIGNAL data_out_sel : std_logic_vector(1 DOWNTO 0);
    SIGNAL empty        : std_logic;
    SIGNAL full         : std_logic;
    SIGNAL header_in    : std_logic_vector(63 DOWNTO 0);
    SIGNAL rd_data      : std_logic_vector(63 DOWNTO 0);
    SIGNAL rd_en        : std_logic;
    SIGNAL wr_data      : std_logic_vector(63 DOWNTO 0);
    SIGNAL wr_en        : std_logic;

    -- Component Declarations
    COMPONENT builder
    PORT (
        clk           : IN     std_logic ;
        data_bx_id    : IN     std_logic_vector (11 DOWNTO 0);
        data_evt_stat : IN     std_logic_vector (7 DOWNTO 0);
        data_evt_ty   : IN     std_logic_vector (3 DOWNTO 0);
        data_lvl_id   : IN     std_logic_vector (23 DOWNTO 0);
        data_source_id : IN    std_logic_vector (11 DOWNTO 0);
        wr_start      : IN     std_logic ;
        rd_data       : IN     std_logic_vector (63 DOWNTO 0);
        reset         : IN     std_logic ;
        rd_start      : IN     std_logic ;
        data_out      : OUT    std_logic_vector (63 DOWNTO 0);
        data_out_sel  : OUT    std_logic_vector (1 DOWNTO 0);
        rd_en         : OUT    std_logic ;
        wr_ready      : OUT    std_logic ;
        wr_data       : OUT    std_logic_vector (63 DOWNTO 0);
        wr_en         : OUT    std_logic ;
        data_evt_lgth : IN     std_logic_vector (23 DOWNTO 0);
        rd_ready      : OUT    std_logic ;
        full          : IN     std_logic ;
        empty         : IN     std_logic ;
    );

```

```

        data_in_en      : IN      std_logic ;
        linkbusy       : IN      std_logic ;
        rd_stop        : IN      std_logic ;
        data_in        : IN      std_logic_vector (63 DOWNT0 0)
    );
END COMPONENT;
COMPONENT fifo
GENERIC (
    addr_bits : natural := 9
);
PORT (
    clk      : IN      std_logic ;
    rd_en    : IN      std_logic ;
    wr_en    : IN      std_logic ;
    wr_data  : IN      std_logic_vector (63 DOWNT0 0);
    reset    : IN      std_logic ;
    rd_data  : OUT     std_logic_vector (63 DOWNT0 0);
    full     : OUT     std_logic ;
    empty    : OUT     std_logic
);
END COMPONENT;
COMPONENT mux
PORT (
    clk      : IN      std_logic ;
    data_in  : IN      std_logic_vector (63 DOWNT0 0);
    header_in : IN     std_logic_vector (63 DOWNT0 0);
    header_sel : IN    std_logic_vector (1 DOWNT0 0);
    reset    : IN      std_logic ;
    ctrl     : OUT     std_logic ;
    data_en  : OUT     std_logic ;
    data_out : OUT     std_logic_vector (63 DOWNT0 0);
    data_in_en : IN    std_logic
);
END COMPONENT;

-- Optional embedded configurations
-- pragma synthesis_off
FOR ALL : builder USE ENTITY FED_DATA_FORMAT.builder;
FOR ALL : fifo USE ENTITY FED_DATA_FORMAT.fifo;
FOR ALL : mux USE ENTITY FED_DATA_FORMAT.mux;
-- pragma synthesis_on

BEGIN
-- Instance port mappings.
builder1 : builder
    PORT MAP (
        clk           => clk,
        data_bx_id    => data_bx_id,
        data_evt_stat => data_evt_stat,
        data_evt_ty   => data_evt_ty,
        data_lvl_id   => data_lvl_id,
        data_source_id => data_source_id,
        wr_start      => wr_start,
        rd_data       => rd_data,
        reset         => reset,
        rd_start      => rd_start,
        data_out      => header_in,
        data_out_sel  => data_out_sel,

```

```

        rd_en      => rd_en,
        wr_ready   => wr_ready,
        wr_data    => wr_data,
        wr_en      => wr_en,
        data_evt_lgth => data_evt_lgth,
        rd_ready   => rd_ready,
        full       => full,
        empty      => empty,
        data_in_en => data_in_en,
        linkbusy   => linkfull,
        rd_stop    => rd_stop,
        data_in    => data_in
    );
    fifol : fifo
        GENERIC MAP (
            addr_bits => fifo_addr_bits
        )
        PORT MAP (
            clk      => clk,
            rd_en    => rd_en,
            wr_en    => wr_en,
            wr_data  => wr_data,
            reset    => reset,
            rd_data  => rd_data,
            full     => full,
            empty    => empty
        );
    mux1 : mux
        PORT MAP (
            clk      => clk,
            data_in  => data_in,
            header_in => header_in,
            header_sel => data_out_sel,
            reset    => reset,
            ctrl     => ctrl,
            data_en  => data_out_en,
            data_out => data_out,
            data_in_en => data_in_en
        );
END fed_data_format;

```

A.2 builder.vhd

```

-- hds header_start
--
-- VHDL Architecture FED_DATA_FORMAT.builder.untitled
--
-- Created:
--     by - corrinep.UNKNOWN (SIMPC)
--     at - 13:25:28 11/12/2001
--
-- Generated by Mentor Graphics' HDL Designer(TM) 2001.5 (Build 170)
--
-- hds header_end
LIBRARY ieee;
USE ieee.std_logic_1164.ALL;

ENTITY builder IS
    PORT(

```

```

        clk            : IN      std_logic;
        data_bx_id     : IN      std_logic_vector (11 DOWNTO 0);
        data_evt_stat  : IN      std_logic_vector (7 DOWNTO 0);
        data_evt_ty    : IN      std_logic_vector (3 DOWNTO 0);
        data_lvl_id    : IN      std_logic_vector (23 DOWNTO 0);
        data_source_id : IN      std_logic_vector (11 DOWNTO 0);
        wr_start       : IN      std_logic;
        rd_data        : IN      std_logic_vector (63 DOWNTO 0);
        reset          : IN      std_logic;
        rd_start       : IN      std_logic;
        data_out       : OUT     std_logic_vector (63 DOWNTO 0);
        data_out_sel   : OUT     std_logic_vector (1 DOWNTO 0);
        rd_en          : OUT     std_logic;
        wr_ready       : OUT     std_logic;
        wr_data        : OUT     std_logic_vector (63 DOWNTO 0);
        wr_en          : OUT     std_logic;
        data_evt_lgth  : IN      std_logic_vector (23 DOWNTO 0);
        rd_ready       : OUT     std_logic;
        full           : IN      std_logic;
        empty          : IN      std_logic;
        data_in_en     : IN      std_logic;
        linkbusy       : IN      std_logic;
        rd_stop        : IN      std_logic;
        data_in        : IN      std_logic_vector (63 DOWNTO 0)
    );

-- Declarations

END builder ;

-- hds interface_end

LIBRARY ieee;
USE ieee.std_logic_arith.ALL;
USE ieee.std_logic_unsigned.ALL;

LIBRARY FED_DATA_FORMAT;
--USE FED_DATA_FORMAT.PCK_CRC16_D64_CCITT.ALL;
USE FED_DATA_FORMAT.PCK_CRC16_D64_X25.ALL;
--USE FED_DATA_FORMAT.PCK_CRC16_D64_SIMPLE.ALL;

ARCHITECTURE builder OF builder IS

    -- Areas in header word, value is ignored, just interested in range
    CONSTANT r_boe:    std_logic_vector(63 DOWNTO 60) := (OTHERS => '0');
    CONSTANT r_evt_ty: std_logic_vector(59 DOWNTO 56) := (OTHERS => '0');
    CONSTANT r_lvl_id: std_logic_vector(55 DOWNTO 32) := (OTHERS => '0');
    CONSTANT r_bx_id:  std_logic_vector(31 DOWNTO 20) := (OTHERS => '0');
    CONSTANT r_src_id: std_logic_vector(19 DOWNTO 8)  := (OTHERS => '0');
    CONSTANT r_fov:    std_logic_vector(7 DOWNTO 4)  := (OTHERS => '0');
    CONSTANT r_last:   std_logic_vector(3 DOWNTO 3)  := (OTHERS => '0');

    -- Areas in trailer word
    CONSTANT r_eoe:    std_logic_vector(63 DOWNTO 60) := (OTHERS => '0');
    CONSTANT r_evt_lgth: std_logic_vector(55 DOWNTO 32) := (OTHERS => '0');
    CONSTANT r_crc:    std_logic_vector(31 DOWNTO 16) := (OTHERS => '0');
    CONSTANT r_evt_stat: std_logic_vector(11 DOWNTO 4) := (OTHERS => '0');

    -- Constants
    CONSTANT c_boe1:   std_logic_vector := "0001"; -- Beginning of event, first word
    CONSTANT c_boe2:   std_logic_vector := "0010"; -- Beginning of event, second word
    CONSTANT c_fov:    std_logic_vector := "0001"; -- Format version
    CONSTANT c_last:   std_logic_vector := "1";    -- Last header word
    CONSTANT c_nlast:  std_logic_vector := "0";    -- Not last header word
    CONSTANT c_eoe:    std_logic_vector := "1001"; -- End of event

```

Common Data Format Implementation

```

CONSTANT CRC_INIT: std_logic_vector := "1111111111111111"; -- Initial value for CRC
calculation

SIGNAL save_evt_stat: std_logic_vector(data_evt_stat'range);
SIGNAL save_evt_lgth: std_logic_vector(data_evt_lgth'range);

TYPE wr_type IS (idle, writing);
SIGNAL wr_state: wr_type;

TYPE rd_type IS (idle, headerstart, header, datastart, data);
SIGNAL rd_state: rd_type;

BEGIN

-- builds header and trailer words and writes them to fifo
proc_wr: PROCESS(clk, reset)
BEGIN
    IF (reset = '0') THEN
        -- reset signals to default:
        wr_state <= idle;
        wr_ready <= '0';
        wr_data <= (OTHERS => '0');
        save_evt_lgth <= (OTHERS => '0');
        save_evt_stat <= (OTHERS => '0');
        wr_en <= '0';
    ELSIF (clk = '1' AND clk'event) THEN
        -- default assignments:
        wr_ready <= NOT full;
        wr_data <= (OTHERS => '0');
        wr_en <= '0';
        --IF (wr_state = idle) THEN
        CASE wr_state IS
        WHEN idle =>
            IF (wr_start = '1') THEN
                ASSERT (full /= '1') REPORT "(builder: proc_wr) Writing to FIFO when full"
                SEVERITY error;
                -- build first word (header)
                wr_data(r_boe'range) <= c_boel;
                wr_data(r_evt_ty'range) <= data_evt_ty;
                wr_data(r_lvl_id'range) <= data_lvl_id;
                wr_data(r_bx_id'range) <= data_bx_id;
                wr_data(r_src_id'range) <= data_source_id;
                wr_data(r_fov'range) <= c_fov;
                wr_data(r_last'range) <= c_last; -- c_nlast if there is another header word
                wr_en <= '1';
                -- Save data needed for trailer word
                save_evt_stat <= data_evt_stat;
                save_evt_lgth <= data_evt_lgth;
                wr_state <= writing;
                wr_ready <= '0';
            END IF;
        WHEN writing =>
            ASSERT (full /= '1') REPORT "(builder: proc_wr) Writing to FIFO when full"
            SEVERITY error;
            ASSERT (wr_start /= '1') REPORT "(builder: proc_wr) Prepare received while
writing to FIFO" SEVERITY error;
            -- build second word (trailer)
            wr_data(r_eoe'range) <= c_eoe; -- EOE
            wr_data(r_evt_lgth'range) <= save_evt_lgth;
            wr_data(r_evt_stat'range) <= save_evt_stat;
            wr_en <= '1';
            wr_state <= idle;
        --WHEN OTHERS =>
        -- wr_state <= idle;
        END CASE;
    END IF;
END PROCESS;

```



```

    END IF;
END PROCESS;

-- reads header & trailer from fifo and sends them to link
proc_rd: PROCESS(clk, reset)
--VARIABLE rd_num: natural RANGE 0 TO max_counter;
--VARIABLE sendstarted: std_logic;
VARIABLE data_counter: unsigned(23 DOWNT0 0);
VARIABLE crc: std_logic_vector(15 DOWNT0 0);
BEGIN
    IF (reset = '0') THEN
        --rd_num := 0;
        --sendstarted := '0';
        rd_state <= idle;
        --sd_state <= 0;
        data_counter := conv_unsigned(0, data_counter'length);
        data_out <= (OTHERS=> '0');

        -- reset signals to default:
        rd_en <= '0';
        data_out_sel <= "00";
        rd_ready <= '0';
        --startcrc <= '0';
        crc := (OTHERS => '0');
    ELSIF (clk = '1' AND clk'event) THEN
        -- default assignments:
        rd_en <= '0';
        data_out_sel <= "00";
        rd_ready <= '0';
        --startcrc <= '0';

        CASE rd_state IS
        WHEN idle =>
            IF (rd_start = '1') THEN
                -- read first word (header)
                ASSERT (empty = '0') REPORT "(builder) Read: fifo empty" SEVERITY error;
                rd_en <= '1';
                rd_state <= headerstart;
            ELSE
                rd_ready <= NOT (linkbusy OR empty);
            END IF;

        WHEN headerstart =>
            -- restart CRC
            --startcrc <= '1';
            crc := CRC_INIT;
            -- read second word (trailer)
            ASSERT (empty = '0') REPORT "(builder) Read: fifo empty" SEVERITY error;
            rd_en <= '1';
            rd_state <= header;

        WHEN header =>
            -- send header
            data_out <= rd_data;
            data_out_sel <= "01";
            rd_state <= datastart;

        WHEN datastart =>
            -- start sending data
            data_out_sel <= "10";
            -- get length of data
            data_counter := unsigned(rd_data(r_evt_lgth'range));
            -- send header, ready for when data ends
            data_out <= rd_data;
            -- add 2 for header and trailer words

```

```

data_out(r_evt_lgth'range) <= std_logic_vector((rd_data(r_evt_lgth'range)) + 2);
rd_state <= data;

WHEN data =>
  data_out_sel <= "10";
  IF (data_in_en = '1') THEN
    data_counter := data_counter - 1;
    crc := nextCRC16_D64(data_in, crc);
  END IF;
  IF (data_counter <= 0) THEN
    data_out_sel <= "11";
    data_out(r_crc'range) <= crc;
    rd_state <= idle;
  END IF;

  --WHEN OTHERS =>
  -- rd_state <= idle;
END CASE;
END IF;
END PROCESS;

END builder;

```

A.3 fifo.vhd

```

-- hds header_start
--
-- VHDL Architecture FED_DATA_FORMAT.fifo.general
--
-- Created:
--   by - corrinep.UNKNOWN (SIMPC)
--   at - 13:07:26 16/01/2002
--
-- Generated by Mentor Graphics' HDL Designer(TM) 2001.5 (Build 170)
--
-- hds header_end
LIBRARY ieee;
USE ieee.std_logic_1164.ALL;

ENTITY fifo IS
  GENERIC(
    addr_bits : natural := 9
  );
  PORT(
    clk      : IN      std_logic;
    rd_en    : IN      std_logic;
    wr_en    : IN      std_logic;
    wr_data  : IN      std_logic_vector (63 DOWNT0 0);
    reset    : IN      std_logic;
    rd_data  : OUT     std_logic_vector (63 DOWNT0 0);
    full     : OUT     std_logic;
    empty    : OUT     std_logic
  );

  -- Declarations

END fifo ;

-- hds interface_end

LIBRARY ieee;
USE ieee.std_logic_arith.ALL;

LIBRARY FED_DATA_FORMAT;

```

```

ARCHITECTURE fifo OF fifo IS
  SIGNAL full_int, empty_int: std_logic;
  --SIGNAL overflow, underflow: std_logic;
  SIGNAL rd_add, wr_add: std_logic_vector(addr_bits-1 DOWNTO 0);
  SIGNAL rd_ptr, wr_ptr: unsigned(addr_bits-1 DOWNTO 0);

  COMPONENT mem64
  GENERIC (
    addr_bits: natural
  );
  PORT (
    clk      : IN      std_logic;
    rd_add   : IN      std_logic_vector (ADDR_BITS-1 DOWNTO 0);
    rd_en    : IN      std_logic;
    wr_add   : IN      std_logic_vector (ADDR_BITS-1 DOWNTO 0);
    wr_data  : IN      std_logic_vector (63 DOWNTO 0);
    wr_en    : IN      std_logic;
    rd_data  : OUT     std_logic_vector (63 DOWNTO 0)
  );
  END COMPONENT;

  FOR ALL : mem64 USE ENTITY FED_DATA_FORMAT.mem64;

BEGIN

  mem: mem64
  GENERIC MAP (
    addr_bits => addr_bits
  )
  PORT MAP(
    clk => clk,
    rd_add => rd_add,
    rd_en => rd_en,
    wr_add => wr_add,
    wr_data => wr_data,
    wr_en => wr_en,
    rd_data => rd_data
  );

  rd_add <= std_logic_vector(rd_ptr);
  wr_add <= std_logic_vector(wr_ptr);
  full <= full_int;
  empty <= empty_int;

  proc: PROCESS(clk, reset)
  BEGIN
    IF (reset = '0') THEN
      rd_ptr <= conv_unsigned(0, rd_ptr'length);
      wr_ptr <= conv_unsigned(0, rd_ptr'length);
      full_int <= '0';
      empty_int <= '1';
      --overflow <= '0';
      --underflow <= '0';
    ELSIF (clk = '1' AND clk'event) THEN
      IF (rd_en = '1') THEN
        IF (empty_int = '1') THEN
          --underflow <= '1';
          ASSERT false REPORT "(fifo) Underflow" SEVERITY error;
        ELSE
          rd_ptr <= rd_ptr + 1;
          IF ((rd_ptr+1) = wr_ptr) THEN empty_int <= '1'; END IF;
          full_int <= '0';
        END IF;
      END IF;
      IF (wr_en = '1') THEN

```

```

    IF (full_int = '1') THEN
        --overflow <= '1';
        ASSERT false REPORT "(fifo) Overflow" SEVERITY error;
    ELSE
        wr_ptr <= wr_ptr + 1;
        IF (rd_ptr = (wr_ptr+1)) THEN full_int <= '1'; END IF;
        empty_int <= '0';
    END IF;
END IF;
--full <= buf_full;
--empty <= buf_empty;
END IF;
END PROCESS;

END fifo;

```

A.4 mem64_general.vhd

```

-- hds header_start
--
-- VHDL Architecture FED_DATA_FORMAT.mem64.general
--
-- Created:
--     by - corrinep.UNKNOWN (SIMPC)
--     at - 13:17:15 11/12/2001
--
-- Generated by Mentor Graphics' HDL Designer(TM) 2001.5 (Build 170)
--
-- hds header_end
LIBRARY ieee;
USE ieee.std_logic_1164.ALL;

ENTITY mem64 IS
    GENERIC(
        addr_bits : natural := 12
    );
    PORT(
        clk      : IN      std_logic;
        rd_add   : IN      std_logic_vector (addr_bits-1 DOWNTO 0);
        rd_en    : IN      std_logic;
        wr_add   : IN      std_logic_vector (addr_bits-1 DOWNTO 0);
        wr_data  : IN      std_logic_vector (63 DOWNTO 0);
        wr_en    : IN      std_logic;
        rd_data  : OUT     std_logic_vector (63 DOWNTO 0)
    );
-- Declarations

END mem64 ;

-- hds interface_end

LIBRARY ieee;
USE ieee.numeric_std.ALL;
LIBRARY FED_DATA_FORMAT;
USE FED_DATA_FORMAT.Utils.ALL;

ARCHITECTURE general OF mem64 IS
    TYPE mem IS ARRAY(2**ADDR_BITS - 1 DOWNTO 0) OF integer;
    SIGNAL buf1, buf2: mem;

```

```

BEGIN

proc: PROCESS(clk)
BEGIN
  IF (clk = '1' AND clk'event) THEN
    IF (wr_en = '1') THEN
      buf1(to_natural(wr_add)) <= to_integer(wr_data(31 DOWNT0 0));
      buf2(to_natural(wr_add)) <= to_integer(wr_data(63 DOWNT0 32));
    END IF;
    IF (rd_en = '1') THEN
      rd_data(31 DOWNT0 0) <= to_slv_signed(buf1(to_natural(rd_add)), 32);
      rd_data(63 DOWNT0 32) <= to_slv_signed(buf2(to_natural(rd_add)), 32);
    ELSE
      --rd_data <= (OTHERS => 'Z');
    END IF;
  END IF;
END PROCESS;

END general;

```

A.5 mux.vhd

```

-- hds header_start
--
-- VHDL Architecture FED_DATA_FORMAT.mux.untitled
--
-- Created:
--       by - corrinep.UNKNOWN (SIMPC)
--       at - 13:25:43 11/12/2001
--
-- Generated by Mentor Graphics' HDL Designer(TM) 2001.5 (Build 170)
--
-- hds header_end
LIBRARY ieee;
USE ieee.std_logic_1164.ALL;

ENTITY mux IS
  PORT(
    clk          : IN    std_logic;
    data_in      : IN    std_logic_vector (63 DOWNT0 0);
    header_in    : IN    std_logic_vector (63 DOWNT0 0);
    header_sel   : IN    std_logic_vector (1 DOWNT0 0);
    reset        : IN    std_logic;
    ctrl         : OUT   std_logic;
    data_en      : OUT   std_logic;
    data_out     : OUT   std_logic_vector (63 DOWNT0 0);
    data_in_en   : IN    std_logic
  );

-- Declarations

END mux ;

-- hds interface_end

ARCHITECTURE mux OF mux IS

  --CONSTANT r_crc: std_logic_vector(31 DOWNT0 16) := (OTHERS => '0');

BEGIN

  mux: PROCESS(clk, reset)

```

```

BEGIN
  IF (reset = '0') THEN
    data_en <= '0';
    ctrl <= '0';
    data_out <= (OTHERS => '0');
  ELSIF (clk = '1' AND clk'event) THEN
    CASE header_sel IS
      WHEN "01" =>
        data_en <= '1';
        ctrl <= '1';
        data_out <= header_in;
        ASSERT data_in_en /= '1' REPORT "(mux) Data being lost while sending header"
SEVERITY error;
      WHEN "10" =>
        ctrl <= '0';
        IF (data_in_en = '1') THEN
          data_en <= '1';
          data_out <= data_in;
        ELSE
          data_en <= '0';
          data_out <= (OTHERS => '0');
        END IF;
      WHEN "11" =>
        data_en <= '1';
        ctrl <= '1';
        data_out <= header_in;
        --data_out(r_crc'RANGE) <= crc_in;
        ASSERT data_in_en /= '1' REPORT "(mux) Data being lost while sending
trailer" SEVERITY error;
      WHEN OTHERS =>
        data_en <= '0';
        ctrl <= '0';
        data_out <= (OTHERS => '0');
        ASSERT data_in_en /= '1' REPORT "(mux) Data being lost" SEVERITY error;
    END CASE;
  END IF;
END PROCESS;

END mux;

```

A.6 pck_crc16_d64_ccitt.vhd

```

-----
-- File: PCK_CRC16_D64.vhd
-- Date: Wed Nov 21 16:54:49 2001
--
-- Copyright (C) 1999 Easics NV.
-- This source file may be used and distributed without restriction
-- provided that this copyright statement is not removed from the file
-- and that any derivative work contains the original copyright notice
-- and the associated disclaimer.
--
-- THIS SOURCE FILE IS PROVIDED "AS IS" AND WITHOUT ANY EXPRESS
-- OR IMPLIED WARRANTIES, INCLUDING, WITHOUT LIMITATION, THE IMPLIED
-- WARRANTIES OF MERCHANTABILITY AND FITNESS FOR A PARTICULAR PURPOSE.
--
-- Purpose: VHDL package containing a synthesizable CRC function
-- * polynomial: (0 2 15 16)
-- * data width: 64
--
-- Info: jand@easics.be (Jan Decaluwe)
-- http://www.easics.com
-----

```

```

library IEEE;
use IEEE.std_logic_1164.all;

package PCK_CRC16_D64_CCITT is

    -- polynomial: (0 2 15 16)
    -- data width: 64
    -- convention: the first serial data bit is D(63)
    function nextCRC16_D64
        ( Data: std_logic_vector(63 downto 0);
          CRC:  std_logic_vector(15 downto 0) )
        return std_logic_vector;

end PCK_CRC16_D64_CCITT;

package body PCK_CRC16_D64_CCITT is

    -- polynomial: (0 2 15 16)
    -- data width: 64
    -- convention: the first serial data bit is D(63)
    function nextCRC16_D64
        ( Data: std_logic_vector(63 downto 0);
          CRC:  std_logic_vector(15 downto 0) )
        return std_logic_vector is

        variable D: std_logic_vector(63 downto 0);
        variable C: std_logic_vector(15 downto 0);
        variable NewCRC: std_logic_vector(15 downto 0);

    begin

        D := Data;
        C := CRC;

        NewCRC(0) := D(63) xor D(62) xor D(61) xor D(60) xor D(55) xor D(54) xor
            D(53) xor D(52) xor D(51) xor D(50) xor D(49) xor D(48) xor
            D(47) xor D(46) xor D(45) xor D(43) xor D(41) xor D(40) xor
            D(39) xor D(38) xor D(37) xor D(36) xor D(35) xor D(34) xor
            D(33) xor D(32) xor D(31) xor D(30) xor D(27) xor D(26) xor
            D(25) xor D(24) xor D(23) xor D(22) xor D(21) xor D(20) xor
            D(19) xor D(18) xor D(17) xor D(16) xor D(15) xor D(13) xor
            D(12) xor D(11) xor D(10) xor D(9) xor D(8) xor D(7) xor
            D(6) xor D(5) xor D(4) xor D(3) xor D(2) xor D(1) xor
            D(0) xor C(0) xor C(1) xor C(2) xor C(3) xor C(4) xor
            C(5) xor C(6) xor C(7) xor C(12) xor C(13) xor C(14) xor
            C(15);

        NewCRC(1) := D(63) xor D(62) xor D(61) xor D(56) xor D(55) xor D(54) xor
            D(53) xor D(52) xor D(51) xor D(50) xor D(49) xor D(48) xor
            D(47) xor D(46) xor D(44) xor D(42) xor D(41) xor D(40) xor
            D(39) xor D(38) xor D(37) xor D(36) xor D(35) xor D(34) xor
            D(33) xor D(32) xor D(31) xor D(28) xor D(27) xor D(26) xor
            D(25) xor D(24) xor D(23) xor D(22) xor D(21) xor D(20) xor
            D(19) xor D(18) xor D(17) xor D(16) xor D(14) xor D(13) xor
            D(12) xor D(11) xor D(10) xor D(9) xor D(8) xor D(7) xor
            D(6) xor D(5) xor D(4) xor D(3) xor D(2) xor D(1) xor
            C(0) xor C(1) xor C(2) xor C(3) xor C(4) xor C(5) xor
            C(6) xor C(7) xor C(8) xor C(13) xor C(14) xor C(15);

        NewCRC(2) := D(61) xor D(60) xor D(57) xor D(56) xor D(46) xor D(42) xor
            D(31) xor D(30) xor D(29) xor D(28) xor D(16) xor D(14) xor
            D(1) xor D(0) xor C(8) xor C(9) xor C(12) xor C(13);

        NewCRC(3) := D(62) xor D(61) xor D(58) xor D(57) xor D(47) xor D(43) xor
            D(32) xor D(31) xor D(30) xor D(29) xor D(17) xor D(15) xor
            D(2) xor D(1) xor C(9) xor C(10) xor C(13) xor C(14);

        NewCRC(4) := D(63) xor D(62) xor D(59) xor D(58) xor D(48) xor D(44) xor
            D(33) xor D(32) xor D(31) xor D(30) xor D(18) xor D(16) xor
            D(3) xor D(2) xor C(0) xor C(10) xor C(11) xor C(14) xor

```

```

        C(15);
NewCRC(5) := D(63) xor D(60) xor D(59) xor D(49) xor D(45) xor D(34) xor
            D(33) xor D(32) xor D(31) xor D(19) xor D(17) xor D(4) xor
            D(3) xor C(1) xor C(11) xor C(12) xor C(15);
NewCRC(6) := D(61) xor D(60) xor D(50) xor D(46) xor D(35) xor D(34) xor
            D(33) xor D(32) xor D(20) xor D(18) xor D(5) xor D(4) xor
            C(2) xor C(12) xor C(13);
NewCRC(7) := D(62) xor D(61) xor D(51) xor D(47) xor D(36) xor D(35) xor
            D(34) xor D(33) xor D(21) xor D(19) xor D(6) xor D(5) xor
            C(3) xor C(13) xor C(14);
NewCRC(8) := D(63) xor D(62) xor D(52) xor D(48) xor D(37) xor D(36) xor
            D(35) xor D(34) xor D(22) xor D(20) xor D(7) xor D(6) xor
            C(0) xor C(4) xor C(14) xor C(15);
NewCRC(9) := D(63) xor D(53) xor D(49) xor D(38) xor D(37) xor D(36) xor
            D(35) xor D(23) xor D(21) xor D(8) xor D(7) xor C(1) xor
            C(5) xor C(15);
NewCRC(10) := D(54) xor D(50) xor D(39) xor D(38) xor D(37) xor D(36) xor
            D(24) xor D(22) xor D(9) xor D(8) xor C(2) xor C(6);
NewCRC(11) := D(55) xor D(51) xor D(40) xor D(39) xor D(38) xor D(37) xor
            D(25) xor D(23) xor D(10) xor D(9) xor C(3) xor C(7);
NewCRC(12) := D(56) xor D(52) xor D(41) xor D(40) xor D(39) xor D(38) xor
            D(26) xor D(24) xor D(11) xor D(10) xor C(4) xor C(8);
NewCRC(13) := D(57) xor D(53) xor D(42) xor D(41) xor D(40) xor D(39) xor
            D(27) xor D(25) xor D(12) xor D(11) xor C(5) xor C(9);
NewCRC(14) := D(58) xor D(54) xor D(43) xor D(42) xor D(41) xor D(40) xor
            D(28) xor D(26) xor D(13) xor D(12) xor C(6) xor C(10);
NewCRC(15) := D(63) xor D(62) xor D(61) xor D(60) xor D(59) xor D(54) xor
            D(53) xor D(52) xor D(51) xor D(50) xor D(49) xor D(48) xor
            D(47) xor D(46) xor D(45) xor D(44) xor D(42) xor D(40) xor
            D(39) xor D(38) xor D(37) xor D(36) xor D(35) xor D(34) xor
            D(33) xor D(32) xor D(31) xor D(30) xor D(29) xor D(26) xor
            D(25) xor D(24) xor D(23) xor D(22) xor D(21) xor D(20) xor
            D(19) xor D(18) xor D(17) xor D(16) xor D(15) xor D(14) xor
            D(12) xor D(11) xor D(10) xor D(9) xor D(8) xor D(7) xor
            D(6) xor D(5) xor D(4) xor D(3) xor D(2) xor D(1) xor
            D(0) xor C(0) xor C(1) xor C(2) xor C(3) xor C(4) xor
            C(5) xor C(6) xor C(11) xor C(12) xor C(13) xor C(14) xor
            C(15);

    return NewCRC;

end nextCRC16_D64;

end PCK_CRC16_D64_CCITT;

```

A.7 pck_crc16_d64_x25.vhd

```

-----
-- File:   PCK_CRC16_D64.vhd
-- Date:   Wed Nov 21 18:01:04 2001
--
-- Copyright (C) 1999 Easics NV.
-- This source file may be used and distributed without restriction
-- provided that this copyright statement is not removed from the file
-- and that any derivative work contains the original copyright notice
-- and the associated disclaimer.
--
-- THIS SOURCE FILE IS PROVIDED "AS IS" AND WITHOUT ANY EXPRESS
-- OR IMPLIED WARRANTIES, INCLUDING, WITHOUT LIMITATION, THE IMPLIED
-- WARRANTIES OF MERCHANTABILITY AND FITNESS FOR A PARTICULAR PURPOSE.
--
-- Purpose: VHDL package containing a synthesizable CRC function
-- * polynomial: (0 5 12 16)

```



```

-- * data width: 64
--
-- Info: jand@easics.be (Jan Decaluwe)
--       http://www.easics.com
-----

library IEEE;
use IEEE.std_logic_1164.all;

package PCK_CRC16_D64_X25 is

    -- polynomial: (0 5 12 16)
    -- data width: 64
    -- convention: the first serial data bit is D(63)
    function nextCRC16_D64
        ( Data: std_logic_vector(63 downto 0);
          CRC:  std_logic_vector(15 downto 0) )
        return std_logic_vector;

end PCK_CRC16_D64_X25;

package body PCK_CRC16_D64_X25 is

    -- polynomial: (0 5 12 16)
    -- data width: 64
    -- convention: the first serial data bit is D(63)
    function nextCRC16_D64
        ( Data: std_logic_vector(63 downto 0);
          CRC:  std_logic_vector(15 downto 0) )
        return std_logic_vector is

        variable D: std_logic_vector(63 downto 0);
        variable C: std_logic_vector(15 downto 0);
        variable NewCRC: std_logic_vector(15 downto 0);

    begin

        D := Data;
        C := CRC;

        NewCRC(0) := D(63) xor D(58) xor D(56) xor D(55) xor D(52) xor D(51) xor
            D(49) xor D(48) xor D(42) xor D(35) xor D(33) xor D(32) xor
            D(28) xor D(27) xor D(26) xor D(22) xor D(20) xor D(19) xor
            D(12) xor D(11) xor D(8) xor D(4) xor D(0) xor C(0) xor
            C(1) xor C(3) xor C(4) xor C(7) xor C(8) xor C(10) xor
            C(15);

        NewCRC(1) := D(59) xor D(57) xor D(56) xor D(53) xor D(52) xor D(50) xor
            D(49) xor D(43) xor D(36) xor D(34) xor D(33) xor D(29) xor
            D(28) xor D(27) xor D(23) xor D(21) xor D(20) xor D(13) xor
            D(12) xor D(9) xor D(5) xor D(1) xor C(1) xor C(2) xor
            C(4) xor C(5) xor C(8) xor C(9) xor C(11);

        NewCRC(2) := D(60) xor D(58) xor D(57) xor D(54) xor D(53) xor D(51) xor
            D(50) xor D(44) xor D(37) xor D(35) xor D(34) xor D(30) xor
            D(29) xor D(28) xor D(24) xor D(22) xor D(21) xor D(14) xor
            D(13) xor D(10) xor D(6) xor D(2) xor C(2) xor C(3) xor
            C(5) xor C(6) xor C(9) xor C(10) xor C(12);

        NewCRC(3) := D(61) xor D(59) xor D(58) xor D(55) xor D(54) xor D(52) xor
            D(51) xor D(45) xor D(38) xor D(36) xor D(35) xor D(31) xor
            D(30) xor D(29) xor D(25) xor D(23) xor D(22) xor D(15) xor

```

```

D(14) xor D(11) xor D(7) xor D(3) xor C(3) xor C(4) xor
C(6) xor C(7) xor C(10) xor C(11) xor C(13);
NewCRC(4) := D(62) xor D(60) xor D(59) xor D(56) xor D(55) xor D(53) xor
D(52) xor D(46) xor D(39) xor D(37) xor D(36) xor D(32) xor
D(31) xor D(30) xor D(26) xor D(24) xor D(23) xor D(16) xor
D(15) xor D(12) xor D(8) xor D(4) xor C(4) xor C(5) xor
C(7) xor C(8) xor C(11) xor C(12) xor C(14);
NewCRC(5) := D(61) xor D(60) xor D(58) xor D(57) xor D(55) xor D(54) xor
D(53) xor D(52) xor D(51) xor D(49) xor D(48) xor D(47) xor
D(42) xor D(40) xor D(38) xor D(37) xor D(35) xor D(31) xor
D(28) xor D(26) xor D(25) xor D(24) xor D(22) xor D(20) xor
D(19) xor D(17) xor D(16) xor D(13) xor D(12) xor D(11) xor
D(9) xor D(8) xor D(5) xor D(4) xor D(0) xor C(0) xor
C(1) xor C(3) xor C(4) xor C(5) xor C(6) xor C(7) xor
C(9) xor C(10) xor C(12) xor C(13);
NewCRC(6) := D(62) xor D(61) xor D(59) xor D(58) xor D(56) xor D(55) xor
D(54) xor D(53) xor D(52) xor D(50) xor D(49) xor D(48) xor
D(43) xor D(41) xor D(39) xor D(38) xor D(36) xor D(32) xor
D(29) xor D(27) xor D(26) xor D(25) xor D(23) xor D(21) xor
D(20) xor D(18) xor D(17) xor D(14) xor D(13) xor D(12) xor
D(10) xor D(9) xor D(6) xor D(5) xor D(1) xor C(0) xor
C(1) xor C(2) xor C(4) xor C(5) xor C(6) xor C(7) xor
C(8) xor C(10) xor C(11) xor C(13) xor C(14);
NewCRC(7) := D(63) xor D(62) xor D(60) xor D(59) xor D(57) xor D(56) xor
D(55) xor D(54) xor D(53) xor D(51) xor D(50) xor D(49) xor
D(44) xor D(42) xor D(40) xor D(39) xor D(37) xor D(33) xor
D(30) xor D(28) xor D(27) xor D(26) xor D(24) xor D(22) xor
D(21) xor D(19) xor D(18) xor D(15) xor D(14) xor D(13) xor
D(11) xor D(10) xor D(7) xor D(6) xor D(2) xor C(1) xor
C(2) xor C(3) xor C(5) xor C(6) xor C(7) xor C(8) xor
C(9) xor C(11) xor C(12) xor C(14) xor C(15);
NewCRC(8) := D(63) xor D(61) xor D(60) xor D(58) xor D(57) xor D(56) xor
D(55) xor D(54) xor D(52) xor D(51) xor D(50) xor D(45) xor
D(43) xor D(41) xor D(40) xor D(38) xor D(34) xor D(31) xor
D(29) xor D(28) xor D(27) xor D(25) xor D(23) xor D(22) xor
D(20) xor D(19) xor D(16) xor D(15) xor D(14) xor D(12) xor
D(11) xor D(8) xor D(7) xor D(3) xor C(2) xor C(3) xor
C(4) xor C(6) xor C(7) xor C(8) xor C(9) xor C(10) xor
C(12) xor C(13) xor C(15);
NewCRC(9) := D(62) xor D(61) xor D(59) xor D(58) xor D(57) xor D(56) xor
D(55) xor D(53) xor D(52) xor D(51) xor D(46) xor D(44) xor
D(42) xor D(41) xor D(39) xor D(35) xor D(32) xor D(30) xor
D(29) xor D(28) xor D(26) xor D(24) xor D(23) xor D(21) xor
D(20) xor D(17) xor D(16) xor D(15) xor D(13) xor D(12) xor
D(9) xor D(8) xor D(4) xor C(3) xor C(4) xor C(5) xor
C(7) xor C(8) xor C(9) xor C(10) xor C(11) xor C(13) xor
C(14);
NewCRC(10) := D(63) xor D(62) xor D(60) xor D(59) xor D(58) xor D(57) xor
D(56) xor D(54) xor D(53) xor D(52) xor D(47) xor D(45) xor
D(43) xor D(42) xor D(40) xor D(36) xor D(33) xor D(31) xor
D(30) xor D(29) xor D(27) xor D(25) xor D(24) xor D(22) xor
D(21) xor D(18) xor D(17) xor D(16) xor D(14) xor D(13) xor
D(10) xor D(9) xor D(5) xor C(4) xor C(5) xor C(6) xor
C(8) xor C(9) xor C(10) xor C(11) xor C(12) xor C(14) xor
C(15);
NewCRC(11) := D(63) xor D(61) xor D(60) xor D(59) xor D(58) xor D(57) xor
D(55) xor D(54) xor D(53) xor D(48) xor D(46) xor D(44) xor
D(43) xor D(41) xor D(37) xor D(34) xor D(32) xor D(31) xor
D(30) xor D(28) xor D(26) xor D(25) xor D(23) xor D(22) xor

```

```

        D(19) xor D(18) xor D(17) xor D(15) xor D(14) xor D(11) xor
        D(10) xor D(6) xor C(0) xor C(5) xor C(6) xor C(7) xor
        C(9) xor C(10) xor C(11) xor C(12) xor C(13) xor C(15);
NewCRC(12) := D(63) xor D(62) xor D(61) xor D(60) xor D(59) xor D(54) xor
        D(52) xor D(51) xor D(48) xor D(47) xor D(45) xor D(44) xor
        D(38) xor D(31) xor D(29) xor D(28) xor D(24) xor D(23) xor
        D(22) xor D(18) xor D(16) xor D(15) xor D(8) xor D(7) xor
        D(4) xor D(0) xor C(0) xor C(3) xor C(4) xor C(6) xor
        C(11) xor C(12) xor C(13) xor C(14) xor C(15);
NewCRC(13) := D(63) xor D(62) xor D(61) xor D(60) xor D(55) xor D(53) xor
        D(52) xor D(49) xor D(48) xor D(46) xor D(45) xor D(39) xor
        D(32) xor D(30) xor D(29) xor D(25) xor D(24) xor D(23) xor
        D(19) xor D(17) xor D(16) xor D(9) xor D(8) xor D(5) xor
        D(1) xor C(0) xor C(1) xor C(4) xor C(5) xor C(7) xor
        C(12) xor C(13) xor C(14) xor C(15);
NewCRC(14) := D(63) xor D(62) xor D(61) xor D(56) xor D(54) xor D(53) xor
        D(50) xor D(49) xor D(47) xor D(46) xor D(40) xor D(33) xor
        D(31) xor D(30) xor D(26) xor D(25) xor D(24) xor D(20) xor
        D(18) xor D(17) xor D(10) xor D(9) xor D(6) xor D(2) xor
        C(1) xor C(2) xor C(5) xor C(6) xor C(8) xor C(13) xor
        C(14) xor C(15);
NewCRC(15) := D(63) xor D(62) xor D(57) xor D(55) xor D(54) xor D(51) xor
        D(50) xor D(48) xor D(47) xor D(41) xor D(34) xor D(32) xor
        D(31) xor D(27) xor D(26) xor D(25) xor D(21) xor D(19) xor
        D(18) xor D(11) xor D(10) xor D(7) xor D(3) xor C(0) xor
        C(2) xor C(3) xor C(6) xor C(7) xor C(9) xor C(14) xor
        C(15);

return NewCRC;

end nextCRC16_D64;

end PCK_CRC16_D64_X25;

```

Appendix B: Common Data Format Verification Code

The verification code for the common data format block includes a testbench, written in VHDL, and a program written in C that analyses the output of the testbench. The testbench includes a top-level block diagram that connects the test code to the device under test (DUT), and the test code itself. For the block diagram, the generated VHDL is listed (*testbench.vhd*). The test code (*tester.vhd*) sends test data to the DUT, and then writes the output signals to a text file. The VHDL code was developed with *HDL Designer*, and run in *ModelSim*, both part of Mentor Graphics *FPGA Advantage*.

The C code reads the text file generated by the test-bench, and verifies its correctness. It includes a reference CRC algorithm (*crcmodel.h* and *crcmodel.c*, adapted from ref [43]) to calculate the CRC of the data and compare it to the VHDL-generated value. It was developed with Microsoft *Visual C++*.

B.1 testbench.vhd

```
-- hds header_start
--
-- VHDL Entity FED_DATA_FORMAT.data_format_tb.symbol
--
-- Created:
--       by - corrinep.UNKNOWN (EMLYN)
--       at - 10:58:41 10/26/02
--
-- Generated by Mentor Graphics' HDL Designer(TM) 2002.1a (Build 22)
--
-- hds header_end

ENTITY data_format_tb IS
-- Declarations

END data_format_tb ;

-- hds interface_end
--
-- VHDL Architecture FED_DATA_FORMAT.data_format_tb.testbench
--
-- Created:
--       by - corrinep.UNKNOWN (EMLYN)
--       at - 10:58:42 10/26/02
--
-- Generated by Mentor Graphics' HDL Designer(TM) 2002.1a (Build 22)
--
LIBRARY ieee;
USE ieee.std_logic_1164.all;
USE ieee.std_logic_arith.all;
```

```

LIBRARY FED_DATA_FORMAT;

ARCHITECTURE testbench OF data_format_tb IS

    -- Architecture declarations

    -- Internal signal declarations
    SIGNAL clk          : std_logic;
    SIGNAL ctrl         : std_logic;
    SIGNAL data_bx_id   : std_logic_vector(11 DOWNTO 0);
    SIGNAL data_evt_lgth : std_logic_vector(23 DOWNTO 0);
    SIGNAL data_evt_stat : std_logic_vector(7 DOWNTO 0);
    SIGNAL data_evt_ty  : std_logic_vector(3 DOWNTO 0);
    SIGNAL data_in      : std_logic_vector(63 DOWNTO 0);
    SIGNAL data_in_en   : std_logic;
    SIGNAL data_lv1_id  : std_logic_vector(23 DOWNTO 0);
    SIGNAL data_out     : std_logic_vector(63 DOWNTO 0);
    SIGNAL data_out_en  : std_logic;
    SIGNAL data_source_id : std_logic_vector(11 DOWNTO 0);
    SIGNAL linkfull     : std_logic;
    SIGNAL rd_ready     : std_logic;
    SIGNAL rd_start     : std_logic;
    SIGNAL rd_stop      : std_logic;
    SIGNAL reset        : std_logic;
    SIGNAL wr_ready     : std_logic;
    SIGNAL wr_start     : std_logic;

    -- Component Declarations
    COMPONENT data_format
    GENERIC (
        fifo_addr_bits : natural := 9;
        length_at_start : boolean := true
    );
    PORT (
        clk          : IN    std_logic ;
        data_bx_id   : IN    std_logic_vector (11 DOWNTO 0);
        data_evt_lgth : IN    std_logic_vector (23 DOWNTO 0);
        data_evt_stat : IN    std_logic_vector (7 DOWNTO 0);
        data_evt_ty  : IN    std_logic_vector (3 DOWNTO 0);
        data_in      : IN    std_logic_vector (63 DOWNTO 0);
        data_in_en   : IN    std_logic ;
        data_lv1_id  : IN    std_logic_vector (23 DOWNTO 0);
        data_source_id : IN    std_logic_vector (11 DOWNTO 0);
        linkfull     : IN    std_logic ;
        rd_start     : IN    std_logic ;
        rd_stop      : IN    std_logic ;
        reset        : IN    std_logic ;
        wr_start     : IN    std_logic ;
        ctrl         : OUT   std_logic ;
        data_out     : OUT   std_logic_vector (63 DOWNTO 0);
        data_out_en  : OUT   std_logic ;
        rd_ready     : OUT   std_logic ;
        wr_ready     : OUT   std_logic
    );
    END COMPONENT;
    COMPONENT data_format_tester
    PORT (
        ctrl          : IN    std_logic ;
        data_out      : IN    std_logic_vector (63 DOWNTO 0);

```

```

data_out_en      : IN      std_logic ;
rd_ready        : IN      std_logic ;
wr_ready        : IN      std_logic ;
clk             : OUT     std_logic ;
data_bx_id      : OUT     std_logic_vector (11 DOWNTO 0);
data_evt_lgth   : OUT     std_logic_vector (23 DOWNTO 0);
data_evt_stat   : OUT     std_logic_vector (7 DOWNTO 0);
data_evt_ty     : OUT     std_logic_vector (3 DOWNTO 0);
data_in         : OUT     std_logic_vector (63 DOWNTO 0);
data_in_en      : OUT     std_logic ;
data_lvl_id     : OUT     std_logic_vector (23 DOWNTO 0);
data_source_id  : OUT     std_logic_vector (11 DOWNTO 0);
linkfull        : OUT     std_logic ;
rd_start        : OUT     std_logic ;
rd_stop         : OUT     std_logic ;
reset           : OUT     std_logic ;
wr_start        : OUT     std_logic ;
);
END COMPONENT;

-- Optional embedded configurations
-- pragma synthesis_off
FOR ALL : data_format USE ENTITY FED_DATA_FORMAT.data_format;
FOR ALL : data_format_tester USE ENTITY FED_DATA_FORMAT.data_format_tester;
-- pragma synthesis_on

BEGIN
-- Instance port mappings.
I0 : data_format
  GENERIC MAP (
    fifo_addr_bits => 9,
    length_at_start => true
  )
  PORT MAP (
    clk           => clk,
    data_bx_id    => data_bx_id,
    data_evt_lgth => data_evt_lgth,
    data_evt_stat => data_evt_stat,
    data_evt_ty   => data_evt_ty,
    data_in       => data_in,
    data_in_en    => data_in_en,
    data_lvl_id   => data_lvl_id,
    data_source_id => data_source_id,
    linkfull      => linkfull,
    rd_start      => rd_start,
    rd_stop       => rd_stop,
    reset         => reset,
    wr_start      => wr_start,
    ctrl          => ctrl,
    data_out      => data_out,
    data_out_en   => data_out_en,
    rd_ready      => rd_ready,
    wr_ready      => wr_ready
  );
I1 : data_format_tester
  PORT MAP (
    ctrl          => ctrl,
    data_out      => data_out,
    data_out_en   => data_out_en,

```

```

        rd_ready      => rd_ready,
        wr_ready      => wr_ready,
        clk           => clk,
        data_bx_id    => data_bx_id,
        data_evt_lgth => data_evt_lgth,
        data_evt_stat => data_evt_stat,
        data_evt_ty   => data_evt_ty,
        data_in       => data_in,
        data_in_en    => data_in_en,
        data_lv1_id   => data_lv1_id,
        data_source_id => data_source_id,
        linkfull      => linkfull,
        rd_start      => rd_start,
        rd_stop       => rd_stop,
        reset         => reset,
        wr_start      => wr_start
    );
END testbench;

```

B.2 tester.vhd

```

-- hds header_start
--
-- VHDL Architecture FED_DATA_FORMAT.data_format_tester.untitled
--
-- Created:
--     by - corrinep.UNKNOWNN (EMLYN)
--     at - 15:59:19 10/03/02
--
-- Generated by Mentor Graphics' HDL Designer(TM) 2002.1a (Build 22)
--
-- hds header_end
LIBRARY ieee;
USE ieee.std_logic_1164.all;
USE ieee.std_logic_arith.all;

ENTITY data_format_tester IS
    PORT(
        ctrl           : IN    std_logic;
        data_out       : IN    std_logic_vector (63 DOWNTO 0);
        data_out_en    : IN    std_logic;
        rd_ready       : IN    std_logic;
        wr_ready       : IN    std_logic;
        clk            : OUT   std_logic;
        data_bx_id     : OUT   std_logic_vector (11 DOWNTO 0);
        data_evt_lgth  : OUT   std_logic_vector (23 DOWNTO 0);
        data_evt_stat  : OUT   std_logic_vector (7 DOWNTO 0);
        data_evt_ty    : OUT   std_logic_vector (3 DOWNTO 0);
        data_in        : OUT   std_logic_vector (63 DOWNTO 0);
        data_in_en     : OUT   std_logic;
        data_lv1_id    : OUT   std_logic_vector (23 DOWNTO 0);
        data_source_id : OUT   std_logic_vector (11 DOWNTO 0);
        linkfull       : OUT   std_logic;
        rd_start       : OUT   std_logic;
        rd_stop        : OUT   std_logic;
        reset          : OUT   std_logic;
        wr_start       : OUT   std_logic
    );

```

```

-- Declarations

END data_format_tester ;

-- hds interface_end

USE std.textio.ALL;

LIBRARY ieee;
USE ieee.std_logic_arith.ALL;
USE ieee.std_logic_unsigned.ALL;

LIBRARY FED_DATA_FORMAT;
USE FED_DATA_FORMAT.RNG.ALL;

ARCHITECTURE tester OF data_format_tester IS

FUNCTION chr(sl: std_logic) RETURN character IS
    VARIABLE c: character;
BEGIN
    CASE sl IS
        WHEN 'U' => c:= 'U';
        WHEN 'X' => c:= 'X';
        WHEN '0' => c:= '0';
        WHEN '1' => c:= '1';
        WHEN 'Z' => c:= 'Z';
        WHEN 'W' => c:= 'W';
        WHEN 'L' => c:= 'L';
        WHEN 'H' => c:= 'H';
        WHEN '-' => c:= '-';
        WHEN OTHERS => c := '?';
    END CASE;
    RETURN c;
END chr;

FUNCTION str(sl: std_logic) RETURN string IS
    VARIABLE s: string(1 TO 1);
BEGIN
    s(1) := chr(sl);
    RETURN s;
END str;

FUNCTION str(slv: std_logic_vector) RETURN string IS
    VARIABLE s: string(1 TO slv'length);
    VARIABLE i, j: integer;
BEGIN
    j := 1;
    FOR i IN slv'RANGE LOOP
        s(j) := chr(slv(i));
        j := j + 1;
    END LOOP;
    RETURN s;
END str;

PROCEDURE RndSlv(rng: INOUT random; ret: OUT std_logic_vector) IS
    VARIABLE r: std_logic_vector(63 DOWNT0 0);
BEGIN
    GenRnd(rng);
    r(63 DOWNT0 48) := conv_std_logic_vector(integer(rng.rnd), 16);

```



```

    GenRnd(rng);
    r(47 DOWNT0 32) := conv_std_logic_vector(integer(rng.rnd), 16);
    GenRnd(rng);
    r(31 DOWNT0 16) := conv_std_logic_vector(integer(rng.rnd), 16);
    GenRnd(rng);
    r(15 DOWNT0 0) := conv_std_logic_vector(integer(rng.rnd), 16);
    ret := r;
END RndSlv;

CONSTANT half_period: time := 12500 ps;
TYPE state_type IS (idle, pause, data);
TYPE arr IS ARRAY(NATURAL RANGE<>) OF NATURAL;
CONSTANT lengths: arr := (24, 10, 15, 0, 70, 1);
FILE output: text IS OUT "tester.txt";
SIGNAL clk_int, trigger: std_logic;

BEGIN

clk <= clk_int;

clock: process(clk_int)
    VARIABLE started: boolean := FALSE;
BEGIN
    IF (NOT STARTED) THEN
        clk_int <= '1';
        STARTED := TRUE;
    ELSIF (clk_int = '0' AND clk_int'event) THEN
        clk_int <= '1' AFTER half_period;
    ELSIF (clk_int = '1' AND clk_int'event) THEN
        clk_int <= '0' AFTER half_period;
    END IF;
END PROCESS;

tester: PROCESS(clk_int)
    VARIABLE count_bx_id, count_lvl_id, count_trig, count_read, read_length,
count_pause : natural;
    VARIABLE done_reset: boolean := false;
    VARIABLE state: state_type;
    VARIABLE data_in_tmp: std_logic_vector(63 DOWNT0 0);
    VARIABLE rng: random := CvRandom(InitUniform(9876, 0.0, 65536.0));
    VARIABLE buf: line;
BEGIN
    IF (clk_int = '1' AND clk_int'event) THEN
        -- default assignments
        data_in      <= (OTHERS => 'Z');
        data_bx_id   <= (OTHERS => 'Z');
        data_evt_lgth <= (OTHERS => 'Z');
        data_evt_stat <= (OTHERS => 'Z');
        data_evt_ty   <= (OTHERS => 'Z');
        data_lvl_id  <= (OTHERS => 'Z');
        data_source_id <= (OTHERS => 'Z');
        data_in_en <= '0';
        wr_start <= '0';
        rd_start <= '0';
        rd_stop <= '0';
        linkfull <= '0';
        reset <= '1';
        trigger <= '0';

```

```

IF (NOT done_reset) THEN
  write(buf, string("Start of run"));
  writeline(output, buf);
  state := idle;
  reset <= '0';
  count_trig := 0;
  count_bx_id := 0;
  count_lvl_id := 0;
  count_read := 0;
  done_reset := true;
END IF;

CASE count_bx_id IS

WHEN 6 | 45 | 47 | 92 | 119 =>
  count_trig := count_trig + 1;
  trigger <= '1';

WHEN 120 TO 160 =>
  linkfull <= '1';

WHEN 250 =>
  writeline(output, buf);
  write(buf, string("End of run"));
  writeline(output, buf);
  ASSERT false REPORT "End of test run" SEVERITY failure;

WHEN OTHERS =>
  -- do nothing
END CASE;

IF (count_trig > 0 AND wr_ready = '1') THEN
  count_trig := count_trig - 1;
  count_lvl_id := count_lvl_id + 1;
  data_evt_ty <= (OTHERS => '1');
  data_lvl_id <= std_logic_vector(conv_unsigned(count_lvl_id,
data_lvl_id'length));
  data_bx_id <= std_logic_vector(conv_unsigned(count_bx_id,
data_bx_id'length));
  data_source_id <= "101100111000";
  data_evt_ty <= (OTHERS => '1');
  data_evt_lgth <= conv_std_logic_vector(lengths(count_lvl_id-1),
data_evt_lgth'length);
  data_evt_stat <= (OTHERS => '0');
  wr_start <= '1';
END IF;

IF (data_out_en = '1') THEN
  write(buf, str(ctrl));
  write(buf, string(" "));
  write(buf, str(data_out));
  writeline(output, buf);
END IF;

CASE state IS
WHEN idle =>
  IF (rd_ready = '1') THEN
    rd_start <= '1';
    read_length := lengths(count_read);

```

```

        count_read := count_read + 1;
        writeline(output, buf);
        write(buf, string("Event "));
        write(buf, count_read);
        write(buf, string(" at "));
        write(buf, count_bx_id);
        writeline(output, buf);
        count_pause := 3;
        state := pause;
    END IF;

    WHEN pause =>
        count_pause := count_pause - 1;
        IF (count_pause <= 0) THEN
            state := data;
        END IF;

    WHEN data =>
        IF (read_length > 0) THEN
            IF (wr_ready = '1') THEN
                RndSlv(rng, data_in_tmp);
                data_in <= data_in_tmp;
                data_in_en <= '1';
                read_length := read_length - 1;
            END IF;
        ELSE
            rd_stop <= '1';
            state := idle;
        END IF;
    END CASE;

    count_bx_id := count_bx_id + 1;
END IF;
END PROCESS;

END tester;

```

B.3 main.c

```

#include <stdlib.h>
#include <stdio.h>
#include <string.h>

#include "crcmodel.h"

void crc64(p_cm_t, char*);
ulong getnum(char*, int);

const ulong POLY_CCITT = 0x8005;
const ulong POLY_X25   = 0x1021;

int main(void) {
    const char *infile = "tester.txt";
    unsigned long num = 0;
    char buf[256];
    int state = 0;
    FILE *in;

    cm_t crc;

```

```

/* Set parameters of CRC */
crc.cm_width = 16;
crc.cm_poly = POLY_CCITT;
crc.cm_init = 0xffff;
crc.cm_refin = FALSE;
crc.cm_refot = FALSE;
crc.cm_xorot = 0;

//printf("CRC = 0x%lX\n", cm_crc(&crc));

in = fopen(infile, "rt");
if (!in) {
    fprintf(stderr, "Error opening %s\n", infile);
    exit(EXIT_FAILURE);
}

for(;;) {
    if (!fgets(buf, sizeof(buf), in)) {
        if (feof(in)) {
            printf("\nEnd of file\n");
            break;
        } else {
            printf("Error reading from file\n");
        }
    }
    //printf("Data: %s\n", buf);
    // process line...
    switch (state) {
    case 0: // default
        if (!strcmp(buf, "Event", 5)) {
            char *ptr = strstr(buf, "at ");
            if (ptr) {
                printf("\nEvent %d, time %d\n", atoi(&buf[6]), atoi(&ptr[3]));
                state = 1;
            }
        }
        break;
    case 1: // header 1
        if (buf[0] == '1') {
            printf("Header:\n");
            printf(" BOE      = %ld\n", getnum(&buf[ 2],  4));
            printf(" Evt_ty   = %ld\n", getnum(&buf[ 6],  4));
            printf(" Lvl_id   = %ld\n", getnum(&buf[10], 24));
            printf(" BX_id    = %ld\n", getnum(&buf[34], 12));
            printf(" Src_id   = %ld\n", getnum(&buf[46], 12));
            printf(" FOV     = %ld\n", getnum(&buf[58],  4));
            printf(" Last    = %ld\n", getnum(&buf[62],  1));
            num = 0;
            /* Initialise the CRC generator */
            cm_ini(&crc);
            if (buf[62] == '0') {
                state = 2;
            } else {
                state = 3;
            }
        } else {
            fprintf(stderr, "Error: header word expected\n");
            exit(EXIT_FAILURE);
        }
    }
}

```

```

        break;
    case 2: // header 2 (optional)
        if (buf[0] == '1') {
            printf("Second Header\n");
            state = 3;
        } else {
            fprintf(stderr, "Error: second header word expected\n");
            exit(EXIT_FAILURE);
        }
        break;
    case 3: // data/trailer
        if (buf[0] == '0') {
            num++;
            crc64(&crc, &buf[2]);
        } else if (buf[0] == '1') {
            printf("Data:\n");
            printf(" Length   = %ld\n", num);
            printf("  CRC      = 0x%.4lX\n", cm_crc(&crc));
            printf("Trailer:\n");
            printf("  EOE      = %ld\n",      getnum(&buf[ 2],  4));
            printf("  Evt_lgth = %ld\n",      getnum(&buf[10], 24));
            printf("  CRC      = 0x%.4lX\n", getnum(&buf[34], 16));
            printf("  Evt_stat = %ld\n",      getnum(&buf[54],  8));
            state = 0;
        } else {
            printf("Unexpected: %s\n", buf);
            state = 0;
        }
        break;
    default:
        // error
        break;
    } // end switch
} // end loop
return EXIT_SUCCESS;
}

ulong getnum(char* src, int len) {
    ulong ret = 0;
    int i;
    for (i = 0; i < len; i++) {
        ret <<= 1;
        if (src[i] == '1') ret |= 1;
    }
    return ret;
}

void crc64(p_cm_t crc, char* src) {
    unsigned char buf[8];
    int i;
    for (i = 0; i < 8; i++) {
        buf[i] = (char)getnum(src + i*8, 8);
    }
    cm_blk(crc, buf, 8);
}

```

B.4 crcmodel.h

```

/*****

```

Common Data Format Verification Code

```

/*          Start of crcmodel.h          */
/*****
/*
/* Author : Ross Williams (ross@guest.adelaide.edu.au.).
/* Date   : 3 June 1993.
/* Status : Public domain.
/*
/* Description : This is the header (.h) file for the reference
/* implementation of the Rocksofttm Model CRC Algorithm. For more
/* information on the Rocksofttm Model CRC Algorithm, see the document
/* titled "A Painless Guide to CRC Error Detection Algorithms" by Ross
/* Williams (ross@guest.adelaide.edu.au.). This document is likely to be in
/* "ftp.adelaide.edu.au/pub/rocksoft".
/*
/* Note: Rocksoft is a trademark of Rocksoft Pty Ltd, Adelaide, Australia.
/*
/*****
/*
/* How to Use This Package
/* -----
/* Step 1: Declare a variable of type cm_t. Declare another variable
/*         (p_cm say) of type p_cm_t and initialize it to point to the first
/*         variable (e.g. p_cm_t p_cm = &cm_t).
/*
/* Step 2: Assign values to the parameter fields of the structure.
/*         If you don't know what to assign, see the document cited earlier.
/*         For example:
/*             p_cm->cm_width = 16;
/*             p_cm->cm_poly   = 0x8005L;
/*             p_cm->cm_init   = 0L;
/*             p_cm->cm_refin  = TRUE;
/*             p_cm->cm_refot  = TRUE;
/*             p_cm->cm_xorot  = 0L;
/*         Note: Poly is specified without its top bit (18005 becomes 8005).
/*         Note: Width is one bit less than the raw poly width.
/*
/* Step 3: Initialize the instance with a call cm_ini(p_cm);
/*
/* Step 4: Process zero or more message bytes by placing zero or more
/*         successive calls to cm_nxt. Example: cm_nxt(p_cm,ch);
/*
/* Step 5: Extract the CRC value at any time by calling crc = cm_crc(p_cm);
/*         If the CRC is a 16-bit value, it will be in the bottom 16 bits.
/*
/*****
/*
/* Design Notes
/* -----
/* PORTABILITY: This package has been coded very conservatively so that
/* it will run on as many machines as possible. For example, all external
/* identifiers have been restricted to 6 characters and all internal ones to
/* 8 characters. The prefix cm (for Crc Model) is used as an attempt to avoid
/* namespace collisions. This package is endian independent.
/*
/* EFFICIENCY: This package (and its interface) is not designed for
/* speed. The purpose of this package is to act as a well-defined reference
/* model for the specification of CRC algorithms. If you want speed, cook up
/* a specific table-driven implementation as described in the document cited
/* above. This package is designed for validation only; if you have found or

```

Common Data Format Verification Code

```

/* implemented a CRC algorithm and wish to describe it as a set of parameters */
/* to the Rocksoft^tm Model CRC Algorithm, your CRC algorithm implementation */
/* should behave identically to this package under those parameters.      */
/*                                                                           */
/*****

/* The following #ifndef encloses this entire */
/* header file, rendering it idempotent.      */
#ifndef CM_DONE
#define CM_DONE

/*****

/* The following definitions are extracted from my style header file which */
/* would be cumbersome to distribute with this package. The DONE_STYLE is the */
/* idempotence symbol used in my style header file.                          */

#ifndef DONE_STYLE

typedef unsigned long   ulong;
typedef unsigned       bool;
typedef unsigned char * p_ubyte_;

#ifndef TRUE
#define FALSE 0
#define TRUE  1
#endif

#endif

/*****

/* CRC Model Abstract Type */
/* ----- */
/* The following type stores the context of an executing instance of the */
/* model algorithm. Most of the fields are model parameters which must be */
/* set before the first initializing call to cm_ini.                       */
typedef struct
{
    int   cm_width;   /* Parameter: Width in bits [8,32].      */
    ulong cm_poly;    /* Parameter: The algorithm's polynomial. */
    ulong cm_init;    /* Parameter: Initial register value.     */
    bool  cm_refin;   /* Parameter: Reflect input bytes?       */
    bool  cm_refot;   /* Parameter: Reflect output CRC?        */
    ulong cm_xorot;   /* Parameter: XOR this to output CRC.     */

    ulong cm_reg;     /* Context: Context during execution.     */
} cm_t;
typedef cm_t *p_cm_t;

/*****

/* Functions That Implement The Model */
/* ----- */
/* The following functions animate the cm_t abstraction. */

void cm_ini(p_cm_t p_cm);
/* Initializes the argument CRC model instance.          */
/* All parameter fields must be set before calling this. */

```

```

void cm_nxt(p_cm_t p_cm,int ch);
/* Processes a single message byte [0,255]. */

void cm_blk(p_cm_t p_cm,p_ubyte_ blk_adr,ulong blk_len);
/* Processes a block of message bytes. */

ulong cm_crc(p_cm_t p_cm);
/* Returns the CRC value for the message bytes processed so far. */

/*****/

/* Functions For Table Calculation */
/* ----- */
/* The following function can be used to calculate a CRC lookup table. */
/* It can also be used at run-time to create or check static tables. */

ulong cm_tab(p_cm_t p_cm,int index);
/* Returns the i'th entry for the lookup table for the specified algorithm. */
/* The function examines the fields cm_width, cm_poly, cm_refin, and the */
/* argument table index in the range [0,255] and returns the table entry in */
/* the bottom cm_width bytes of the return value. */

/*****/

/* End of the header file idempotence #ifndef */
#endif

/*****/
/*                               End of crcmodel.h                               */
/*****/

```

B.5 crcmodel.c

```

/*****/
/*                               Start of crcmodel.c                               */
/*****/
/*                               */
/* Author : Ross Williams (ross@guest.adelaide.edu.au.). */
/* Date   : 3 June 1993. */
/* Status : Public domain. */
/*                               */
/* Description : This is the implementation (.c) file for the reference */
/* implementation of the Rocksofttm Model CRC Algorithm. For more */
/* information on the Rocksofttm Model CRC Algorithm, see the document */
/* titled "A Painless Guide to CRC Error Detection Algorithms" by Ross */
/* Williams (ross@guest.adelaide.edu.au.). This document is likely to be in */
/* "ftp.adelaide.edu.au/pub/rocksoft". */
/*                               */
/* Note: Rocksoft is a trademark of Rocksoft Pty Ltd, Adelaide, Australia. */
/*                               */
/*****/
/*                               */
/* Implementation Notes */
/* ----- */
/* To avoid inconsistencies, the specification of each function is not echoed */
/* here. See the header file for a description of these functions. */
/* This package is light on checking because I want to keep it short and */

```


Common Data Format Verification Code

```

/* simple and portable (i.e. it would be too messy to distribute my entire
/* C culture (e.g. assertions package) with this package.
/*
/*
/*****

#include "crcmodel.h"

/*****

/* The following definitions make the code more readable. */

#define BITMASK(X) (1L << (X))
#define MASK32 0xFFFFFFFFL
#define LOCAL static

/*****

static ulong reflect(ulong v, int b) {
/* Returns the value v with the bottom b [0,32] bits reflected. */
/* Example: reflect(0x3e23L,3) == 0x3e26 */
    int i;
    ulong t = v;
    for (i=0; i<b; i++) {
        if (t & 1L) {
            v|= BITMASK((b-1)-i);
        } else {
            v&= ~BITMASK((b-1)-i);
        }
        t>>=1;
    }
    return v;
}

/*****

static ulong widmask(p_cm_t p_cm)
/* Returns a longword whose value is (2^p_cm->cm_width)-1. */
/* The trick is to do this portably (e.g. without doing <<32). */
{
    return (((1L<<(p_cm->cm_width-1))-1L)<<1) | 1L;
}

/*****

void cm_ini(p_cm_t p_cm) {
    p_cm->cm_reg = p_cm->cm_init;
}

/*****

void cm_nxt(p_cm_t p_cm, int ch) {
    int i;
    ulong uch = (ulong) ch;
    ulong topbit = BITMASK(p_cm->cm_width-1);

    if (p_cm->cm_refin) uch = reflect(uch,8);
    p_cm->cm_reg ^= (uch << (p_cm->cm_width-8));
    for (i=0; i<8; i++) {
        if (p_cm->cm_reg & topbit) {

```

```

    p_cm->cm_reg = (p_cm->cm_reg << 1) ^ p_cm->cm_poly;
  } else {
    p_cm->cm_reg <<= 1;
  }
  p_cm->cm_reg &= widmask(p_cm);
}
}

/*****/

void cm_blk(p_cm_t p_cm, p_ubyte_blk_adr, ulong blk_len) {
  while (blk_len-->0) cm_nxt(p_cm, *blk_adr++);
}

/*****/

ulong cm_crc(p_cm_t p_cm) {
  if (p_cm->cm_refot) {
    return p_cm->cm_xorot ^ reflect(p_cm->cm_reg, p_cm->cm_width);
  } else {
    return p_cm->cm_xorot ^ p_cm->cm_reg;
  }
}

/*****/

ulong cm_tab(p_cm_t p_cm, int index) {
  int i;
  ulong r;
  ulong topbit = BITMASK(p_cm->cm_width-1);
  ulong inbyte = (ulong) index;

  if (p_cm->cm_refin) inbyte = reflect(inbyte, 8);
  r = inbyte << (p_cm->cm_width-8);
  for (i=0; i<8; i++) {
    if (r & topbit) {
      r = (r << 1) ^ p_cm->cm_poly;
    } else {
      r<<=1;
    }
  }
  if (p_cm->cm_refin) r = reflect(r, p_cm->cm_width);
  return r & widmask(p_cm);
}

/*****/
/*                                     End of crcmodel.c                                     */
/*****/

```

References

1. ALEPH DELPHI L3 and OPAL Collaborations (2002). **Search for the Standard Model Higgs Boson at LEP. ICHEP'02 (Amsterdam, July 2002)** .
http://lephiggs.web.cern.ch/LEPHIGGS/papers/July2002_SM/index.html
2. ALEPH DELPHI L3 and OPAL Collaborations (2002). **Search for the Standard Model Higgs Boson at LEP. ICHEP'02 (Amsterdam, July 2002)** .
http://lephiggs.web.cern.ch/LEPHIGGS/papers/July2002_SM/index.html
3. Denegri D. *et al.* (1994). **B Physics and CP Violation Studies with the CMS Detector at LHC.** *Int. J. Mod. Phys. A* 9, 4211-4255.
4. CMS Collaboration (1994). **The Compact Muon Solenoid Technical Proposal.** (CERN/LHCC 94-38).
5. CMS Collaboration (1997). **CMS: The Magnet Project - Technical Design Report.** (CERN/LHCC 97-010).
6. CMS Collaboration (1998). **CMS Tracker Project Technical Design Report.** (CERN/LHCC 98-6).
7. CMS Collaboration (2000). **Addendum to the CMS Tracker TDR.** (CERN/LHCC 2000-016).
8. CMS Collaboration (1997). **CMS Electromagnetic Calorimeter Technical Design Report.** (CERN/LHCC 97-33).
9. CMS Collaboration (1997). **CMS Hadron Calorimeter Project Technical Design Report.** (CERN/LHCC 97-32).
10. CMS Collaboration (1997). **CMS Muon System Technical Design Report.** (CERN/LHCC 97-32).
11. Wultz C.-E. (2001). **Concept of the First Level Global Trigger for the CMS experiment at LHC.** *Nucl. Instrum. Meth.* A473 (3), 231-242.
12. Brown S. & Rose J. (1996). **Architecture of FPGAs and CPLDs: A Tutorial.** *IEEE Design and Test of Computers* 13 (2), 42-57.
<http://www.eecg.toronto.edu/~jayar/pubs/brown/survey.ps.gz>
13. McCalmont S. (2002). **EE465 - Digital IC Design.** (Iowa State University, Course Notes).
<http://class.ee.iastate.edu/ee465/>
14. Smith M.J.S. (1997). **Application Specific Integrated Circuits.** (Addison-Wesley).

15. Cheung P.Y.K. (2002). **Digital System Design**. (Imperial College London Department of Electrical and Electronic Engineering, Course Notes).
http://www.ee.ic.ac.uk/pcheung/teaching/ee3_DSD/
16. **Virtex-II 1.5V Platform FPGAs Data Sheet (2002). Summary of Virtex-II Features**. (Xilinx).
<http://www.xilinx.com/partinfo/ds031-1.pdf>
17. **Virtex-II 1.5V Platform FPGAs Data Sheet (2001). Detailed Description**. (Xilinx).
<http://www.xilinx.com/partinfo/ds031-2.pdf>
18. Smith D.J. (2002). **VHDL & Verilog Compared & Contrasted**. (Veribest Inc.).
<http://www.angelfire.com/in/rajesh52/verilogvhdl.html>
19. **A Designer's Guide to Verilog (2002)**. (Doulos).
http://www.doulos.com/fi/dgvlog_fr.html
20. **A Designer's Guide to VHDL (2002)**. (Doulos).
http://www.doulos.com/fi/dgvhdl_fr.html
21. Thacker E. (2001). **System Ace: Configuration Solution for Xilinx FPGAs**. (White Paper, Version 1.0). (Xilinx Inc.).
http://www.xilinx.com/publications/whitepapers/wp_pdf/wp151.pdf
22. Hall G. (1992). **Modern charged particle detectors**. *Contemporary Physics* 33 (1), 1-14.
23. Jones L. (2001). **APV25S1 Design Overview**.
http://www.te.rl.ac.uk/INS/Electronic_Systems/Microelectronics_Design/Projects/High_Energy_Physics/CMS/APV25-S1/files/Overview.pdf
24. Fulcher J.R. (2001). **Radiation Effects in Electronics for the CMS Tracking Detector**. (Imperial College).
25. Jones L. (2001). **APV25-S1 User Guide**. (Version 2.2).
http://www.te.rl.ac.uk/med/projects/High_Energy_Physics/CMS/APV25-S1/pdf/User_Guide_2.2.pdf
26. Jones L.L. *et al.* (1999). **The APV25 Deep Submicron Readout Chip for CMS Detectors**. *5th Workshop on Electronics for LHC Experiments, Snowmass, Colorado*.
27. Hall G. (2000). **The Deconvolution Method of Pulse Shaping**.
28. **The I²C Bus Specification (2000)**. (Version 2.1). (Philips).
<http://www.semiconductors.philips.com/buses/i2c/>
29. Murray P. (2000). **APVMUX User Guide**. (Version 1.0).

30. **CMS Tracker Optical Readout Link Specification (2001). Part 2: Analogue opto-hybrid.** (Version 3.2).
31. Coughlan J.A. *et al.* (2002). **The Front-End Driver Card for the CMS Silicon Strip Tracker Readout.** *8th Workshop on Electronics for LHC Experiments, Colmar, France.*
32. Racz A. *et al.* (2002). **CMS data to surface transportation architecture.** (8th Workshop on Electronics for LHC Experiments).
<http://lhc-electronics-workshop.web.cern.ch/LHC-electronics-workshop/2002/DAQ/B42.pdf>
33. Boyle O. *et al.* (1997). **The S-LINK Interface Specification.**
<http://hsi.web.cern.ch/HSI/s-link/>
34. Racz A. *et al.* (2000). **The S-LINK 64 bit extension specification: S-LINK64.**
<http://hsi.web.cern.ch/HSI/s-link/>
35. CMS Collaboration (2002). **The TriDAS Project Technical Design Report, Volume 2: Data Acquisition and High Level Trigger.** (Version 3.0).
36. Christiansen J. *et al.* (1999). **TTCrx Reference Manual. A Timing, Trigger and Control Receiver ASIC for LHC Detectors.** (Version 3.0). (RD12 Project Collaboration, CERN).
37. Bell K.W. *et al.* (2002). **User Requirements Document for the Final FED of the CMS Silicon Strip Tracker.** (Version 0.51).
http://www.te.rl.ac.uk/esdg/cms-fed/hardware/fed_urd_v0.51.pdf
38. **CMS Tracker Front-End Driver Schematics (2002).**
39. Gannon B. (2002). **Compact Muon Solenoid (CMS) Front End Driver (FED) Front-End FPGA Technical Description.** (Version 1.1).
http://www.te.rl.ac.uk/esdg/cms-fed/hardware/fed_fe_fpga.pdf
40. Gill K.A. & Marinelli N. (2001). **Start-up Synchronization Procedure of the CMS Tracker.**
41. Reid I.D. (2002). **The effect of the FED ADC range on the Silicon Strip Tracker Coordinate Resolution.**
42. **CMS DAQ horizontal pages (2002).**
<http://cmsdoc.cern.ch/cms/TRIDAS/horizontal/>
43. Williams R. (1993). **A Painless Guide to CRC Error Detection Algorithms.** (Version 3). (Rocksoft™).
44. **CRC Tool .** (Easics).
<http://www.easics.com/webtools/crctool>

45. Iles G. & Foudas C. (2001). **APVE Working Document**. (Draft Version 1.10).
46. Tomalin I.R. (2001). **Personal Communication**.
47. Caner A. & Tomalin I. (2000). **On Balancing Data Flow from the Silicon Tracker**.